UNIVERSITY OF CALIFORNIA
SANTA CRUZ

FERNS LIVING ON THE EDGE: ECOPHYSIOLOGY OF FERNS UNDER SEVERE WATER DEFICIT

A dissertation submitted in partial satisfaction
of the requirements for the degree of

DOCTOR OF PHILOSOPHY

in

ECOLOGY AND EVOLUTIONARY BIOLOGY

by

Helen I. Holmlund

June 2020

The Dissertation of Helen I. Holmlund is approved:

_____
Professor Jarmila Pittermann, chair

_____
Professor Ingrid Parker

_____
Professor Rita Mehta

_____
Professor Marilyn Ball

_____
Quentin Williams
Acting Vice Provost and Dean of Graduate Studies

Table of Contents

Abstract……vi

Acknowledgments……..viii

Introduction……1

Chapter 1……7

Tables and Figures……...31

Chapter 2……..46

Tables and Figures……...73

Chapter 3……..87

Tables and Figures…….108

Conclusion…….115

Appendix 1…….121

Appendix 2…….125

Literature Cited……..126

List of Figures

Chapter 1

Figure 1……32

Figure 2……33

Figure 3……35

Figure 4……36

Figure 5……38

Figure 6……40

Figure 7……42

Figure 8……44

Figure S1……121

Figure S2……123

Figure S3……124

Chapter 2

Figure 1……74

Figure 2……75

Figure 3……77

Figure 4……79

Figure 5……81

Figure 6……82

Figure 7……84

Figure 8……85

Chapter 3

Figure 1……..108

Figure 2……..110

Figure 3……..112

Figure 4……..113

Figure S1……125

Abstract

Ferns Living on the Edge: Ecophysiology of Ferns under Severe Water Deficit

Helen I. Holmlund

Ferns are the second most diverse lineage of vascular plants, yet we know little about how ferns have adapted to survive in habitats with limited fresh water. In this dissertation, I examined two groups of ferns that thrive in freshwater-limited ecosystems: the salt-tolerant mangrove ferns and the desiccation-tolerant "resurrection" ferns.

In Chapter 1, I characterized adaptations to high salinity and high evaporative demand in the mangrove fern *Acrostichum speciosum* along salinity and rainfall gradients in Australia. I found that mangrove ferns exhibit the same key adaptations as salt-tolerant angiosperms: excluding the majority of salt at the roots and osmotically adjusting leaves to maintain turgor. Furthermore, the mangrove ferns showed differing responses to high salinity and high evaporative demand; only high salinity decreased water potential and rates of gas exchange.

In Chapters 2 and 3, I characterized mechanisms of recovery in resurrection ferns, which completely desiccate (< -100 MPa) and revive when rehydrated. In Chapter 2, I experimentally determined that root pressure plays a critical role in restoring hydraulic flow through the vascular system during resurrection. High concentrations of sucrose in desiccated rhizomes may contribute to developing this root pressure. In Chapter 3, I discovered that vascular tissues experience reversible

desiccation patterns using high resolution micro-computed tomography (microCT). Auto-fluorescence revealed that the chemical composition of these tissues likely facilitates reversible desiccation in the vascular system.

Although mangrove and resurrection ferns are distinct in many ways, both rely on osmotic adjustment to survive periods of limited freshwater availability.

Acknowledgments

First, I want to thank my thesis advisor, Jarmila Pittermann. Jarmila is responsible for inspiring my love of ferns, for which I will be forever grateful. I will always appreciate how Jarmila encouraged me to develop my research interests, however crazy they sounded. Beyond giving me freedom to pursue these ideas, she actively supported me and helped me achieve my goals. Jarmila is also a particularly gifted writer, and I appreciate the many hours she has invested in helping me improve my own writing. I am so grateful for the tools she has given me to continue my life as a scientist.

I want to thank Steve Davis, who first sparked my fascination with research, teaching, and the chaparral. Dr. Davis has had a profound impact on my life as my friend and mentor. After my first day in the field with Dr. Davis, I never looked at nature, ferns, or the chaparral the same way again. Over the past seven years, Dr. Davis has continually supported and inspired my curiosity for how ferns can thrive in water-limited ecosystems. It is a powerful mentor who changes the way you see the world and helps you move from consuming knowledge to producing it, and that is what Dr. Davis has done for me. I hope I can inspire the next generation of students as he has inspired me.

I would like to thank Marilyn Ball for all the ways that she has blessed my life. Besides introducing me to the wonders of Australia and the mangrove ecosystem, she has helped me earn prestigious titles in the field such as “the croc lady” and “swamp

sheila." From the moment I set foot in Canberra, Marilyn welcomed me into her home and her lab group, going above and beyond the obligations of a PI to make me feel welcome in a new country. Collaborating with Marilyn has completely transformed my perspective on leaves and salt tolerance, inspiring a vast sea of questions that I hope to answer someday.

Over the last several years, I have had the pleasure to work with many other incredible scientists. I am grateful to Ingrid Parker and Rita Mehta, who served on my thesis committee. I thank Anna Jacobsen and Brandon Pratt for collaborating with me and introducing me to new questions about histology, 3D imaging, and the chaparral. I also want to thank Frank Ewers for investing in my development as a scientist and all the early mornings he spent carrying water with me into the field. Thank you also to Hua Chen, Joanne Lee, and Daryl Webb at ANU's Centre for Advanced Microscopy, for conducting CEDX measurements on the mangrove ferns and for the hours they spent training me in cryo technique. I have had the joy of working with many other scientists who inspired me over the last few years, including Martin Venturas, Aaron Ramirez, Marcia Murry-Ewers, Gretchen North, John Sperry, Robin Dunkin, Eddie Watkins, Courtney Campany, Robbin Moran, Anna Sala, Gerard Sapes, Teresa Neeman, Pete Raimondi, Eldon Ball, Jack Egerton, Nigel Brothers, and Catherine Bone.

I am grateful to all the Pepperdine students who studied ferns alongside me, including Victoria Lekson, Samantha Fiallo, Natalie Aguirre, Katie Sauer, Brandon

Grinovich, Karagan Smith, Cristian Garcia, Marissa Ochoa, Amanda Burns, Gabriella Palmeri, Shaquetta Reese, Amir Mahmoud, Ala Mahmoud, Nate Gruendemann, Guinevere Mesh, Luis Ballasteros, Jamille Lockhart, Logan Meeks, Alexandra Case, and Briana Arquilevich. I learned so much from these students, and my work would not have been possible without them. I am also grateful to the graduate students and post-docs who cheerfully assisted me in the lab and the field, including Katharine Cary, Marta Percolla, Ryan Salladay, Alex Baer, Jim Wheeler, Tomas Fuenzalida, Callum Bryant, Alonso Zavaleta Fernandez de Cordova, Holly Beckett, Sabrina Shirazi, Regina Spranger, Ana Valenzuela Toro, and Sara Gonzales. I especially thank Katharine Cary for years of mentorship, moral support, and camping adventures. I also want to thank Shelby Boyd and Jessie Hampton for moral support and coaching me through the writing process.

I want to thank the land managers, field station directors, and administrators who facilitated my field work. I am grateful to the California state parks and the National Park Service for permission to study ferns in the Santa Monica Mountains. Thank you to Anne Hoggett and Lyle Vail at the Lizard Island Research Station for facilitating my project on Lizard Island. Thank you to Nigel Brothers and Catherine Bone for outstanding support of field work conducted in mangrove forest along the Daintree River. Thank you to Lyndal Laughrin for facilitating my work on Santa Cruz Island. Thank you to Jim Velzy and Sylvie Childress at the UCSC greenhouses and to the staff at the ANU greenhouses for growing my ferns and providing horticultural support. Thank you to Daphne Green and all the faculty and staff in Pepperdine's

Natural Science Division for welcoming and supporting my continued research at Pepperdine. I also want to thank the incredible administrative staff in UCSC's EEB department for always connecting me to the help I needed, including Sarah Amador, Judy Straub, Jacqueline Rose, and Stephanie Zakarian.

Thank you to my family and friends for all their love, support, and enthusiasm for my work. I am especially grateful to my parents for homeschooling me and teaching me that learning is fun. Thank you also to my Malibu family, including Steve and Janet Davis and the University Church of Christ congregation, who have made Pepperdine feel like home to me. I am also grateful to the communities of Vintage Faith Church and Hope Church Canberra, who welcomed me and invested in my growth as a scientist and a Christian.

Finally, I am so grateful for the people who have financially contributed to my education and my research. Thank you to the National Science Foundation for my Graduate Research Fellowship and my GROW award, and for supporting the SURB program at Pepperdine, where I first discovered my passion for research. Thank you to UC Santa Cruz for my Chancellor's Fellowship, Langenheim Fellowship, and summer support from the EEB department. Thank you to Pepperdine University and the Natural Science Division for supporting my work through the SURB program and for supporting the incredible students who worked alongside me. I especially want to thank Frank and Regina Merritt for their support of the SURB program. Thank you to the Southern California Research Learning Center for funding my research on Santa Cruz

Island. Thank you also to the Ecological Society of America, Botanical Society of America, the Gordon Conference organizers, and the UCSC Graduate Student Association for conference travel awards. My work was also made possible by the funding granted to my collaborators, including the National Science Foundation (NSF grant IOS-1258186 to Jarmila Pittermann, NSF HRD-1547784 to Brandon Pratt and Anna Jacobsen, and NSF IOS-1252232 to Anna Jacobsen) and the Australian Research Council (ARC Discovery Grant DP180102969 awarded to Marilyn Ball at Australian National University). I also want to recognize the support of the Department of Defense (Army Research Office proposal No. 68885-EV-REP and contract No. W911NF-16-1-0556 to Brandon Pratt) and of the CSUB Biology 3D Imaging Center, which made possible our use of microCT to visualize water movement in resurrection ferns.

Chapters 2 and 3 were originally published as the following articles in the *Journal of Experimental Botany* and *New Phytologist*:

Holmlund HI, Davis SD, Ewers FW, Aguirre NM, Sapes G, Sala A, Pittermann J. 2020. Positive root pressure is critical for whole-plant desiccation recovery in two species of terrestrial resurrection ferns. *Journal of Experimental Botany* 71(3): 1139-1150.

Holmlund HI, Pratt RB, Jacobsen AL, Davis SD, Pittermann J. 2019. High-resolution computed tomography reveals dynamics of desiccation and rehydration in fern petioles of a desiccation-tolerant fern. *New Phytologist* 224(1): 97-105.

Introduction

As early vascular plants that evolved 200 million years prior to the appearance of flowering plants, ferns are interesting to physiologists because of their ancestral traits (Pittermann *et al*., 2015). Today, ferns are the second most diverse plant lineage with twelve thousand species worldwide, surpassed only by flowering plants (PPG I, 2016). However, ferns remain understudied. Ferns are major players in a variety of ecosystems, including the tropics, subtropics, and temperate rainforest. Ferns may act as ecological filters, controlling which angiosperm tree species dominate the overstory (Maguire and Forman, 1983; George and Bazzaz, 1999). Furthermore, ferns have been speculated to be an "untapped source of biodiversity" for crop development (Rathinasabapathi, 2006). Studying ferns can inform our understanding of evolution, past and present, by helping us understand key transitions in vascular plant evolution and by revealing current ecological interactions of diverse ecosystems.

Ferns typically inhabit wet, shady habitats, such as tropical rainforests and temperate forest understories. Ferns reproduce by means of spores with an independent gametophyte generation that requires surface water for fertilization, further augmenting the relation between most ferns and mesic habitats. However, some fern species thrive in water-limited habitats, including the desert and chaparral ecosystems (Gaff, 1977; Nobel, 1978; Kirkpatrick, 2008; Hietz, 2010; Pittermann *et al*., 2015; Holmlund *et al*., 2016). Ferns growing in saline habitats are also water-limited in a different way, because the greater selectivity of ion uptake at the roots slows water movement into the

plant (Ball, 1988c). Studying fern adaptations to water deficit has the potential to expand our understanding of how plants in general may tolerate drought and salinity, which is relevant to our changing climate.

My dissertation explores two strategies that ferns use to cope with water stress: salt tolerance and desiccation tolerance. While both of these strategies have been studied in flowering plants, no previous works have focused on ferns at the level of whole-plant water relations. Interestingly, both these groups of ferns occur in the family Pteridaceae, which has been documented to have a high proportion of ferns that thrive in water-limited habitats (Schuettpelz *et al*., 2009; Mahley *et al*., 2018). The salt-tolerant mangrove ferns (*Acrostichum* spp.) thrive pan-tropically in mangrove swamps, yet we know so little about the mechanisms through which mangrove ferns exclude salt, secrete salt, or osmotically adjust cells in order to cope with surrounding salinity. In contrast, desiccation-tolerant "resurrection" ferns survive in deserts worldwide by hibernating through dry spells (up to ~6 months) in a completely desiccated state. Our knowledge of the mechanisms of whole-plant recovery is limited in vascular resurrection plants and basically non-existent in resurrection ferns. Both of these fern groups are ecologically relevant as denizens of ecosystems where most plants would die. Furthermore, both salt tolerance and desiccation tolerance have been explored as a means of crop improvement, albeit with limited success (Flowers, 2004; Toldi *et al*., 2009). Ferns are indeed understudied sources of biodiversity, and understanding their physiology will provide further insight into the diversity of mechanisms vascular plants have for persisting in a dynamic environment.

In **Chapter 1**, I collaborated with Dr. Marilyn Ball at the Australian National University to address the question of fern salt tolerance by characterizing the water relations of *Acrostichum speciosum* growing along a salinity gradient and an atmospheric moisture gradient in tropical Australia. The Daintree River system in Queensland, Australia, provides a natural salinity gradient, and the range of *A. speciosum* extends from upstream locations (nearly freshwater) to the mouth of the river (approx. 100% seawater). To examine the effect of atmospheric moisture on *A. speciosum*, I compared ferns along the Daintree River on the mainland (high rainfall) to ferns growing on Lizard Island (low rainfall). At each site, I measured aspects of tissue hydration (predawn and midday water potential), osmotic adjustment (osmotic potential at saturation and full turgor), gas exchange (photosynthesis and transpiration), and anatomical traits related to water use (stomatal size, stomatal density, leaf vein density, leaf mass per unit area). My results show that these plants adjust their cellular osmotic potential along a salinity gradient in order to cope with increasing salinity. However, the ability to thrive in more saline soils comes at the cost of decreasing photosynthesis and increased anatomical investments to cope with water loss. Although no osmotic adjustments or reduction in gas exchange were associated with the atmospheric moisture gradient, I found substantial shifts in leaf anatomical traits of low-salinity plants between the mainland (high rainfall) and island (low rainfall) sites, perhaps to maximize water use efficiency with changing atmospheric moisture availability. Taken together, these findings reveal a suite of adaptations that allows *A. speciosum* to thrive in the saltwater mangrove swamp.

In Chapters 2 and 3, I characterize the dynamics of whole-plant recovery in vascular resurrection ferns. As vascular plants, resurrection ferns face challenges during the resurrection process that are not experienced by most desiccation-tolerant (DT) plants, including mosses. While nonvascular DT plants rehydrate fairly quickly, vascular DT plants face the added challenges of rehydrating distinct tissue types and organs of varying function and chemical composition, as well as restoring hydraulic flow through the vascular system. In these chapters, I used several methodological approaches to develop an integrated perspective on the mechanisms of reversible desiccation and recovery in these ferns.

In **Chapter 2**, I use targeted irrigation experiments *in situ* to test whether root water or leaf water contributes more to whole plant recovery. To study these plants in their natural setting, I collaborated with Drs. Stephen Davis and Frank Ewers at Pepperdine University, located in the chaparral ecosystem of southern California where these resurrection ferns thrive. I also collaborated with Drs. Anna Sala and Gerard Sapes at the University of Montana to measure the dynamics of non-structural carbohydrates in the rhizome, stipe, and leaf tissue of resurrecting plants *in situ*. These experiments showed that root water can resurrect the entire plant, but leaf water uptake expedites recovery in distal leaves. Importantly, I also found that root pressure is critical for whole plant recovery and that concentrations of non-structural carbohydrates change during resurrection. My results indicate that sucrose may function as a desiccation protectant in the stipes and rhizomes of these resurrection ferns, as shown previously in other plants (Moore *et al*., 2007; Peters *et al*., 2007).

Furthermore, it is possible that high concentrations of sucrose in the desiccated rhizome tissues may contribute to the development of root pressure early in resurrection, thus contributing to the recovery process as well as the protected, desiccated state.

Although some knowledge is best obtained through field studies, advanced imaging techniques, such as micro-computed tomography (microCT), can provide powerful insight into the processes of xylem embolism formation and recovery by generating three-dimensional images of the vascular system of intact plants (Brodersen *et al*., 2010). In **Chapter 3**, I collaborated with Drs. Anna Jacobsen and Brandon Pratt at California State University, Bakersfield, using high-resolution microCT to visualize the dynamics of desiccation and rehydration in several stipe tissues. Our microCT analysis revealed reversible desiccation of stipe tissues, with several patterns unique to these resurrection ferns, including perennially desiccated cortex tissue and a compressible vascular bundle. We complemented these results by examining stipe cross sections with light and fluorescence microscopy, revealing several anatomical and histochemical traits that might contribute to the patterns of desiccation and rehydration seen using microCT.

As a whole, my dissertation begins to explore the diverse strategies that ferns use to thrive in water-limited niches. Both these groups of ferns belong to the family Pteridaceae, which has been previously noted for diversity of adaptations and niches (Schuettpelz *et al*., 2009; Mahley *et al*., 2018). Although the saltwater mangrove swamp and the dry chaparral ecosystem appear quite distinct, both the mangrove and resurrections ferns have adapted to thrive with limited freshwater availability. A better

understanding of the traits that convey drought tolerance is particularly relevant given our changing climate, as ferns that thrive in the "extremes" may be survivors in a hotter and drier climate.

Chapter 1

The mangrove fern, *Acrostichum speciosum*, exhibits responses to salinity consistent with halophytic angiosperms: separating the effects of rhizospheric and atmospheric water availability on leaf structure and function

Abstract

Halophytes (salt-loving plants) have evolved a suite of adaptations to thrive in salt water. Most halophytes are flowering plants, but there is one known genus of salt-loving ferns, *Acrostichum spp*. I tested natural populations of *Acrostichum speciosum* growing along a salinity gradient to determine whether mangrove ferns have adaptations similar to those that angiosperms use to thrive in high salinity. I found that *A. speciosum* shared some key halophytic traits with angiosperms, including greater exclusion of ions at the roots and cellular osmotic adjustment to maintain turgor. Furthermore, I found that *A. speciosum* growing in high estuarine salinity had some characteristics consistent with conservative water use, including reduced rates of gas exchange and anatomical traits that would ease the water potential gradient in the leaf tissues. An island population of *A. speciosum* growing in low salinity but with reduced atmospheric moisture maintained water potentials and gas exchange rates consistent with a well-hydrated status, yet the island plants had anatomical traits that would ease the water potential gradient inside the leaf. My findings provide insight into the adaptations shared by halophytic ferns and angiosperms, which may contribute to our understanding of the evolution of salt tolerance.

Introduction

All plants need water to live, grow, and reproduce. The greatest source of water on our planet is seawater, but unfortunately, most plants cannot use this resource. Seawater contains high concentrations of Na^+ and Cl^- (483 mM Na^+ and 558 mM Cl^-; Harvey 1966), which pose obstacles to plant water use. Excess Na^+ and Cl^- ions in the cytosol are toxic to plant cells, impairing essential enzyme functions (Flowers *et al*., 2015). Consequently, plants are faced with an osmotic challenge of extracting a safely dilute solution from high salinity seawater. Plants need to filter the seawater before they can absorb the water into their vascular system, leaving behind most of the Na^+, Cl^-, and other ions. Failure to filter out these ions would rapidly lead to toxic ion concentrations in the cells of the roots, stems, and leaves, and the plants would die.

Despite these apparent challenges, salt-loving plants (halophytes) spend most or all of their life cycles in saline environments. Studies over the last several decades have revealed two primary adaptations that allow halophytes to thrive in saline water (Flowers and Colmer, 2008). 1) Halophytes have greater specificity of ion uptake at the roots, enabling the entry of low-salinity water into the xylem rather than allowing unregulated flow of Na^+ and Cl^- ions into the plant (Scholander 1968; Moon. *et al* 1986; Ball, 1988c; Stuart *et al*., 2007). This greater specificity is facilitated by an effective barrier to apoplastic (unregulated) uptake of water and ions and maintained by selective symplastic pathways (Moon *et al*., 1986). 2) Halophytes lower their cellular osmotic potential to maintain positive turgor pressure and growth even when their total water

potential is relatively low (Scholander *et al*., 1964; Scholander *et al*., 1966). Maintaining a tissue osmotic potential more negative than that of the surrounding estuarine water allows halophytes to generate a water potential gradient that will draw water into the plant, even when the water outside the plant is saline. The plants need a continuous supply of freshwater from the roots to keep their cells turgid (rigid), a state that permits growth and normal cellular function. Most plants use these same physiological processes to cope with soil salinity, but halophytes more successfully implement these traits under saline conditions (Flowers *et al*., 2010). Saline water may even enhance growth in some halophytes (Ball and Pidsley, 1995; Flowers and Colmer, 2008; Nguyen *et al*, 2015).

Halophytism has evolved in approximately 60 plant families (Flowers *et al*., 2010). Most halophytes are angiosperms or algae; there are no halophytic gymnosperms, a few halophytic mosses, and only one known genus of salt-tolerant ferns (Flowers *et al*., 2010). These halophytic ferns (*Acrostichum spp.*) pose interesting questions in the context of the evolution of salt-tolerant plants. Since the ancestors of these ferns are not salt tolerant, *Acrostichum spp*. may have evolved the suite of traits associated with halophytism separately from other halophytes. Although the oldest ferns predate the first angiosperms, most extant fern species (including the family Pteridaceae with the genus *Acrostichum*) have evolved relatively recently in the Cretaceous following the diversification of angiosperms (Schneider *et al*., 2004). This recent appearance of the polypod ferns likely reflects an opportunistic exploitation of the niches created by angiosperm diversity (Schneider *et al*., 2004; Schettpelz and

Pryer, 2009). Other ferns in Pteridaceae have shown adaptations to extremely water-limited environments (Watkins *et al*., 2007; Pittermann *et al*., 2013; Mahley *et al*., 2018). For instance, many Cheilanthoid ferns are desiccation-tolerant "resurrection" ferns, thriving in arid climates like the desert and chaparral ecosystems (Nobel, 1978; Kirkpatrick, 2008; Pittermann *et al*., 2015; Holmlund *et al*., 2016).

Apparently, the mangrove ferns have a similar potential to adapt to a freshwater-limited habitat: the saltwater mangrove swamp. Mangrove swamps are pantropical plant communities that include many halophytes. These ecosystems are especially worthy of study given the ecological and economic importance of the mangrove swamps (Spalding *et al*., 1997; Brander *et al*., 2012). Although the mangrove swamps are dominated by halophytic trees, other plants thrive in the understory, including the mangrove ferns. These ferns often grow adjacent an estuarine water source, slightly elevated on tree roots (Tomlinson, 2016).

Mangrove ferns represent a previously under-studied halophytic system. Several studies have begun to explore the ecological range and physiological adaptations of *Acrostichum spp*. (Medina *et al* 1990; Sharpe, 2010; Werth *et al*., 2015). Furthermore, Medina *et al*. (1990) found a correlation between soil salinity and leaf sap osmotic potential in *A. aureum*, suggesting that halophytic ferns and angiosperms may have similar adaptations, using root ion selectivity and leaf osmotic adjustment to thrive in saline soil. Although the genus *Acrostichum* only includes three widely-recognized species, they are pantropical, thriving in mangrove ecosystems around the

world (Tomlinson, 2016). In some locations, these ferns are even weedy and pose challenges to post-hurricane restoration of the mangrove trees (Sharpe 2010; Tomlinson, 2016). Given that halophytism is so rare in ferns (3 out of c. 12,000 species), in this study I investigate what adaptations allow *Acrostichum spp*. to thrive in the saltwater habitat.

I hypothesized that mangrove ferns have adapted to thrive in saline water with greater ion selectivity at the roots and cellular osmotic adjustment. Given that most halophytic angiosperms share these two key adaptations, it seems likely that halophytic ferns also have evolved these traits at the cellular and whole-plant levels. To characterize these adaptations, I examined native populations of *Acrostichum speciosum* growing along a naturally occurring salinity gradient in the Daintree River system in Queensland, Australia. First, I used cryo-SEM with energy dispersive x-ray analysis (CEDX) to quantify cellular element concentrations in the apoplast and symplast of ferns growing in low versus high estuarine salinity. I predicted that most Na^+ and Cl^- ions would be excluded at the roots, causing low ion concentrations in the apoplast (xylem). I also predicted that ferns growing near high estuarine salinity would have higher cellular salt concentrations than ferns growing near low salinity. This adjustment would decrease the leaf osmotic potential of ferns near saline water, allowing the plants to maintain turgor in spite of decreasing xylem water potentials.

In some respects, tissue dehydration due to high salinity may be similar to dehydration due to evaporative demand. In addition to growing along a salinity

gradient, the mangrove ferns in north Queensland also thrive in areas with dissimilar rainfall. The Daintree River system on the mainland receives 2284 ± 99 mm annual precipitation (mean ± SE, see methods), while nearby Lizard Island receives only 1333 ± 81 mm annually ($p < 0.05$). Since the roots of all mangrove ferns grow in soil soaked by the nearby estuary, this difference in rainfall likely reflects a difference in fresh water available to the leaves, which is known to be a critical water resource for some mangrove tree species (Nguyen *et al*., 2017; Fuenzalida *et al*., 2019). In order to test the effects of estuarine salinity and evaporative demand on *Acrostichum* water relations, I measured physiological and anatomical traits *in situ* along the salinity gradient (mainland, low salinity versus high salinity) and along the evaporative demand gradient (low estuarine salinity, mainland versus island).

Despite some apparent similarities between habitats with high salinity and high evaporative demand, I hypothesized that mangrove ferns will have different physiological adaptations to high estuarine salinity (fresh water limitation at the roots) versus high evaporative demand (fresh water limitation at the leaves). Xylem tensions may only be impacted when water entry is limited at the roots, resulting in a more negative water potential in the high salinity group compared to the high evaporative demand group. Furthermore, I predict that all ferns osmotically adjust their leaves *only as needed* to maintain turgor throughout the day, leading to more negative osmotic potentials in the high salinity group but not the high evaporative demand group. Increased xylem tensions may in turn reduce gas exchange in the high salinity group, as either stomata close to reduce water loss or photosynthetic capacity is impacted by

tissue dehydration. Conversely, ferns experiencing dilute estuarine salinity but high evaporative demand should sustain high rates of gas exchange since water entry into the roots is not limited.

However, I predicted that both freshwater-limited groups (high salinity and high evaporative demand) will have the leaf hydraulic architecture to support improved tissue hydration during high transpiration. Although the high evaporative demand group has abundant water entry into the roots, the increased evaporative demand may create extreme water potential gradients within the leaf unless the plants compensate with adapted leaf architecture. Thus, both freshwater-limited groups would need leaf hydraulic architecture to support increased water supply to the leaves, which would shorten the hydraulic pathway from the xylem to the mesophyll cells and alleviate extreme water potential gradients within the leaf. For instance, higher vein density and smaller, denser stomata would likely improve water supply to the leaf mesophyll cells by shortening the hydraulic pathway (Zwieniecki *et al*., 2004; Sommerville *et al*., 2010; Scoffoni *et al*., 2011). Also, smaller and thicker leaves (which are often associated with denser veins) may provide more space for water storage (Nguyen *et al*., 2017).

Mangrove ecosystems are frequently subject to dynamic conditions, as landscapes evolve and rivers and coastlines change course over time. Consequently, I characterized the physiological plasticity of individual plants by transplanting ferns to a glasshouse and gradually exposing the roots to increasing salinity. I hypothesized that exposure to increasing estuarine salinity in the greenhouse would induce adjustment of

osmotic potential consistent with maintenance of hydration and turgor in fronds, possibly at the cost of slower carbon assimilation and gas exchange.

Methods

Plant material

I obtained plant material from three field sites in northern Queensland, Australia: two along the Daintree River and one on Lizard Island (Fig. S1). The Daintree River system has a natural salinity gradient with a population of *Acrostichum speciosum* ranging from high salinity (3.3% NaCl, 94% seawater) near the mouth of the river to low salinity (0.6% NaCl, 18% seawater) upstream (Fig. 1A). Ferns growing at these mainland sites were compared to ferns on Lizard Island, growing near low salinity water (0.2% NaCl, 6% seawater) (Fig. 1A). Ferns at the mainland sites received approximately twice as much rainfall as the ferns on Lizard Island (Fig. 1B), while ferns at all sites grew in wet soil (> 25% soil water content, Fig. S2). Accordingly, the three sites were classified as low estuarine salinity/high rainfall and high estuarine salinity/high rainfall at the two mainland sites along the Daintree River and low estuarine salinity/low rainfall at the Lizard Island site.

In order to test the extent of physiological plasticity, I tested the ferns' response to increasing estuarine salinity by transplanting eight mature individuals from the low salinity mainland site to a glasshouse at the Australian National University in Canberra, ACT, Australia. These ferns were established hydroponically for six months in a low

salinity solution (0.5% NaCl, 15% seawater) prior to these experiments using a commercial seawater mix (Reef Essential Mixed Macro Probiotic Salt, Quantum USA, Fort Walton Beach, FL, USA). Several nutrients were added to the hydroponic solution, including 5 mM NH_4NO_3, 0.2 mM PO_4^{3-}, and 2 mM Fe-EDTA, as described by Ball and Pidsley (1995). During this experiment, I increased the salinity of the hydroponics solution for half the plants (treatment group, n = 4), while the other half were maintained at a constant low salinity (control group, n = 4). Salinity of the treatment group was increased gradually at a rate of 0.17% NaCl (5% seawater) three times per week until the plants reached 1.7% NaCl (50% seawater). The water relations and gas exchange of all plants were characterized before and after the estuarine salinity was increased for the treatment group, allowing approximately one month for a gradual adjustment to increased salinity.

Environmental conditions

I measured estuarine salinity using a hand-held refractometer (n = 3-6 water samples per site; A.S.T. Co. Ltd., Japan). I assessed soil water content by sampling approximately 10 g of wet soil surrounding the fern roots in the field and measuring the mass before and after 48 hours of drying at 60ºC. Precipitation data for the years 1979-2018 were obtained from the Low Isles Meteorological Station (mainland, Australian Government Bureau of Meteorology) and from Dr. Anne Hoggett (Lizard Island, personal communication). Mainland precipitation data for 1999-2005 were not available.

Cellular elemental concentrations

To determine the cellular elemental concentrations of leaf tissues, I used cryo-scanning electron microscopy (cryo-SEM) with energy-dispersive X-ray microanalysis (CEDX). These methods have been described previously in Stuart *et al*. (2007) and reviewed in McCully *et al*. (2010). Fern fronds were collected at the Daintree site in Queensland, sealed in two plastic bags with wet paper towels, and transported back to Canberra. Ferns from Lizard Island were not included in CEDX analyses. A single healthy, fully expanded pinna from the middle of each frond was frozen using cryo-pliers chilled in liquid N_2 as described by McCully *et al*. (2000). Samples were cryo-planed using a cryo-microtome (Ultramicrotome EM UC7, Leica Microsystems Inc., Buffalo Grove, IL, USA). The prepared samples had a cryo-planed surface of approximately 5-10 mm^2, revealing a cross-section of 2-4 leaf veins. The samples were coated with aluminum prior to analysis (CT1500B LN_2 Cryotrans cold stage and coating unit, Oxford Instruments plc, Abingdon, UK). Plant samples were analyzed using cryo-SEM with CEDX (Hitachi 4300 SE/N Schottky Field Emission, Hitachi, Krefeld, Germany; INCA X-MAX EDXA system, 80mm^2 Silicon Drift Detector (ATW2, 129eV), Oxford Instruments plc, Abingdon, UK). All sample preparation and analyses were conducted at the Centre for Advanced Microscopy (Canberra, Australia).

I used standard calibration curves to convert the signal for each element (Na, Cl, K, Mg, P, S, and Ca) to units of concentration (molarity, Fig. S3). To obtain the calibration curves, I froze single droplets from serial dilutions in liquid ethane, cryo-

planed each droplet, and coated it with aluminum prior to CEDX. For the elements Na and P, a false pile-up peak was detected due to interference from oxygen and aluminum signals, as has been reported previously for Na (Marshall, 2017). I corrected for the false pile-up signal by creating another calibration curve relating the false pile-up Na peak to the oxygen peak. (The oxygen signal was varied by changing the thickness of the aluminum coating on this set of standards.) Once a satisfactory calibration curve was obtained for each element, the linear relationship between element concentration and signal peak in the standard dilutions was used to calculate cellular element concentrations in the leaf tissue samples (Fig. S3). In the final analysis, some negative values for element concentrations were recorded, especially in sample groups with consistently low ion concentrations. Since negative element concentrations are theoretically impossible, I recorded these values as zero. The results presented in this study do not change substantially if these values are omitted from the analyses.

I focused my analyses on seven elements commonly found in seawater and mangrove leaf tissues: Na, Cl, K, Mg, P, S, and Ca. In each leaf sample, I identified four tissue types based on appearance in cryo-SEM: xylem, phloem, bundle sheath cells (BSC), and mesophyll cells. Xylem conduits were evident based on thick cell walls and a lack of cellular contents. In some samples, scalariform pits were visible in the xylem conduit walls. BSC were identified based on their position surrounding the vascular bundle and their uniformly dense cellular contents. Mesophyll cells were identified based on their large size and position outside the vascular bundle. For the purposes of this study, I used the term “phloem” to characterize all living cells inside the vascular

bundle that were not xylem cells; however, cryo-SEM does not allow distinction between different cell types within the phloem tissue, or between phloem and parenchyma. Therefore, the "phloem" cells identified in this study likely include several phloem and parenchyma cell types that could be distinguished in future studies.

Within each leaf sample, I measured n = 2-11 cells per cell type. I used the average values for each cell type for each plant in the analyses. I compared plants growing in high estuarine salinity (n = 4 plants) to plants growing in low estuarine salinity (n = 3 plants) along the Daintree River on the mainland.

Water relations

I used a Scholander-Hammel pressure chamber (model 1050D, PMS Instrument, Albany USA) to measure pre-dawn and midday water potentials (Ψ_{pd} and Ψ_{md}) of the tips (15-20 cm long) of fully expanded, healthy fronds from plants in the field. Frond tips were excised in air, sealed in two plastic bags, and transported immediately to the field station for analysis (n = 7-8 individuals).

Pressure-volume analyses were conducted according to the methods described by Tyree and Hammel (1972) and Bartlett *et al*. (2012). Fern fronds were cut under water and transported back to the laboratory. I rehydrated the fronds for 2-4 hours by placing the cut ends of the stipes in 1% seawater and spraying the leaf tissue with fresh water. After rehydration, I cut the frond tips under water (approximately 15 cm long) and used these tips for the pressure-volume analysis. Key parameters were inferred as

described in Barlett *et al*. (2012) from the relationship between frond mass and water potential as the fronds dried. I determined the osmotic potential at saturation ($\Psi_{\Pi, sat}$) and at the turgor loss point ($\Psi_{\Pi, tlp}$) and also the relative water content at the turgor loss point (RWC_{tlp}) using the linear relationship between $1/\Psi$ and the relative water content (RWC) after the turgor loss point. Capacitance was calculated as $\Delta RWC/\Delta\Psi$ before turgor loss (C_{ft}) and after turgor loss (C_{tlp}). Bulk modulus of elasticity (ε) was calculated as $\Delta\Psi_P/\Delta RWC$ for values less negative than the turgor loss point.

Gas exchange

I used a Li-Cor 6400XT portable gas exchange system (Li-COR Biosciences, Inc, Lincoln, NE, USA) to measure gas exchange parameters in the field, including maximum carbon assimilation (A_{max}), transpiration rates (E), and stomatal conductance to water vapor (g_s). Water use efficiency (WUE) was calculated as CO_2 assimilation rates divided by transpiration rates (mmol CO_2 assimilated mol^{-1} H_2O transpired). All gas exchange measurements were taken with saturating light (1000 μmol m^{-2} s^{-1}) and a reference CO_2 of 400 ppm. Pinnae from the middle of a healthy frond were selected for gas exchange measurements.

Leaf anatomical traits

To further elucidate the effects of variable salinity and atmospheric moisture on hydraulic function, I measured anatomical traits related to water relations in the leaves. LMA was calculated as leaf dry mass per unit fresh leaf area. I measured vein density,

stomatal size and stomatal density by photographing leaf surfaces using a microscope (Axiostar Plus Epifluorescence Microscope, Zeiss, Germany). Stomatal size was calculated as the product of stomatal length and width (Franks and Beerling, 2009). A total of 20 stomata were measured for each plant, taken from three leaf surface sections. Stomatal density was measured by counting the number of stomata present in a 400X view (approximately 0.25 mm^2 area) on the abaxial side of the leaf, with three replicates per plant. No stomata were found on the adaxial surface. I calculated vein density as total vein length divided by leaf area in a leaf surface section approximately 12 mm^2. Three leaf micrographs were measured to obtain average vein density for each individual plant.

Statistics

When I compared three plant groups (e.g., island, low salinity mainland, high salinity mainland), I used a one-way ANOVA with a Tukey's HSD post-hoc test at a significance level of $\alpha = 0.05$. For the CEDX data, I used a two-way ANOVA with estuarine salinity and cell type as fixed effects. I applied a Tukey's HSD post-hoc test to further tease apart the differences among elemental concentrations in different cell types. For the glasshouse experiments, I used a repeated measures ANOVA to test the significance of the interaction between time and treatment at $\alpha = 0.05$. Repeated measures ANOVAs were conducted using JMP Pro vs. 14.2.0, and all other analyses were computed in R vs 3.5.2 (R Core Team, 2018). Plots were created using the ggplot2 package (Wickham, 2016).

Results

Environmental conditions

Environmental conditions varied among the three sites. Estuarine salinity was higher at both mainland sites than the island site, where the salinity was only 0.23 ± 0.03% NaCl (means ± SE, Fig. 1A). However, there was approximately a five-fold difference in estuarine salinity on the mainland at the mouth of the Daintree river (3.31 ± 0.02% NaCl) compared to the low-salinity site upstream (0.58 ± 0.01% NaCl, Fig. 1A). Annual rainfall was significantly lower on the island (1333 ± 81 mm yr^{-1}) than on the mainland (2284 ± 99 mm yr^{-1}, Fig. 1B). Since the soil at each site was quite hydrated (>25% water content, Fig. S2), I interpreted the difference in rainfall as a difference in evaporative demand (i.e., atmospheric moisture available to the ferns).

Cellular elemental concentrations

Estuarine salinity significantly affected cellular concentrations of two elements (Na and Cl), with leaves from the low salinity sites having lower cellular concentrations of Na and Cl (Fig. 2B, C). There were significant effects of cell type on cellular concentrations of five elements (Na, Cl, K, Mg, and P; Fig. 2B-F). The elemental concentrations inside mature xylem conduits were generally lower than those of other cell types. For Na and K, xylem concentrations of each element were lower than those of all other cell types as determined by a Tukey's HSD post-hoc test (Figs. 2B, D). Xylem concentrations of Cl were lower than those in the phloem and mesophyll but

not significantly different from the BSC (Fig. 2C). For Mg, BSC had elevated concentrations compared to xylem and mesophyll cells (Fig. 2E). For P, xylem had significantly lower concentrations than phloem cells, but no other differences were significant (Fig. 2F). There was no significant effect of estuarine salinity or cell type on cellular concentrations of S and Ca (Fig. 2G, H).

Water potential

Frond water potential tracked estuarine salinity among the three sites, with ferns from the island (lowest salinity) having the least negative water potential and ferns from the mainland high salinity site (highest salinity) having the most negative water potential at both pre-dawn and midday (Ψ_{pd} and Ψ_{md}; Fig. 3). Notably, Ψ_{md} approached the osmotic potential at the turgor loss point ($\Psi_{\Pi,tlp}$) at each site, indicating that the ferns may wilt at midday under these conditions (Figs. 3B, 4B).

Pressure-volume analyses

The osmotic potential at saturation ($\Psi_{\Pi,sat}$) and at the turgor loss point ($\Psi_{\Pi,tlp}$) were more negative at the high salinity site (mainland) than either of the low salinity sites (island or mainland) (Fig. 4A, B). Capacitance before and after turgor loss (C_{ft}, C_{tlp}) was also lower at the mainland high salinity site (Fig. 4C, D). The ferns from the mainland high salinity site had a higher bulk modulus of elasticity (Fig. 4E). However, the relative water content at the turgor loss point (RWC_{tlp}) was not statistically different among the three sites (Fig. 4F).

Gas exchange

Ferns growing near high estuarine salinity had lower rates of gas exchange compared to ferns at either low salinity site (island or mainland), including lower maximum CO_2 assimilation rates (A_{max}), transpiration rates (E), and stomatal conductance to water vapor (g_s) (Fig. 5A-C). The lower annual rainfall received on the island (Fig. 1B) appeared to have no significant effect on gas exchange rates compared to the low salinity site on the mainland. Water use efficiency (WUE) was not significantly different among sites (Fig. 5D).

Leaf anatomical traits

Anatomical traits were similar among fronds of ferns grown at sites characterized by either high estuarine salinity/high rainfall on the mainland or low estuarine salinity/low rainfall on Lizard Island (Fig. 6). Fronds of these two groups had significantly higher LMA, higher vein density, and smaller and more densely packed stomata than fronds of ferns grown at the low salinity/high rainfall site on the mainland (Fig. 6A-D).

Glasshouse experiments

Plants exposed to increasing estuarine salinity in the glasshouse had no significant physiological differences compared to the low salinity control plants (Figs. 7-8). A few parameters from the pressure-volume analyses revealed slight trends consistent with differences between high and low salinity plants under field conditions

(Figs. 7C, E), but these trends were not significant at $\alpha = 0.05$. No significant differences were seen in gas exchange characteristics between the treatment and control groups (Fig. 8).

Discussion

This study revealed that mangrove ferns thrive in saline habitats by sharing some of the adaptations common to many halophytic angiosperms, including greater specificity of ion uptake at roots and osmotic adjustment to maintain cell turgor. These adaptations were manifested at both the cellular level and the whole-plant level. Coordination of cellular and whole-plant responses to salinity is a key element of halophytism that enables maintenance of favorable balances between carbon gain, water loss, and ion uptake (Ball, 1988a; Ball, 1996; Flowers *et al*., 2010).

Elemental concentrations of Na, Cl, K, Mg, and P in mature xylem conduits were consistently lower than those in some living cells, likely indicating effective selectivity of ion uptake at the roots. These findings are compatible with the mass balance problem associated with transporting large quantities of salt through the xylem, especially considering that mangrove ferns have no mechanism for secreting salt from the leaves (Ball, 1988c). Greater selectivity of ion uptake may help mangrove ferns thrive in saline water by preventing ions from accumulating and reaching toxic concentrations in living cells (Flowers *et al*., 2010). Several previous studies have also found dilute salt concentration in the xylem sap of mangrove trees (Ball, 1988c; Stuart *et al*., 2007). However, analyses of cellular element concentrations using CEDX

revealed greater cellular concentrations of Na and Cl in leaf cells from the high salinity site, perhaps indicating that mangrove ferns accumulate more ions in their living cells as needed to adapt to high estuarine salinity. Presumably, excess Na^+ and Cl^- ions would be stored in the vacuole of most cells to prevent interference with enzyme function (Flowers *et al*., 2010; Flowers *et al*., 2015). As phloem sieve cells do not have a vacuole, the high concentrations of Na and Cl reported here for the phloem likely reflect the pooling of analyses made on other types of phloem cells, which may vary in function and cellular composition. Further analyses with cryo-transmission electron microscopy (cryo-TEM) are needed to distinguish between distinct cell types within the phloem tissue in these ferns.

The CEDX results (at the cellular level) may provide insight into other adaptations at the whole-plant level. The pressure-volume analyses tested for osmotic adjustment across leaf tissues. My results show that plants growing in high estuarine salinity adjusted the osmotic potential at saturation and turgor loss, perhaps to cope with greater xylem tensions induced by increased estuarine salinity. Adjusting the osmotic potential below the midday leaf water potential would allow the leaves to maintain turgor needed for growth and stomatal opening (Bartlett *et al*., 2012). Increased cellular concentrations of Na and Cl in the leaf tissues may have contributed to this osmotic adjustment, which can be achieved by enhanced concentrations of ions in the vacuole and compatible solutes in the cytosol (Flowers *et al*., 2010). Notably, the relative water content at the turgor loss point (RWC_{tlp}) did not change with increasing salinity. It seems likely that the plants also adjusted other components of tissue-water

relations (particularly the bulk modulus of elasticity, ε) to maintain RWC_{tlp} above a critical hydration threshold (Bartlett *et al*., 2012).

Although adjustment of leaf osmotic potential enables maintenance of the turgor and hydration required to thrive in high salinity, exploitation of this niche by the mangrove ferns may come at a cost of productivity. In my study, the ferns growing in high estuarine salinity had lower rates of gas exchange, including the maximum rate of carbon assimilation (A_{max}). Greater selectivity of ion uptake at the roots may slow water uptake, reducing the supply of water to the shoot and hence also reducing overall gas exchange rates (Ball, 1988c). In this study, I measured gas exchange during the dry season at both sites (arrows in Fig. 1B) at the presumed peak performance between 0900 and 1100. However, it is possible that plants growing in high estuarine salinity experience a burst of photosynthetic activity early in the morning, which compensates for negligible carbon assimilation later in the day. Future studies may further characterize the nature and causes of photosynthetic limitations associated with ferns growing in high estuarine salinity.

I combined these instantaneous measures of gas exchange with leaf anatomical traits, reflecting a more integrated picture of the ferns' response to estuarine salinity. High salinity plants had thicker leaves, higher vein density, and smaller and more densely packed stomata compared to low salinity plants. In terms of gas exchange, these anatomical traits may seem surprising given that the high salinity plants had four-fold lower rates of CO_2 assimilation and transpiration, whereas high stomatal and vein

densities could possibly facilitate higher gas exchange rates (Boyce *et al*., 2009; Franks *et al*., 2009; McElwain *et al*., 2016). However, these traits may still be consistent with adaptation to the demands of a high salinity environment, which slows water supply through the roots. For instance, increased vein density facilitates efficient water transport to the leaf tissues, keeping the leaves hydrated with minimal decrease in total leaf water potential during peak daily transpiration and alleviating tissue damage due to extreme water potential gradients (Sack and Frole, 2006; Sommerville *et al*., 2012). Increased stomatal density would improve CO_2 uptake, improving water use efficiency at a given rate of water loss (Franks and Beerling, 2009). Also, smaller leaf area in halophytic plants contributes to minimizing increase in leaf temperature relative to air temperature with minimal evaporative cooling during periods of high insolation, thus improving water use efficiency by minimizing water loss (Ball *et al*., 1988b; Ball, 1988c).

Although small leaf size tends to correlate with denser veins and stomata (Sack *et al.,* 2012), these anatomical adjustments in high salinity plants may be adaptive to prevent excessive tension on the water column due to the slow supply of water through the selective roots (Ball, 1996). Thus, even though higher stomatal and vein density may not slow gas exchange rates directly, these traits may improve plant hydration and water use within the plant, maximizing tissue hydration and carbon gain. Furthermore, as estuarine salinity varies with the tide and season, it is possible that this increased capacity for leaf hydraulic conductance may allow the high salinity plants to capitalize on periods of low salinity with a burst of high photosynthetic activity.

How does high evaporative demand from the leaves impact *Acrostichum* water relations compared to freshwater limitation at the roots? The island plants maintained high rates of gas exchange yet showed similar anatomical traits to the high salinity plants on the mainland. The island ferns may have adapted these leaf anatomical traits that minimize leaf tissue dehydration in order to cope with lower atmospheric moisture on Lizard Island. This finding provides support for the hypothesis that slower gas exchange in high salinity plants is driven by limitations of water supply from the roots, rather than leaf anatomical traits. Perhaps a key adaptation is improved stomatal control, as previous studies have shown that smaller stomata can open and close more rapidly than large stomata (Drake *et al*., 2013; but see Raven, 2014). In that case, smaller stomata may afford the high salinity plants and the low rainfall (island) plants improved control of gas exchange rates, in case the environmental conditions should necessitate water conservation.

The mangrove swamp is a dynamic ecosystem, with changes occurring over short and long time scales. To determine how mangrove ferns adjust to increasing estuarine salinity over time, I exposed ferns in a glasshouse to gradually increasing estuarine salinity over the course of one month. Although the glasshouse ferns had no significant changes in osmotic adjustment or gas exchange rates, the capacitance before turgor loss and the bulk modulus of elasticity had trends consistent with the acclimation seen under field conditions. It is possible that mangrove ferns would exhibit physiological adaptations over a longer time scale or with the growth of new leaves. Previous studies on mangrove trees have used mangrove propagules to test for

responses to salinity (Ball, 1988c; Nguyen *et al.,* 2015); similar studies on ferns may require a multi-year study due to slower growth rates and the physiological shock of transplanting. Further experiments over longer time scales are needed to determine the extent to which physiological plasticity and genetic adaptations play a role in the differences between plants growing in low and high salinity (or island versus mainland). A reciprocal transplant experiment would be appropriate in this case, but field-intensive transplant experiments are rare in regions inhabited by large reptiles.

My results are consistent with a previous report of elevated Na and Mg in leaf cell sap of *A. aureum* growing in high soil salinity (Medina *et al*., 1990). An advantage of CEDX technology is the ability to distinguish element concentrations among cell types. Consequently, my findings expand our understanding of salt in *Acrostichum* leaves because now we know that the xylem salt concentrations may be relatively low while salt accumulates in most living cells. This result is also consistent with the results of Werth *et al*. (2015), which found increasing Na concentration with leaf age in *A. danaeifolium*, implying that salt concentrations in the leaves may accumulate as salts are gradually transported via the xylem.

Why are there so few species of halophytic ferns compared to the biodiversity of halophytic angiosperms? Approximately 0.25% of angiosperms are known halophytes (Flowers *et al*., 2010), whereas ferns show an even lower rate of halophytism, with approximately 3 species in a single genus out of 12,000 known fern species (0.025%; PPG I, 2016). Previous studies have suggested that the salt tolerance

of the independent gametophyte may prove a substantial obstacle to the establishment of halophytic ferns (Medina *et al*., 1990). Studies have found that the gametophytes showed a degree of salt tolerance but grew best in fresh water or low estuarine salinity (Lloyd and Buckley, 1986; Xiao-Ping and Bee-Lian, 1998), consistent with patterns of *A. speciosum* recruitment in this study (H. Holmlund, personal observation). Previous studies have hypothesized that selection must act on both the sporophyte and gametophyte generations (Pittermann *et al*., 2013).

Although halophytism may be a rare trait in ferns, adaptations to cope with limited fresh water are slightly more common. In particular, the family Pteridaceae (which includes the genus *Acrostichum*) has remarkable ecological and morphological diversity, including many ferns which have adapted to arid habitats (Schuettpelz *et al*., 2007; Mahley *et al*., 2018). As the Pteridaceae have evolved "in the shadow of angiosperms" (Schneider *et al*., 2004), it seems that *Acrostichum spp.* may be well adapted to fill the understory saltwater niche created by the mangrove trees. Future studies might further characterize the limits and mechanistic basis for the adaptations that allow *Acrostichum spp.* to thrive in the mangrove swamp.

Table 1: Abbreviations used throughout this chapter.

Parameter	Units	Meaning
Elemental analyses		
CEDX		cryo-SEM with energy dispersive x-ray analysis
x		xylem
p		phloem
b, BSC		bundle sheath cell
m		mesophyll
Na	mM	sodium
Cl	mM	chlorine
K	mM	potassium
Mg	mM	magnesium
P	mM	phosphorus
Ca	mM	calcium
S	mM	sulfur
Water relations		
Ψ_{pd}	MPa	pre-dawn frond water potential
Ψ_{md}	MPa	midday frond water potential
$\Psi_{\Pi, sat}$	MPa	osmotic potential at saturation
$\Psi_{\Pi, tlp}$	MPa	osmotic potential at the turgor loss point
C_{ft}	g MPa^{-1}	capacitance before turgor loss
C_{tlp}	g MPa^{-1}	capacitance after turgor loss
ε	MPa	bulk modulus of elasticity
RWC_{tlp}	%	relative water content at the turgor loss point
Gas exchange		
A_{max}	μmol CO_2 $m^{-2}s^{-1}$	maximum carbon assimilation
E	mmol H_2O $m^{-2}s^{-1}$	evapotranspiration
g_s	mol $m^{-2}s^{-1}$	stomatal conductance to water vapor
WUE	mmol CO_2 mol^{-1} H_2O	water use efficiency, A/E
Anatomical traits		
LMA	g m^{-2}	leaf mass per unit area
VD	mm mm^{-2}	leaf vein density
SS	mm^2	stomatal size (length x width)
SD	mm^{-2}	stomatal density

Figure 1: Environmental conditions at the three study sites, one at Lizard Island (Island) and two along the Daintree River (Mainland). Boxplots represent estuarine salinity, n = 3-6 samples per site (Panel A). Data in Panel B are monthly rainfall (mean ± SE), n = 39 years (island) and 32 years (mainland) from 1979-2018. In this study, annual rainfall was used as a surrogate for evaporative demand, since ferns at all sites grew in wet soil near a river. Arrows in Panel B indicate the month in which I conducted field experiments for mainland (gray) and island (white) plants. Annual rainfall was significantly different between the two sites at $\alpha = 0.05$. Data were analyzed using a one-way ANOVA with a Tukey's HSD post-hoc test (Panel A) or a Student's t test (comparing annual rainfall, Panel B) at a significance level of $\alpha = 0.05$. Different letters indicate differences among groups.

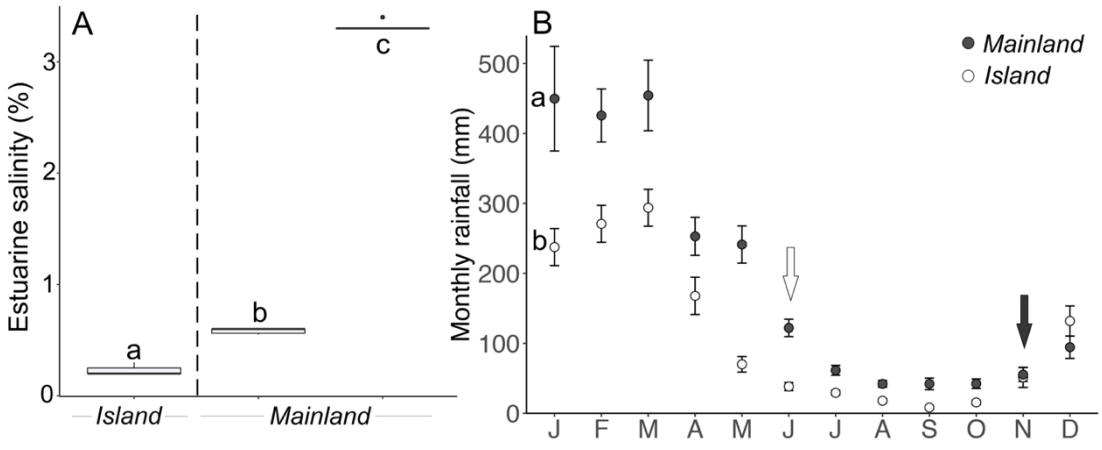

Figure 2: Elemental composition as determined by CEDX of selected cell types within different leaf tissues in *A. speciosum* grown naturally at high and low salinity sites along the Daintree River (n = 4 high salinity plants, 3 low salinity plants). Panel A: Cryo-preserved vein as visualized by cryo-SEM to identify tissue types for CEDX analysis. Tissue types were identified as xylem conduits (x), phloem (p), bundle sheath cells (b, BSC), and mesophyll (m). Cryo-SEM did not allow us to distinguish cell types among the phloem tissue, so the cells identified as "phloem" likely include several types of phloem and parenchyma cells. Bar indicates 25 μm. Panels B-H: Box plots displaying cellular concentrations, respectively, of Na, Cl, K, Mg, P, Ca, and S in four cell types (x, p, b, and m) in leaves of plants grown at low (grey) and high (black) salinity. Estuarine salinity had a significant effect on cellular concentrations of Na and Cl ($p < 0.05$). Cell type had a significant effect on cellular concentrations of Na, Cl, K, Mg, and P ($p < 0.05$). Data were analyzed using a two-way ANOVA on the average values for each cell type (n = 2-11 cells per cell type per plant), with estuarine salinity and cell type as fixed effects. A Tukey's HSD post-hoc test was applied to discern differences among cell type (different letters represent differences among cell types, $p < 0.05$).

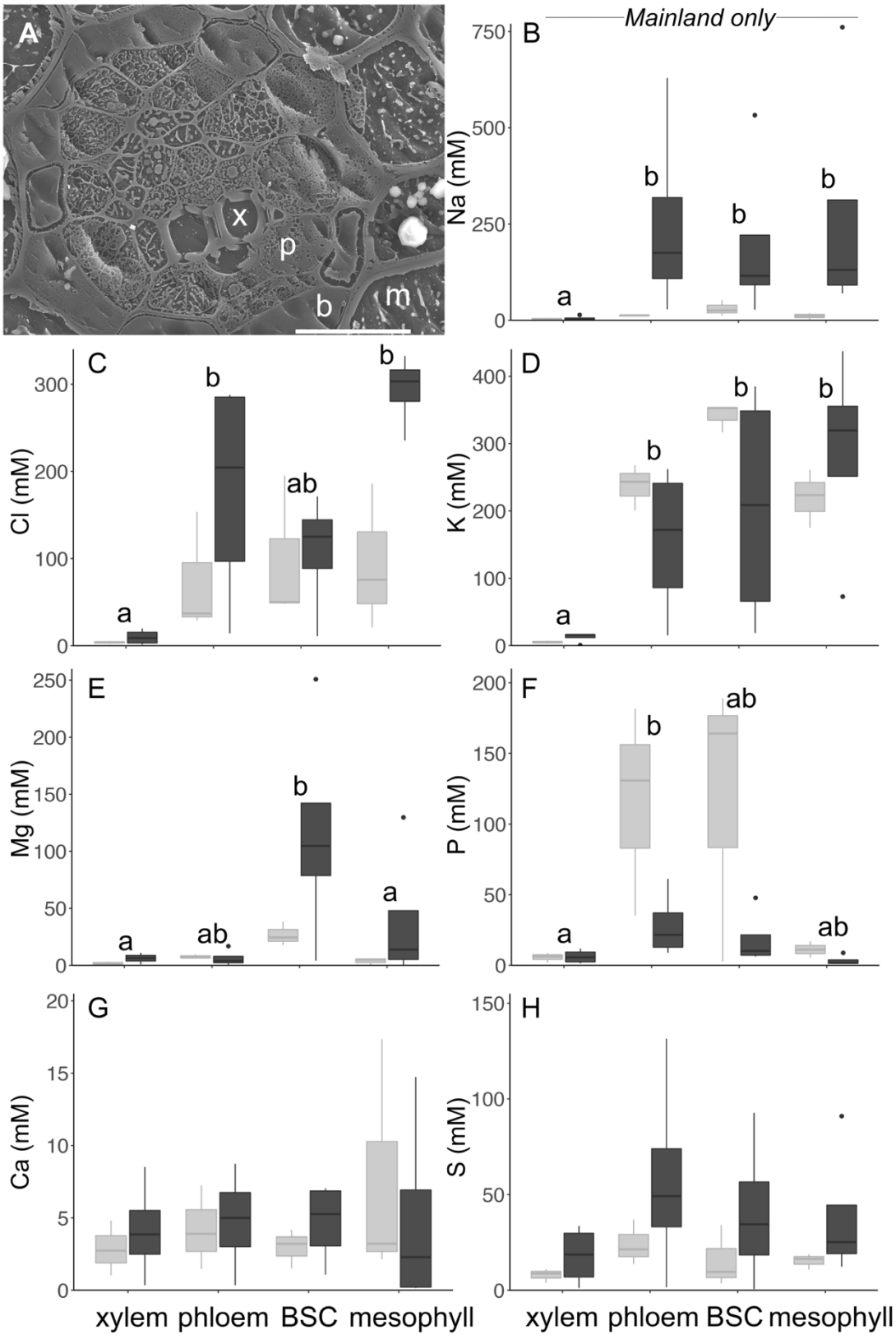
A
x
p
b
m
B
Mainland only
Na (mM)
750
500
250
0
a
b
b
b
C
Cl (mM)
300
200
100
0
a
b
ab
b
D
K (mM)
400
300
200
100
0
a
b
b
b
E
Mg (mM)
250
200
150
100
50
0
a
ab
b
a
F
P (mM)
200
150
100
50
0
a
b
ab
ab
G
Ca (mM)
20
15
10
5
0
H
S (mM)
150
100
50
0
xylem
phloem
BSC
mesophyll
xylem
phloem
BSC
mesophyll

Figure 3: Frond water potential at pre-dawn (Panel A) and midday (Panel B) under the field conditions shown in Fig. 1 (n = 7-8 plants per group). Horizontal dashed lines in panel B indicate the mean osmotic potential at the turgor loss point at each site. Differences were determined using a one-way ANOVA with a Tukey's HSD post-hoc test (letters indicate significant differences, $p < 0.05$).

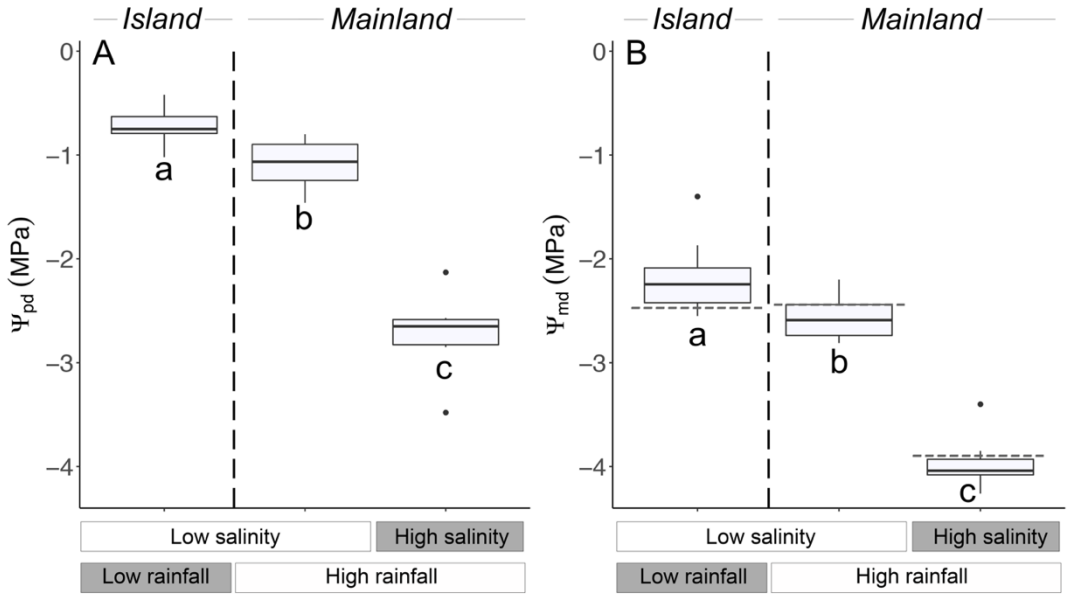

Figure 4: Pressure-volume analyses from plants growing *in situ* under the field conditions shown in Fig. 1 (n = 6-8 plants per group), including the osmotic potential at saturation ($\Psi_{\Pi, sat}$, Panel A), the osmotic potential at the turgor loss point ($\Psi_{\Pi, tlp}$, Panel B), capacitance before turgor loss (C_{ft}, Panel C), capacitance after turgor loss (C_{tlp}, Panel D), bulk modulus of elasticity (ε, Panel E), and the relative water content at the turgor loss point (RWC_{tlp}, Panel F). Differences were determined using a one-way ANOVA with a Tukey's HSD post-hoc test (letters indicate significant difference, $p < 0.05$).

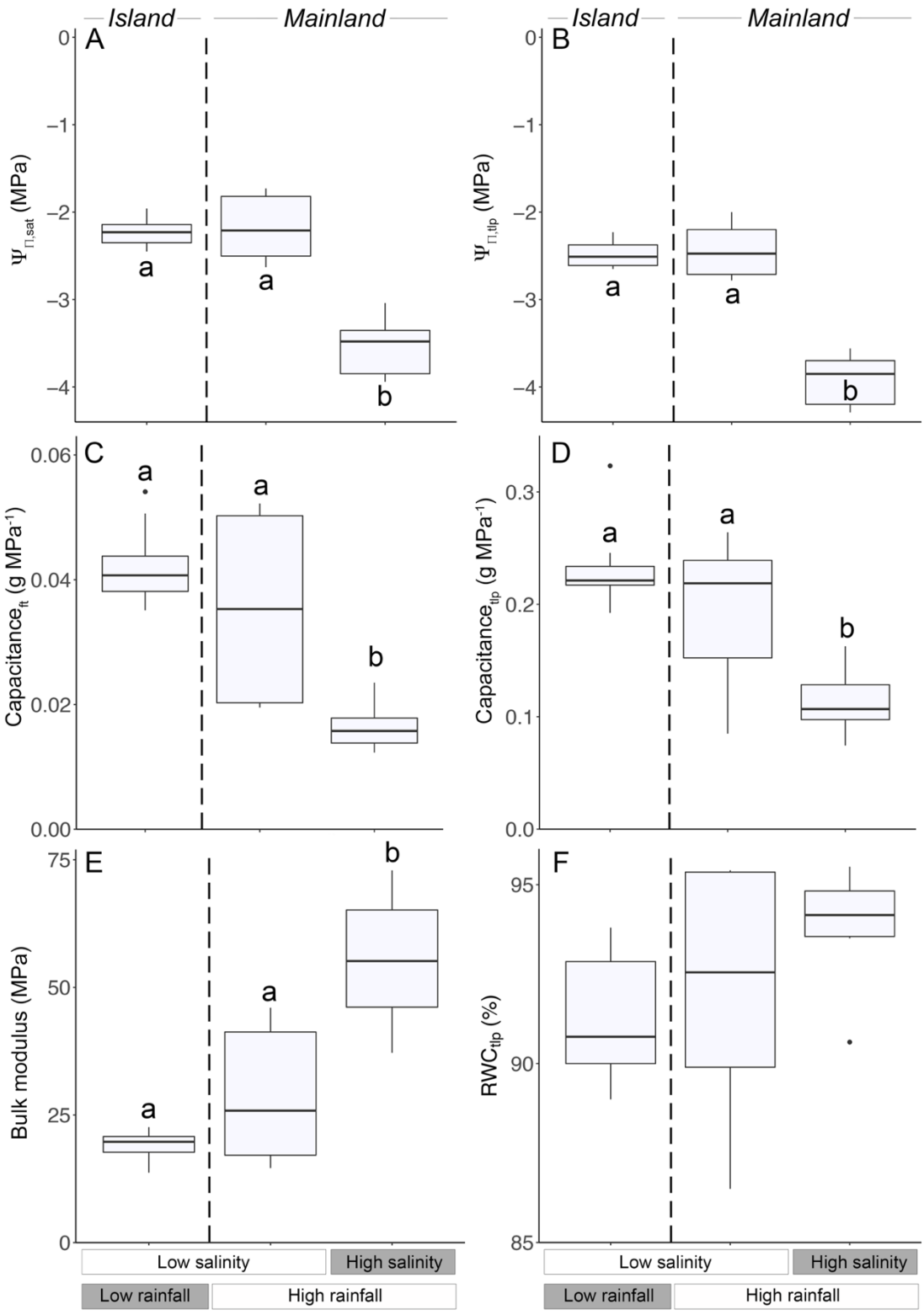
Island
Mainland
A
B
C
D
E
F
$\Psi_{\Pi,sat}$ (MPa)
$\Psi_{\Pi,tlp}$ (MPa)
Capacitance$_{ft}$ (g MPa^{-1})
Capacitance$_{tlp}$ (g MPa^{-1})
Bulk modulus (MPa)
RWC$_{tlp}$ (%)
0
−1
−2
−3
−4
0.06
0.04
0.02
0.00
0.3
0.2
0.1
0.0
75
50
25
0
95
90
85
a
b
Low salinity
High salinity
Low rainfall
High rainfall

Figure 5: Gas exchange characteristics measured *in situ* on intact, attached fronds of plants growing under the environmental conditions described in Fig. 1 (n = 6-8 plants per group), including maximum carbon assimilation rate (A_{max}, Panel A), transpiration (E, Panel B), stomatal conductance to water vapor (g_s, Panel C), water use efficiency (WUE, Panel D), leaf internal CO_2 (C_i, Panel E), and vapor pressure deficit based on leaf temperature (VPD_L, Panel F). WUE was calculated as CO_2 assimilation rates divided by transpiration rates (mmol CO_2 assimilated mol^{-1} H_2O transpired). Data were analyzed using a one-way ANOVA with a Tukey's HSD post-hoc test (letters indicate significant difference, $p < 0.05$).

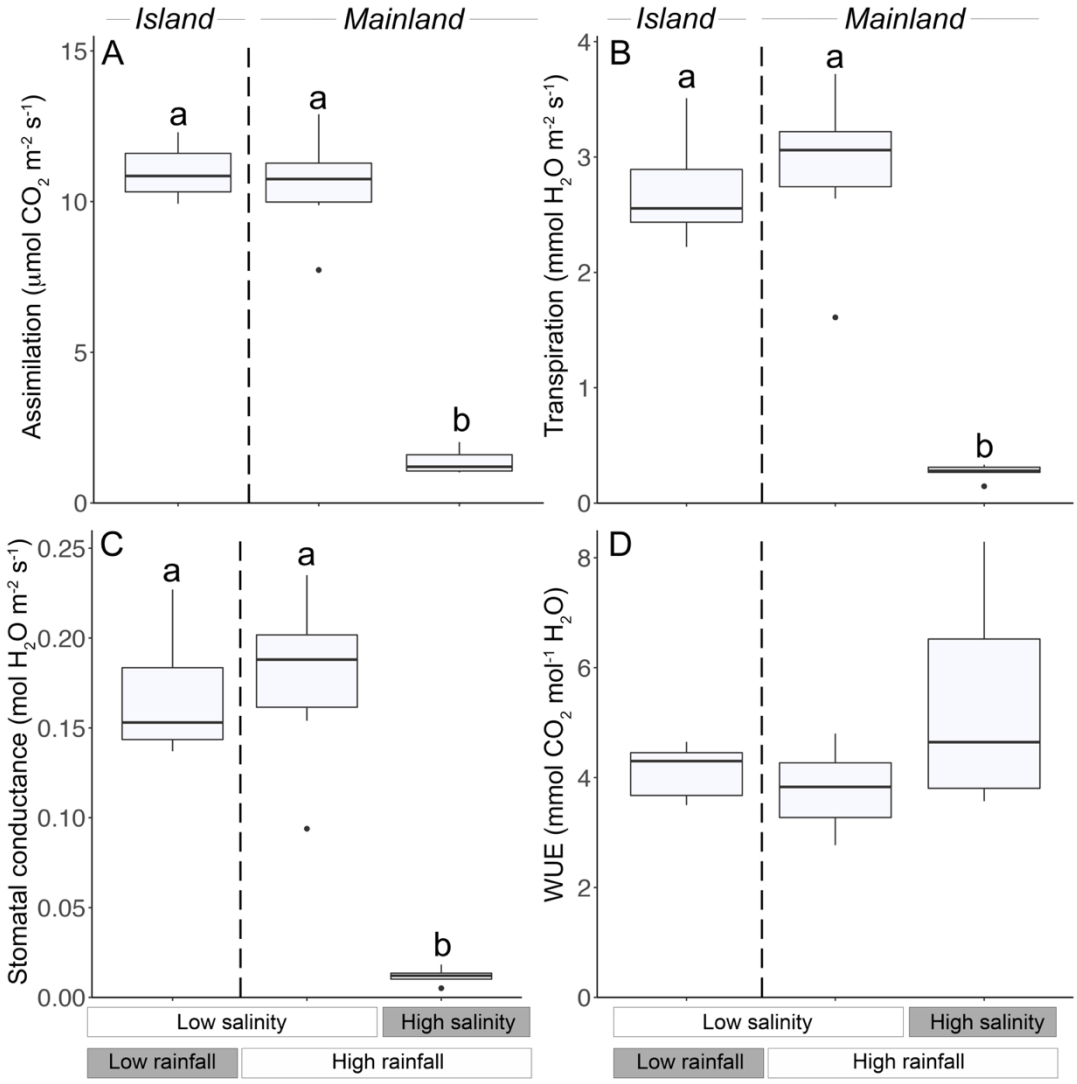
Island
Mainland
A
B
C
D
a
b
Assimilation (µmol CO2 m-2 s-1)
Transpiration (mmol H2O m-2 s-1)
Stomatal conductance (mol H2O m-2 s-1)
WUE (mmol CO2 mol-1 H2O)
Low salinity
High salinity
Low rainfall
High rainfall

Figure 6: Leaf anatomical traits from plants growing *in situ* under the environmental conditions described in Fig. 1 (n = 8 plants per group), including leaf mass per unit area (LMA, Panel A), leaf vein density (Panel B), leaf stomatal size (Panel C), and leaf stomatal density (Panel D). All traits were measured on a single pinna taken from the middle of a mature frond. Stomatal size was calculated as the product of stomatal length and width. Differences were determined using a one-way ANOVA with a Tukey's HSD post-hoc test (letters indicate significant difference, $p < 0.05$).

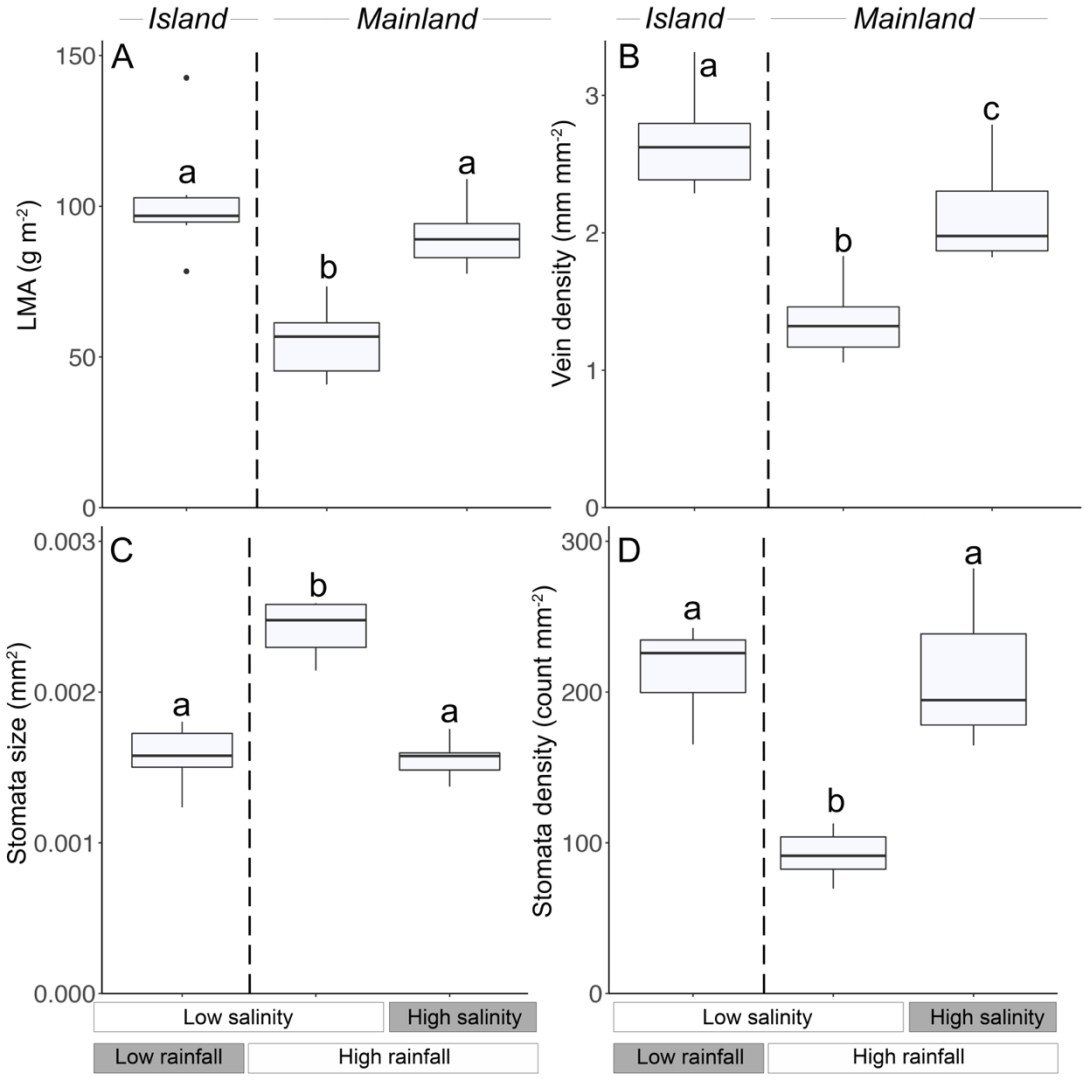
Island
Mainland
A
LMA (g m-2)
150
100
50
0
a
b
a
B
Vein density (mm mm-2)
3
2
1
0
a
b
c
C
Stomata size (mm2)
0.003
0.002
0.001
0.000
a
b
a
D
Stomata density (count mm-2)
300
200
100
0
a
b
a
Low salinity
High salinity
Low rainfall
High rainfall

Figure 7: Pressure-volume analyses from plants growing in the glasshouse in low salinity (0.5% seawater) or high salinity (50% seawater), including the osmotic potential at saturation ($\Psi_{\Pi, sat}$, Panel A), the osmotic potential at the turgor loss point ($\Psi_{\Pi, tlp}$, Panel B), capacitance before turgor loss (C_{ft}, Panel C), capacitance after turgor loss (C_{tlp}, Panel D), bulk modulus of elasticity (ε, Panel E), and the relative water content at the turgor loss point (RWC_{tlp}, Panel F). All plants were grown for six months in low salinity (0.5% seawater). Once established, plants were either gradually transitioned from low to high salinity (treatment group, gray boxes) or maintained in 0.5% seawater (control group, white boxes). All plants were measured before and after this treatment was applied (pre and post). Data were analyzed using a repeated measures ANOVA. There were no significant effects of time or of the interaction between time and treatment at a significance level of $\alpha = 0.05$. n = 4 control plants (low salinity) and 4 treatment plants (low to high salinity).

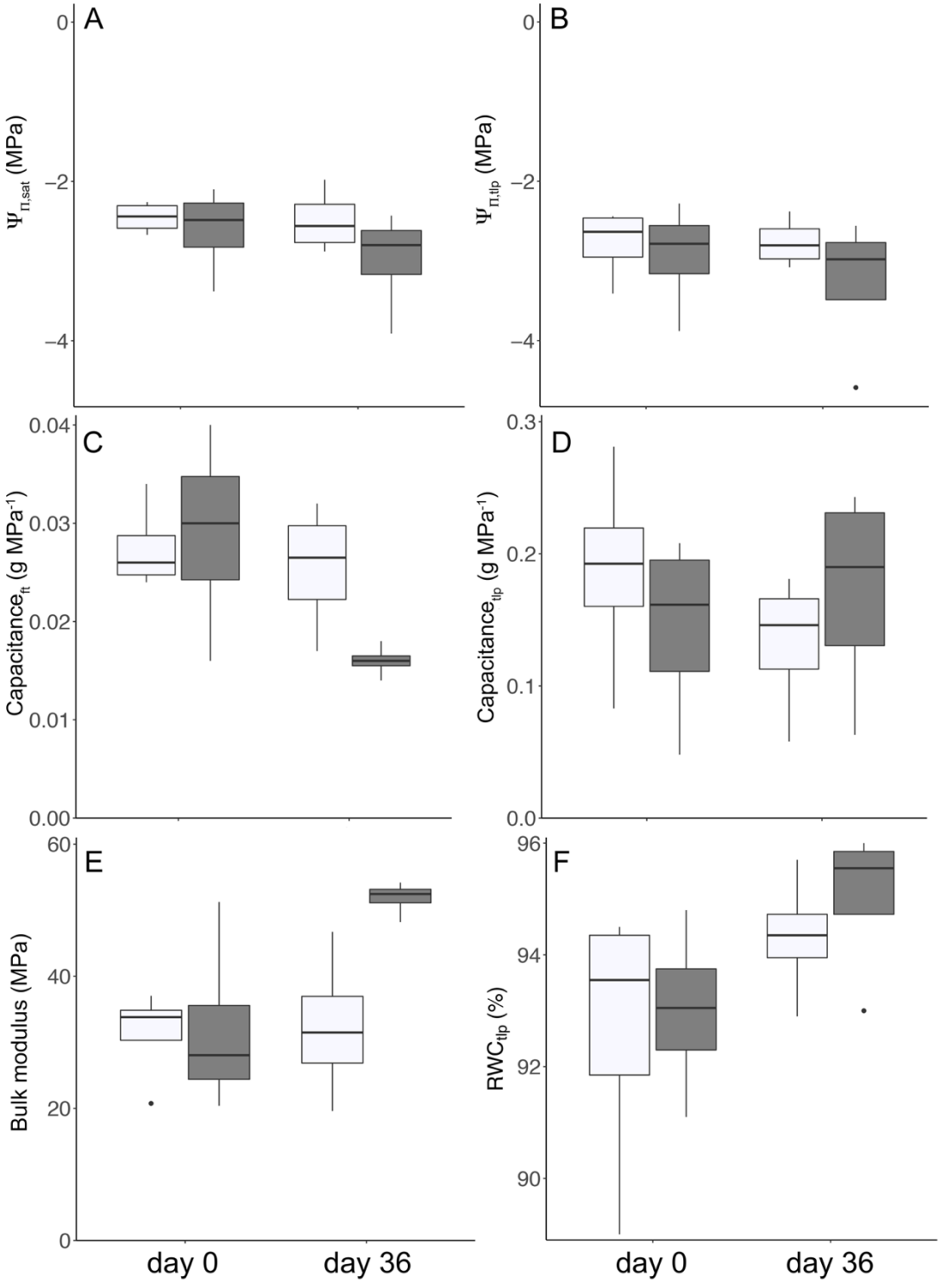
A
B
C
D
E
F
$\Psi_{\pi,sat}$ (MPa)
$\Psi_{\pi,tlp}$ (MPa)
Capacitance$_{ft}$ (g MPa^{-1})
Capacitance$_{tlp}$ (g MPa^{-1})
Bulk modulus (MPa)
RWC$_{tlp}$ (%)
0
−2
−4
0.04
0.03
0.02
0.01
0.00
0.3
0.2
0.1
0.0
60
40
20
0
96
94
92
90
day 0
day 36

Figure 8: Gas exchange characteristics from plants growing in the glasshouse in low salinity (0.5% seawater) or high salinity (50% seawater), including maximum carbon assimilation rate (A_{max}, Panel A), transpiration (E, Panel B), stomatal conductance to water vapor (g_s, Panel C), and water use efficiency (WUE, Panel D). WUE was calculated as CO_2 assimilation rates divided by transpiration rates (mmol CO_2 assimilated mol^{-1} H_2O transpired). All plants were grown for six months in low salinity (0.5% seawater). Once established, plants were either gradually transitioned from low to high salinity (treatment group, gray boxes) or maintained in 0.5% seawater (control group, white boxes). All plants were measured before and after this treatment was applied. Data were analyzed using a repeated measures ANOVA. There were no significant effects of time or of the interaction between time and treatment at a significance level of $\alpha = 0.05$. n = 4 control plants (low salinity) and 4 treatment plants (low to high salinity).

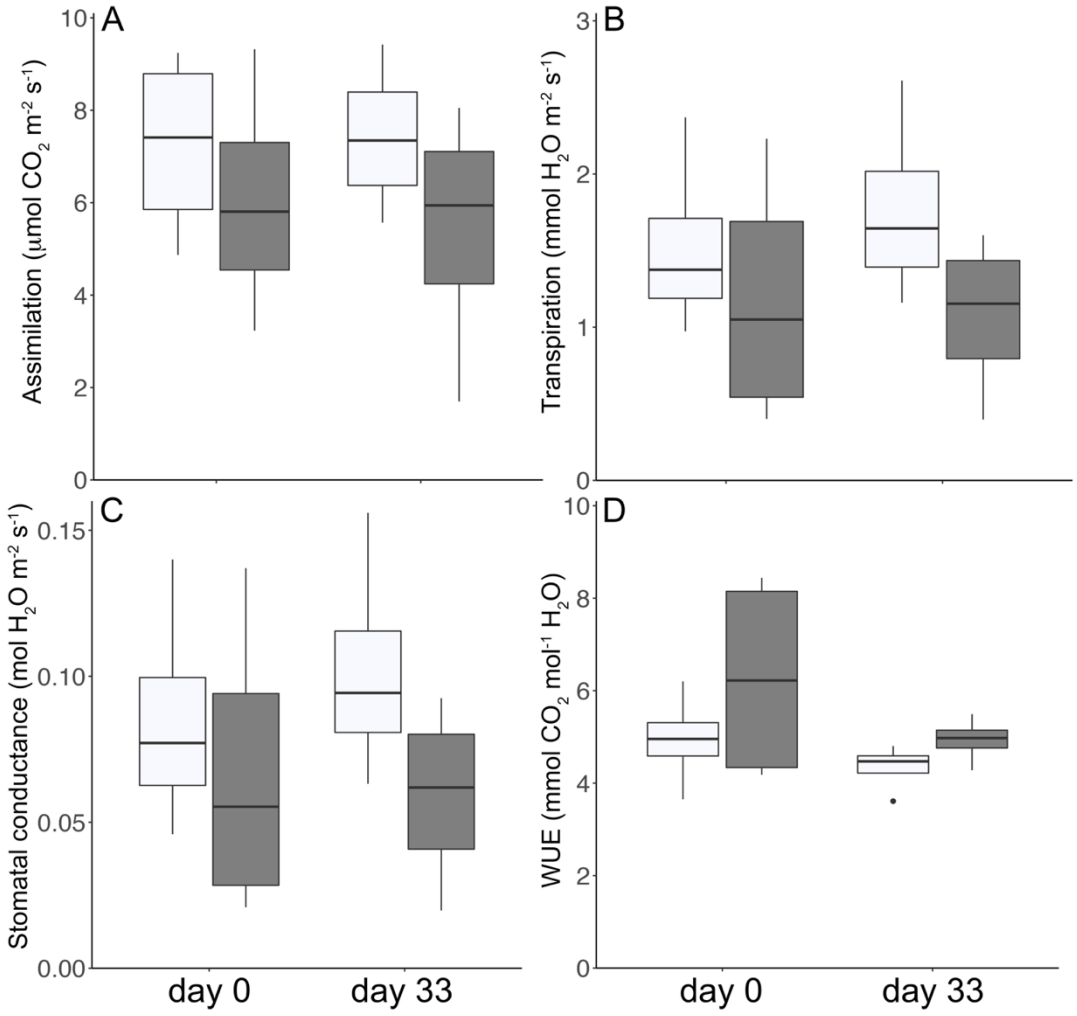
A
B
C
D
Assimilation (μmol CO_2 m^{-2} s^{-1})
Transpiration (mmol H_2O m^{-2} s^{-1})
Stomatal conductance (mol H_2O m^{-2} s^{-1})
WUE (mmol CO_2 mol^{-1} H_2O)
0
2
4
6
8
10
1
3
0.00
0.05
0.10
0.15
day 0
day 33

Chapter 2

Positive root pressure is critical for whole-plant desiccation recovery in two species of terrestrial resurrection ferns

Abstract

Desiccation-tolerant (DT) organisms can lose nearly all their water without dying. Desiccation tolerance allows organisms to survive in a nearly completely dehydrated, dormant state. At the cellular level, sugars and proteins stabilize cellular components and protect them from oxidative damage. However, there are few studies of the dynamics and drivers of whole-plant recovery in vascular DT plants. In vascular DT plants, whole-plant desiccation recovery (resurrection) depends not only on cellular rehydration, but also on the recovery of organs with unequal access to water. In this study, *in situ* natural and artificial irrigation experiments revealed the dynamics of desiccation recovery in two DT fern species. Organ-specific irrigation experiments revealed that the entire plant resurrected when water was supplied to roots, but leaf hydration alone (foliar water uptake) was insufficient to rehydrate the stele and roots. In both species, pressure applied to petioles of excised desiccated fronds resurrected distal leaf tissue, while capillarity alone was insufficient to resurrect distal pinnules. Upon rehydration, sucrose levels in the rhizome and stele dropped dramatically as starch levels rose, consistent with the role of accumulated sucrose as a desiccation protectant. These findings provide insight into traits that facilitate desiccation recovery in dryland ferns associated with chaparral vegetation of southern California.

Introduction

Desiccation tolerance (DT) describes an organism's ability to dry to equilibrium with the air and then recover metabolic activity upon rehydration. Functionally, this means that DT organisms can tolerate the loss of most of their water (10% water content or -100 MPa; Alpert, 2005). The evolution of DT likely allowed early plants to colonize land before stomata and a vascular system regulated water loss (Gaff and Oliver, 2013). Desiccation tolerance protects most bryophytes from frequent dry periods (reviewed in Proctor *et al*., 2007). Almost all vascular plants have retained DT in the seed or spore stage, but a few ferns and angiosperms have re-evolved DT in their leaves, stems, or roots (Oliver *et al*., 2000; Gaff and Oliver, 2013; VanBuren *et al*., 2017). Plants that express DT in these vegetative tissues are colloquially referred to as resurrection plants. Vascular resurrection plants thrive in seasonally dry regions where desiccation-sensitive plants have lower survival rates and fitness, and they are most common on sandy slopes and rocky outcrops (Gaff, 1977; Gaff, 1987; Porembski and Barthlott, 2000; Alcantara *et al*., 2015).

Cellular recovery from near-complete dehydration is complex and requires the coordination of physical and chemical processes. The desiccated state presents at least three challenges at the cellular level: photo-oxidative stress caused by reactive oxygen species, the metabolic requirements of resurrection, and the mechanical stress of cell and tissue deformation (Farrant *et al*., 2007). While desiccated, the cellular components are usually stabilized by protective sugars and proteins, forming a "glassy" state

(Moore *et al*., 2007; Peters *et al*., 2007). This glassy state reduces the damage caused by reactive oxygen species, and the sugars may also provide energy to fuel metabolic processes during rehydration (Scott, 2000). Mechanical stress is alleviated by tissue structures that facilitate cell folding and prevent extensive tissue damage (Moore *et al*., 2007).

Most DT organisms are relatively small and composed of only one or a few cell layers (e.g., algae, lichens, bryophytes, fern gametophytes), making rehydration a relatively simple process. When water first contacts these desiccated tissues, it easily spreads on the surface or through adjoining cells (Proctor, 2000; Proctor *et al*., 2007). However, vascular DT plants such as ferns and angiosperms face the added challenge of resurrecting distinct tissues and organs with unequal access to water, adding another layer of complexity to whole-plant recovery. For instance, the roots of a desiccated vascular plant have a reliable water source after rain (wet soil) for days or weeks, but the leaf surfaces may be subject to ephemeral wetting and high atmospheric water demand, likely drying within a day following a rainfall event. Although previous studies have tried to elucidate the mechanism of whole-plant recovery in a DT angiosperm, *Myrothamnus flabellifolius* (Sherwin *et al*., 1998; Schneider *et al*., 2000), these studies found contradicting results regarding the role of root pressure in whole-plant recovery of this species. Furthermore, this question remains untested in DT ferns. Ferns and angiosperms have contrasting hydraulic anatomy and may show different patterns of whole-plant recovery.

Several species of resurrection ferns thrive in the rocky soils of the California chaparral ecosystem, including locally abundant *Pellaea andromedifolia* and *Pentagramma triangularis*. These plants have small stature, with fronds rarely exceeding 50 cm and 20 cm tall, respectively. Their rhizomes are typically found 2 cm below the soil surface, and their roots are fibrous and shallow (Holmlund *et al*., 2016). These two species co-occur in the rocky outcrops and shallow soil characteristic of exposed chaparral slopes, and they grow in niches with higher irradiance compared to other chaparral fern species (Holmlund *et al*., 2016). The southern California chaparral ecosystem is subject to long summer droughts (Cowling *et al*., 1996). During drought, these two DT species completely desiccate but normally resurrect within several days of the first rain event. However, we observed that only the smallest fronds or basal pinnules (leaflets) resurrected following a small rain event (5 mm, 28 Feb 2014, Fig. 1); more precisely, only the leaf tissue closest to the root water source resurrected. This observation suggested that water from the roots contributed more to whole-plant recovery than did leaf water uptake. In contrast, if leaf water uptake were the primary water source for resurrected ferns, then all fronds or pinnules would have resurrected equally following a small rain event.

Consequently, we hypothesized that these ferns resurrect via bottom-up rehydration (root water uptake) rather than top-down rehydration (leaf water uptake). We tested this hypothesis using three sets of natural and artificial irrigation treatments on desiccated plants by quantifying recovery in the root, stele, and leaf tissue (Fig. 2). First, we quantified desiccation recovery following a natural rain event in which we

excluded water from the leaves of some plants *in situ*. This experiment demonstrated that root water alone was sufficient to resurrect all parts of the plant. Next, we used organ-specific *in situ* irrigation experiments during the dry season to determine if leaf water uptake alone can resurrect the whole plant. Pilot data revealed that these resurrection ferns consistently generated root pressure during the early stages of recovery. Thus, we suspected that positive root pressure rather than capillary action alone is necessary for whole-plant recovery. We tested this hypothesis by resurrecting excised fronds using either simulated root pressure or capillary action alone.

Additionally, we theorized that changes in non-structural carbohydrate (NSC) content in the leaves, stipe vascular bundles (stele), and rhizomes might provide further insight into the desiccation and recovery dynamics in these ferns. Therefore, we tracked the NSC content of leaves, steles, and rhizomes in *P. andromedifolia* during recovery following a natural rain event. Since sucrose is a known desiccation protectant, we hypothesized that all organs would have high sucrose concentrations per unit dry weight in the desiccated state. Taken together, our field and lab experiments examine whether root pressure and NSC variation contribute to recovery from desiccation.

Materials and Methods

Plant Material

We examined two DT fern species in the chaparral understory of the Santa Monica Mountains (Los Angeles County, California, USA). We selected these two

species because they have contrasting frond size and shape, representing extremes in the frond morphology of DT fern species growing in the southern California chaparral (Fig. 1, 3, 4). *Pentagramma triangularis* (formerly *Pentagramma triangularis* Kaulf. subsp. *triangularis*, see Schuettpelz *et al*., 2015) has pinnate-pinnatifid fronds and short stature (generally less than 20 cm tall). In the desiccated state, the entire frond curls upward to form a single curled structure. *Pellaea andromedifolia* Kaulf. is 2-pinnate or 3-pinnate and about 50 cm tall. In the desiccated state, the smallest leaf segments (pinnules) curl downward, while the entire frond retains its open position. We used two similar study sites along the Backbone Trail of the Santa Monica Mountains for all field experiments and collections: the intersection of the Backbone trail and Piuma Road (34°04′34″N, 118°41′10″W) and the Newton Canyon trailhead on Kanan Dume Road (34°04’34.0“N, 118°48’57.2”W). Our nomenclature is that of Baldwin *et al*. (2012) with modifications by Schuettpelz *et al*. (2015).

Experimental overview

Our study consisted of three experiments: a natural rain experiment *in situ* at the onset of the wet season, a root vs leaf irrigation experiment *in situ* during the dry season, and a water pressure vs capillary action experiment on stipes of excised fronds in an environmental chamber (Fig. 2). In the first experiment, we excluded rain water from the leaves of plants *in situ* during the first rain event of the wet season to test whether root water alone could resurrect the entire plant (“rain” experiment in Fig. 2A; n = 4-5 plants per treatment). We compared desiccation recovery between the “wet

leaf" and "dry leaf" treatments in this experiment. In the second experiment, we conducted *in situ* organ-specific irrigation experiments during the dry season to test whether leaf water alone could resurrect the entire plant ("dry season" experiment in Fig. 2B; n = 6 plants per treatment). We assessed which plant organs recovered when we watered the roots alone ("root irrigated") or leaves alone ("leaf irrigated"). In the last experiment, we applied water to the cut ends of excised fronds to test whether root pressure was needed for full recovery of the leaf tissue ("pressure" experiments in Fig. 2C; n = 6 plants per treatment). Water was either forced into the cut end of the stipe using applied pressure ("30 kPa" in Fig. 2C) or applied to the cut end without pressure ("0 kPa" in Fig. 2C).

During resurrection, leaf tissue uncurls and photosynthetic capacity increases. We assessed increasing photosynthetic capacity by measuring dark-adapted chlorophyll fluorescence (F_v/F_m), which indicates the maximum efficiency of photosystem II and has previously been used as a measure of desiccation recovery (Proctor & Tuba, 2002; Watkins *et al.*, 2007; see also Maxwell & Johnson, 2000). Furthermore, we have found that F_v/F_m correlates with maximum photosynthetic rate during resurrection in *P. triangularis* (Samantha Fiallo, unpublished data). Therefore, in our experiments, we quantified desiccation recovery in four ways, measuring 1) increase in dark-adapted chlorophyll fluorescence (F_v/F_m), 2) increase in width of the frond or pinnule (leaflet) relative to the desiccated state, 3) development of positive root pressure, and 4) increase in water potential of the soil, stipe cortex, stipe vascular bundle, and leaf tissue. Plants were selected using haphazard sampling in the field.

We selected fronds of similar size across individuals within species to avoid confounding effects of size on recovery. For both species, we selected a single representative frond on each plant before the experiment. Since recovery response was sometimes highly variable among individual fronds and pinnules, choosing fronds and pinnules *a priori* helped prevent sampling bias towards the resurrected pinnules. The leaf tissue on the selected frond was used to estimate the degree of recovery from desiccation once each day. For *P. andromedifolia*, two individual pinnules on the frond were chosen: one at the bottom and one at the top of the same frond. All pinnules chosen were located within 5 cm of the central rachis. The bottom pinnule was selected from the lowest branch on the frond. The top pinnule was selected within 5 cm of the frond tip.

The fronds are much smaller in *P. triangularis*, and the pinnae are often fused (Fig. 1). Unlike *P. andromedifolia*, the pinnae of *P. triangularis* are densely placed on the distal end of the frond and curl or uncurl as a unit while desiccating and resurrecting. Thus, only one measurement of F_v/F_m was taken per frond in *P. triangularis*.

Leaf recovery: F_v/F_m and pinnule width

We measured F_v/F_m and frond or pinnule width daily during all experiments using a pulse-modulated fluorometer and digital Vernier calipers (model OS1p, Opti Sciences, Hudson, New Hampshire, USA). In the field, dark-adaptation clips or pieces of black cotton cloth were used to dark-adapt the leaf tissue for at least 20 minutes prior to F_v/F_m measurements, following the methods of Holmlund *et al*. (2016). We found

that dark adaptation for a minimum of 20 minutes was sufficient for ferns to reach recovered F_v/F_m values above 0.8.

Stele recovery: F_v/F_m

Additionally, we measured the desiccation recovery of the photosynthetic tissue surrounding the vascular bundle (stele) inside the stipe using F_v/F_m (Fig. 4, inset photo). Only *P. andromedifolia* had a large enough stele for this measurement. The steles of *P. triangularis* also contain chlorenchyma; however, these steles were too small to reliably measure fluorescence. F_v/F_m of the stele was measured by carefully shaving away approximately 1 cm of the outer desiccated cortex (longitudinally) in the center third of the stipe (Fig. 4, inset photo). A stipe was selected that was not supplying water to the pinnules we were measuring (i.e., we used a different frond on the same plant). This exposed stele was wrapped in parafilm, and then dark-adaptation clips were used to dark-adapt the stele as for the leaf tissue.

Root or rhizome recovery: Root pressure

Preliminary field irrigation experiments on desiccated plants indicated that positive root pressures peaked about two days after irrigation began. Since a frond is sacrificed for each root pressure measurement, root pressure was measured in the morning only near the beginning of the rain experiment and near the beginning and end of the dry-season experiments using bubble manometers as in Ewers *et al*. (1997). Although we refer to the observed pressure as "root pressure," our current methods do

not allow us to distinguish between root pressure and rhizome pressure. Briefly, capillary tubes that had been sealed on one end were attached via flexible tubing to freshly cut stipes 2 cm above the soil. Before attaching the manometer to the plant, a bubble was inserted into the distal end of the manometer, and the rest of the tubing was filled with 20 mM KCl solution. Manometers were attached in the morning between 0600 and 0900 hrs and allowed to equilibrate 90 min before reading. The length of the bubble was measured before and after relieving the pressure by puncturing the tubing with a needle. This ratio was used to calculate root pressure using Equation 1:

Equation 1: $$P = 100[\left(\frac{L_{atm}}{L_{pressure}}\right) - 1]$$

in which L_{atm} is the length of the bubble when the pressure is relieved and $L_{pressure}$ is the length of the bubble under root pressure (Ewers *et al*., 1997). Manometers were not equilibrated overnight because changes in temperature caused additional small bubbles to form in the manometers, preventing an accurate reading. A small positive root pressure was observed in many of the desiccated unwatered controls (less than 3 kPa); however, this is likely an artifact of the method. It is likely that the lack of connection between the water in the bubble manometer and the embolized xylem conduits did not allow the manometer to fully equilibrate with desiccated plants, resulting in a slight positive pressure, which was generated when the manometer was attached to the stipe. This hypothesis is supported by our finding of slight positive pressures in desiccated control plants, which would have no water source to generate root pressure. Thus, root pressure values less than 3 kPa in all treatment groups were omitted from all analyses,

since these values were likely generated by this minor artifact.

Water potential

Water potential was measured at the end of the field experiments using a dew point hygrometer (WP4C Dewpoint PotentiaMeter, METER Group, Inc., Pullman, WA, USA). For *P. triangularis*, we measured soil and leaf water potential. For *P. andromedifolia*, we also measured the water potentials of the steles and outer parenchyma (cortex) layers by quickly dissecting the stipes and rachises inside a humid bag before placing chopped samples in the dew point hygrometer (Fig. 4, inset). *Pentagramma triangularis* lacked sufficient stipe material to measure stele and cortex water potential.

Rainy season experiments

To determine the contribution of leaf water to desiccation recovery, we took advantage of the first rain event of the wet season to conduct an experiment for 13 days to test the effects of leaf wetness on desiccation recovery (Fig. 2). On 7 Jan 2018, we covered all fronds of five individuals of each species with plastic bags to keep the leaves dry during a forecasted rain event. On 8 Jan to 9 Jan 2018, our western study site received 69 mm of precipitation (obtained from Lechuza Patrol weather station, Los Angeles Department of Public Works). Prior to this rain event, all ferns at our field sites had been desiccated for approximately seven months. Following the rain, we concluded that the roots of the plants were thoroughly soaked (based on excavations of

some control plants), and all plants began to resurrect. All plastic bags were removed on the morning of 10 Jan, after the rain stopped. The effect of the plastic bags on the vapor pressure deficit (VPD) around the leaves was judged to be minimal since it was raining almost the entire time the bags were covering the plants.

No data was obtained on 9 Jan 2018 due to hazardous storm conditions. F_v/F_m and leaf width was measured daily from days 2 to 12 following the rain event. Root pressure was measured in the morning near the beginning of the experiment (day 2). Tissue and soil water potentials were measured on day 13 post rain. Some dew formed on *P. andromedifolia* leaves on the mornings of days 3 and 4. The effect of dew was judged to be minimal considering that all plants were affected equally, and that rain water on leaves should already have had an effect on leaves during the first two days.

Dry season irrigation experiments

During the dry season, we conducted organ-specific field irrigation experiments for 16 days each to separately test the effects of root irrigation and leaf irrigation on the plants' resurrection response (Fig. 2). We used two types of irrigation. Root irrigation was achieved by daily watering the surrounding soil with 9.5 liters of water (days 0-15, total of 152 liters per plant over the course of 16 days; Ψ_{soil} = -0.05 ± 0.00 MPa, -0.10 ± 0.01 MPa, Table 1). Each plant was watered *in situ* with 9.5 liters daily in the late afternoon. Leaf irrigation was achieved by repeatedly spraying the leaves with de-ionized water during the day. De-ionized water was used to prevent accumulation of ions on the leaf surface following repeated spray treatments and evaporation. Due to

high temperatures and low relative humidity, it was difficult to keep all the leaves wet even while repeatedly spraying them. Therefore, we covered the leaves with plastic bags to keep them wet. During the day, we removed the bags every 1-2 hrs to spray the leaves and prevent the buildup of gases. We left the bags on the plants overnight to keep the leaves wet. The leaves were usually still wet in the morning, except for days 13-15 of the leaf irrigation experiment for *P. andromedifolia*, when the Santa Ana winds occurred at our study site, creating exceptionally hot, dry, and windy conditions. The bottom (proximal) pinnules occasionally dried out overnight since they were close to the bag opening. This difference in overnight wetting probably accounts for the difference in the recovery of top versus bottom pinnules in the leaf irrigation treatment of *P. andromedifolia* (Fig. 4I-J). The water potential of the soil surrounding the rhizomes of the leaf irrigation plants was thoroughly dry on day 16 of the experiment (-141 ± 1 MPa, -117 ± 5 MPa, Table 1), indicating that the leaf spraying had not hydrated the soil.

We measured F_v/F_m and pinnule width daily from day 0 (prior to watering) through day 15. Root pressure was measured in the mornings on days 2 and 16 after starting irrigation. Samples for soil, stele, cortex, and leaf water potentials were collected at midday on day 16 after starting irrigation. In addition to the root irrigation and leaf irrigation treatments, we tracked twelve unmanipulated desiccated plants to confirm that plants remained desiccated throughout the experiment, not rehydrated by fog or dew. However, we did not include these plants in our statistical analyses.

Applied pressure experiments

In the lab, we performed applied pressure experiments under controlled conditions for five days to determine the relative contributions of root pressure and capillary action to whole-plant desiccation recovery (Fig. 2). To achieve this goal, we applied positive water pressure to the cut end of desiccated fronds in the lab under controlled conditions to mimic root pressures observed in plants resurrecting in the field. The resurrection response of these fronds was compared to the response of a control treatment subjected to capillary action alone (no pressure applied to the cut end of the stipe). Entire fronds were excised from the field while desiccated. Fronds were resurrected in a growth chamber (diurnal relative humidity = 50-70%, temperature = 20°C daytime, 15°C night, 14-hour days). The relative humidity in our growth chamber fell within the range observed in the field (14-75%). Fans circulated air throughout the chamber to promote uniform conditions. Plant positions were rotated regularly. For the root pressure simulation, water pressure was applied to the cut end of the stipe using an elevated pressure head (30 kPa ± 0.5 kPa). For the control treatment, fronds were secured with the cut end submerged 1 cm deep in KCl solution in a 50-mL conical vial. F_v/F_m and frond/pinnule width were measured daily on the leaves on days 0 through 5. Prior to F_v/F_m measurements, plants were dark-adapted by turning off the lights for at least 20 minutes. In both capillary action and applied pressure treatments, we used filtered (0.1 μm filter) and degassed 20 mM KCl solution to slow bacterial and fungal growth in the xylem conduits. Additionally, all tubing and vials were bleached prior to the experiment.

Non-structural carbohydrate analyses in P. andromedifolia

Non-structural carbohydrate (NSC) content was quantified in the natural rain experiment using the enzymatic methods of Lloret *et al*. (2018). NSC content was only examined in *P. andromedifolia* because individuals of *P. triangularis* were too small, lacking sufficient rhizome and stipe material for the analysis. Leaves of *P. triangularis* were not sampled because individual plants had too few leaves for repeated sampling. Briefly, rhizome, stele, and leaf tissue samples were collected from six *P. andromedifolia* individuals in the desiccated state (day 0) and on days 2, 5, and 8 after the natural rain event on 8-9 Jan 2018. Samples were transported on ice back to the lab, where they were microwaved 30-60 seconds at 1500 W to stop enzymatic breakdown of sugars (i.e., consumption of NSC pools). Samples were dried in an oven at 60°C to a constant mass and finely ground into a homogenous powder. Eleven milligrams of powder were dissolved in water and placed into a water bath at 80°C to extract soluble sugars (i.e., sucrose, glucose, and fructose). We quantified soluble sugar by using enzymes to separately convert each soluble sugar to glucose-6-phosphate, which was then quantified optically at 340 nm using spectrophotometry. Total NSC content was separately determined by enzymatically digesting all NSCs into glucose-6-phosphate. Starch was then estimated as the difference between total NSCs and soluble sugars.

Statistical analyses

In the rain experiment, F_v/F_m and frond/pinnule width data were compared between wet leaf (rained) and dry leaf (bagged) treatments using a univariate repeated-

measures ANOVA with a Greenhouse-Geisser correction factor to account for lack of sphericity (Figs. 3-5). The same individuals were sampled repeatedly throughout the experiment, allowing the effect of time to be included in the analysis. P-values refer to the significance of the interaction between treatment and time effects (significant when $p < 0.05$). The same analyses were used for the applied pressure versus capillarity experiment in the growth chamber (Fig. 6). In the rain experiment, root pressure and water potential data were compared between wet leaf and dry leaf treatments using a Student's t-test assuming equal variance ($p < 0.05$, Figs. 3-4, Table 1). NSC data were analyzed using a one-way ANOVA within a given organ and sugar type followed by a Tukey's HSD post-hoc test ($p < 0.05$, Figs. 7-8). Repeated measures analyses were not appropriate for the NSC data because different individuals were sampled each time so that subsequent measurements would not be affected by previous rhizome excavations. All analyses were conducted using JMP Pro software (vs 14.2.0).

Results

Recovery following rain or dry season irrigation

Following a 69-mm natural rain event on 8-9 January 2018, ferns rehydrated either naturally (wet leaf control) or with water excluded from the leaves covered by a bag (dry leaf treatment, Fig. 2). All individuals had been thoroughly desiccated for at least seven months prior to this rain event. To further tease apart whether recovery could occur by either root water uptake alone or leaf water uptake alone, two additional treatments were implemented during the dry season using either daily root irrigation

(days 0-15) or frequent leaf irrigation by spraying (Fig. 2).

Recovery of P. triangularis

Pentagramma triangularis is smaller than *P. andromedifolia* and responds differently to desiccation. As *P. triangularis* desiccates, water loss triggers inward curling of the pinnae, forming a cluster that exposes the yellow indument on the abaxial side of the leaf (Fig. 1A). The abaxial side of the leaf is presumably protected by the pale, waxy indument. Desiccation recovery was monitored in both the leaf tissue (uncurling frond) and the roots. After the rain, leaves in both the wet leaf (uncovered) and dry leaf (covered) groups uncurled and recovered healthy F_v/F_m (above 0.8) and frond width within six days, but the wet leaf group resurrected slightly faster than the dry leaf group ($p = 0.039$, 0.002, Fig. 3A-B). However, this effect was localized to the leaf tissue, as there was no significant difference between the root pressure of the wet leaf and dry leaf groups on day 2 post rain ($p = 0.969$, Fig. 3C).

During the dry season, the root irrigation treatment showed a similar but delayed resurrection response compared to both treatments in the rain experiment (Fig. 3D-F). The root irrigation treatment showed recovery in both roots and leaves, even though no water was applied directly to the leaves. The root-irrigated plants showed root pressure on day 2 post start of irrigation (16.2 ± 9.1 kPa, Fig. 3F), consistent with root/rhizome recovery. However, leaf recovery was delayed until day 8 (Fig. 3D-E). In contrast, individuals in the leaf irrigation treatment only showed recovery in the leaves and not in the roots (Fig. 3G-I), indicating that no or insufficient water traveled from

the leaves to the roots. No root pressure was observed at the end of the dry-season irrigation experiment (day 16), with the exception of one plant in the leaf irrigation treatment showing slight pressure (4.5 kPa).

Recovery of P. andromedifolia

In contrast to *P. triangularis*, the desiccating fronds of *P. andromedifolia* maintain their open structure, while the terminal segments (pinnules) curl individually. In this species, width of the individual pinnules was monitored instead of the width of the entire frond, since frond width remained approximately constant throughout recovery. Furthermore, *P. andromedifolia* is a larger plant, allowing recovery of the stele to be monitored as well as the leaves and roots. In the stipes, recovery of the inner vascular system (stele, including the endodermis and pericycle surrounding the vascular tissue) was monitored by measuring F_v/F_m because the stele contained chlorenchyma surrounding the phloem and xylem (Fig. 4, inset photo).

Following the natural rain event, the stele chlorenchyma of the stipe of both wet leaf and dry leaf plants recovered F_v/F_m in a manner similar to the leaf tissue (Fig. 4C). Individuals with either wet (uncovered) or dry (covered) leaves recovered F_v/F_m equally well in the top pinnule (Fig. 4A, $p = 0.713$), bottom pinnule (Fig. 4B, $p = 0.548$), stele (Fig. 4C, $p = 0.261$), and roots/rhizome (Fig. 4D, $p = 0.819$). The F_v/F_m values above 0.8 in recovered tissues were consistent with the hydrated tissue and soil water potentials at the end of the experiment (day 13 post rain; Fig. 4, Table 1).

In the dry-season root irrigation treatment, all plant organs (root/rhizome, stele, leaf) improved F_v/F_m even though water was only applied to the roots (Fig. 4E-H); however, the water did not reach most top pinnules during the course of the experiment (Fig. 4E). This result contrasted with the recovery observed in the dry leaf treatment from the natural rain experiment, in which only the roots received water and yet all pinnules recovered (including the top pinnules). This difference is likely due to the high temperatures and low relative humidity during the dry season, which probably slowed recovery of the dry-season root-irrigated plants. The soil surrounding the roots was thoroughly hydrated in both experiments ($\Psi_{soil} \geq$ -0.10 MPa, Table 1). Soil and tissue water potentials of root-irrigated plants at the end of the dry season experiment showed a clear gradient from the soil near the roots (-0.1 MPa) to the stele (-1.2 MPa) to resurrected leaf tissue (-2.0 MPa; Fig. 4B-D, Table 1). The stipe cortex tissue appeared to be hydraulically isolated from the neighboring stele tissue (-34.4 ± 4.0 MPa vs -1.23 ± 0.06 MPa) and showed no signs of recovery (Table 1; Fig. 4, inset). The root-irrigated plants showed root pressure on day 2 post start of irrigation (16.4 ± 4.4 kPa, Fig. 4H). Most root pressure had dissipated by the end of the dry-season irrigation experiments; only two plants in the root irrigation treatment showed root pressure on day 16 (12.4 and 4.8 kPa). These data are consistent with the finding that root pressure dissipated by day 6 following the natural rain event in the wet season (data not shown).

In the leaf-irrigated plants from the dry season experiment, only leaf tissue resurrected; the stele and roots remained desiccated (Fig. 4I-L). Top pinnules resurrected more quickly and more completely (higher F_v/F_m and leaf width) than

bottom pinnules, perhaps due to more thorough overnight wetting farther inside the bag (Fig. 4I-J), or perhaps because the bottom pinnules were losing more water to the stele. Pinnule expansion closely followed F_v/F_m recovery in the leaf tissue (Fig. 5). However, steles in the leaf irrigation treatment showed no signs of F_v/F_m recovery, and this result is consistent with their dehydrated status on day 16 of the experiment (-19.4 ± 9.2 MPa, Fig. 4K, Table 1). No root/rhizome recovery was observed in the leaf irrigation treatment on days 2 or 16 (Fig. 4L).

Applied pressure experiments

Given that root water uptake appeared to be critical for whole-plant desiccation recovery, this subsequent experiment tested whether the root pressure observed in intact, rehydrating plants *in situ* was actually necessary for desiccation recovery, or if capillary action alone inside xylem conduits can resurrect the stele and leaves. We rehydrated excised fronds in a growth chamber either by applying 30 kPa of water pressure to the cut end of the stipe (simulated root pressure) or by placing the cut end of the stipe in water (capillary action alone) (Fig. 2). F_v/F_m of the bottom pinnules of *P. andromedifolia* recovered equally well with capillary action alone and with simulated root pressure (Fig. 6C, ns). However, the leaf tissue of *P. triangularis* and the top pinnules of *P. andromedifolia* showed improved recovery when pressure was applied to the cut end of the stipe compared to capillary action alone (Fig. 6A-B, $p = 0.014$, 0.004). Frond or pinnule width closely followed F_v/F_m in these experiments; however, there was high variability in pinnule size (Fig. 6D-F). Changes in frond width

of *P. triangularis* were marginally significant between treatments (Fig. 6D, $p = 0.051$). Pinnule width of *P. andromedifolia* increased more rapidly with applied pressure for the top pinnule (Fig. 6E, $p = 0.022$) and not significantly different between treatments for the bottom pinnule (Fig. 6F, ns).

Non-structural carbohydrate analysis in P. andromedifolia

Non-structural carbohydrate (NSC) content was analyzed enzymatically in the leaves, steles, and rhizomes of resurrecting *P. andromedifolia* individuals following the 69-mm rain event on 8-9 January 2018 (i.e., natural rain experiment). Insufficient material was available to measure NSC content in *P. triangularis* due to the small size and number of leaves on each plant. Desiccated plant tissue was collected before the rain, and resurrecting plant tissue was collected 2, 5, and 8 days after the rain. Total NSC content did not change over time in the leaf tissue and rhizomes of recovering individuals, but NSC content decreased in the steles during the resurrection process ($p < 0.05$; Fig. 7). However, separate analyses of starch, sucrose, and glucose/fructose content revealed more complex patterns (Fig. 8). Further analysis indicated that leaf tissue showed no change in any of the three NSC components (starch, sucrose, and glucose/fructose) over time ($p = 0.36, 0.76, 0.97$; Fig. 8A). In contrast, both the steles and rhizomes showed decreased sucrose in the resurrected state compared to the desiccated state ($p < 0.05$; Fig. 8B-C). Both the steles and rhizomes showed a slight peak in glucose/fructose content on day 2 post rain (Fig. 8B-C). Starch was absent from both the steles and the rhizomes in the desiccated state; however, starch rose steadily

in the rhizome throughout the recovery process ($p < 0.05$; Fig. 8C).

Discussion

Our results show that three factors contribute to desiccation recovery in *P. andromedifolia* and *P. triangularis*: root pressure, capillary action, and foliar water uptake. Experimentally excluding natural rain from a desiccated leaf showed that a combination of root pressure and capillary action resurrected all plant organs (root, stipe, and leaf) without the aid of foliar water uptake. Root irrigation during the dry season showed that positive hydraulic root pressure and capillary action resurrected all plant organs, although some distal pinnules never recovered, possibly due to the higher VPD in the dry season. However, leaf recovery happened most rapidly via foliar water uptake, as in the dry season leaf irrigation experiment and the wet-leaf treatment in the natural rain experiment. Therefore, desiccation recovery in natural conditions likely involves all three mechanisms.

However, root pressure likely plays a critical role in recovering the stipe. Stipe F_v/F_m in *P. andromedifolia* only recovered when water was applied to the roots; foliar water uptake did not rehydrate the stipe despite 15 days of wetting the leaves (Fig. 4K). In the chamber experiment, capillary action succeeded in resurrecting proximal pinnules in *P. andromedifolia*, but applied water pressure was needed to resurrect distal pinnules in *P. andromedifolia* and the fronds of *P. triangularis* (Fig. 6). Thus, root pressure likely drives stipe recovery (including xylem embolism repair) in natural conditions. Indeed, our previous study (chapter 3 of this thesis) found that gas

embolism is repaired in stipe xylem early in the resurrection process when only the roots were watered (Holmlund *et al.*, 2019). Restoring hydraulic flow through the vascular system would be essential for long-term water supply to the leaf blades and pinnules. Without stipe hydraulic flow, the leaf blades and pinnules would likely desiccate after the leaf surface water evaporated or was absorbed.

Further experiments are needed to determine whether a combination of capillary action and foliar water uptake could enable whole-plant recovery without the aid of root pressure. However, this scenario is probably not representative of natural conditions, given that root pressure was nearly always observed whenever water was applied to the roots (Figs. 3C, 3F, 4D, 4H). The data presented here suggest that root pressure likely initiates whole-plant recovery by rehydrating the vascular system while foliar water uptake concurrently expedites leaf recovery.

Root pressure has been shown to occur in non-DT ferns (Sperry, 1983; Fisher *et al*., 1997), but the role of root pressure in desiccation recovery in DT ferns was previously unknown. *Pleopeltis polypodioides*, a subtropical epiphyte, is perhaps the most commonly studied DT fern, but we are unaware of any reports of root pressure in this species. Instead, previous studies have shown that *P. polypodioides* relies on specialized scales for leaf water uptake (John and Hasenstein, 2017). Our study on chaparral ferns may provide an interesting contrast to previous work on *P. polypodioides*, since these two groups of ferns may have re-evolved different DT mechanisms to fill their respective niches. Resurrection fern species may have evolved

diverse strategies for tolerating desiccation because DT in the vegetative tissues has apparently re-evolved in vascular plants (Gaff and Oliver, 2013; VanBuren *et al*., 2017). Root pressure may help terrestrial ferns take full advantage of a timely seasonal rain event, whereas subtropical epiphytic ferns may capture sufficient water through foliar water uptake following frequent rain events.

Previous studies on DT angiosperm *Myrothamnus flabellifolius* have produced conflicting reports regarding the role of root pressure in angiosperm desiccation recovery. Schneider *et al*. (2000) found that root pressure was required to remove a lipid layer lining the tracheary elements in *M. flabellifolius*. Sherwin *et al*. (1998) found that capillary action, and not root pressure, was likely responsible for whole-plant recovery, since they only observed 2.4 kPa of root pressure in resurrecting plants. Evidence was found for capillary refilling, and excised stems even resurrected under -8 kPa of tension (Sherwin *et al*., 1998). However, root pressure generation may have been hindered by the fact that the plants in that study were potted, because subsequent studies found up to 13 kPa root pressure for this species *in situ* (Canny, 2000). Although no one has directly compared hydraulic recovery in DT ferns and DT angiosperms, some ferns lacking specialized structures for foliar water uptake may require root pressure for resurrection even if angiosperms do not. Ferns have tracheid-based xylem with less xylem per unit stipe transverse area, which contributes to higher xylem resistance per unit stipe transverse area than those of angiosperms and gymnosperms (Pittermann *et al*., 2011; Pittermann *et al*., 2013). Reduced xylem transverse area in ferns might hinder rapid resurrection in the absence of root pressure, at least for the

most distal leaf tissue.

Although root pressure is critical for whole-plant recovery in these two DT fern species, many other factors likely affect the speed and success of desiccation recovery. High ambient temperature and low relative humidity (high VPD) likely slowed desiccation recovery during the dry season root irrigation experiment, even though the soil was fully hydrated in both the dry season root irrigation experiment and the natural rain experiment (Table 1). Warmer and drier atmospheric conditions likely cause more water to evaporate from the liquid to the gas phase in the stipe xylem conduits of resurrecting plants, slowing the movement of liquid water to the leaf blades. Reduced path length and xylem resistance might explain why the bottom (proximal) pinnules of *P. andromedifolia* resurrected with capillary action alone in the chamber experiment while the top (distal) pinnules required applied pressure to resurrect. However, the low VPD experienced by the plants during the natural winter rain experiment is likely more typical of the conditions usually experienced during resurrection in the Santa Monica Mountains. It is possible that root pressure would be less critical for whole-plant recovery if high atmospheric moisture (low VPD) was maintained until all plant organs had resurrected, although this hypothesis was not tested in our study.

Our study of the NSC dynamics in three organs of resurrecting *P. andromedifolia* may provide some insight into the mechanism of desiccation protection in this chaparral DT fern species. Sucrose was concentrated in some of the desiccated tissues, especially the stele (Fig. 8B). These data are consistent with other studies

identifying sucrose as a desiccation protectant in other DT species (reviewed in Scott, 2000). The photosynthetic stele (Fig. 4, inset) showed the highest NSC content throughout the experiment, perhaps due to the densely packed chloroplasts surrounding the xylem and phloem. Notably, the three organs showed different NSC dynamics. Sucrose and starch fluctuated in the rhizome. During recovery, sucrose content dropped rapidly while starch content increased steadily. The rhizome sucrose may have been converted into starch for long-term storage, perhaps as a resource for the next desiccation event. The progressive storage of starch is consistent with the role of rhizomes in carbon storage (Martínez-Vilalta *et al*., 2016). Conversion to starch may also maximize assimilation by preventing buildup of the product (sucrose). Sucrose in the stele also decreased on day 2 post rain, and glucose and fructose decreased by day 5 post rain. It is possible that these sugars in the stipe may have declined after first providing energy for xylem embolism repair and possibly solutes for the rapid buildup of positive hydrostatic pressure in the stipe, although our study did not directly test either of those hypotheses. Previous studies have suggested that sucrose may facilitate embolism reversal, even in the absence of root pressure (Secchi and Zwieniecki, 2011; Secchi and Zwieniecki, 2012; Savi *et al*., 2016). Furthermore, Schmitz *et al*. (2012) found a correlation between hydraulic conductivity and light availability to xylary chloroplasts in a non-DT angiosperm, implying that xylary chloroplasts may facilitate embolism repair. Although our study did not directly test the role of NSCs or xylary chloroplasts in desiccation recovery, this concept may be an interesting direction for future study, especially in DT species lacking root pressure.

Holmlund *et al*. (2016) speculated that DT ferns would fare better than other fern species in the future as climate change leads to longer and more severe droughts in southern California. The results from this study may provide support for this hypothesis, since the first seasonal rain event came unusually late in January 2018 and still the ferns resurrected rapidly and fully. These results, combined with future studies, will elucidate the mechanisms of desiccation recovery on a whole-plant scale, thus providing insight into the minimum survival requirements of the resurrection ferns.

Author contributions

This chapter was originally published as the following article in the *Journal of Experimental Botany*:

Holmlund HI, Davis SD, Ewers FW, Aguirre NM, Sapes G, Sala A, Pittermann J. 2020. Positive root pressure is critical for whole-plant desiccation recovery in two species of terrestrial resurrection ferns. *Journal of Experimental Botany* 71(3): 1139-1150.

H.I.H., J.P., F.W.E., and S.D.D. conceived the original ideas; H.I.H., S.D.D., F.W.E., N.M.A., G.S., and J.P. collected the data; H.I.H. and J.P. wrote the article with contributions of all the authors; H.I.H. agrees to serve as the author responsible for contact and ensures communication.

Table 1: Tissue and soil water potential (in MPa) after resurrection *in situ* following rain, root irrigation, leaf irrigation, and a dry control group. Data are means ± SE. Plants resurrected by the natural rain event belonged either to the dry leaf treatment group (italics) or the wet leaf control group (regular letters). No significant differences were observed in tissue or soil water potentials between wet leaf and dry leaf groups following rain (Student's t test with equal variances, $p < 0.05$). One outlier was removed from the *P. andromedifolia* leaf irrigation group (Ψ_{leaf} = -27.97 MPa); this leaf dried out in transit from field to lab.

	P. triangularis				*P. andromedifolia*			
	Rain	Root irrigation	Leaf irrigation	Dry control	Rain	Root irrigation	Leaf irrigation	Dry control
Ψ_{leaf}	-1.80 ± 0.06 *-1.78 ± 0.05*	-2.08 ± 0.21	-0.88 ± 0.10	-91.1 ± 2.7	-1.92 ± 0.07 *-2.13 ± 0.07*	-1.96 ± 0.06	-2.33 ± 0.29	-77.3 ±7.4
Ψ_{stele}					-2.10 ± 0.28 *-3.35 ± 0.69*	-1.23 ± 0.06	-19.4 ± 9.2	-81.7 ± 7.3
Ψ_{cortex}					-74.7 ± 14.6 *-88.0 ± 7.7*	-34.4 ± 4.0	-46.0 ± 6.7	-86.0 ± 4.6
Ψ_{soil}	-0.05 ± 0.02 *-0.07 ± 0.03*	-0.05 ± 0.00	-141.1 ± 1.2	-100.3 ± 10.4	-0.07 ± 0.04 *-0.09 ± 0.03*	-0.10 ± 0.01	-117.3 ± 5.1	-104.9 ± 5.5

Figure 1: Two partially resurrected chaparral ferns following 5 mm rainfall in February 2014. (A) Only the shorter fronds (green, uncurled) of this *Pentagramma triangularis* individual have resurrected, while the taller fronds remain desiccated (yellow, curled). (B) Only the lower pinnules (leaflets) of this *Pellaea andromedifolia* frond have resurrected (green, uncurled), while the upper pinnules remain desiccated (purple, curled).

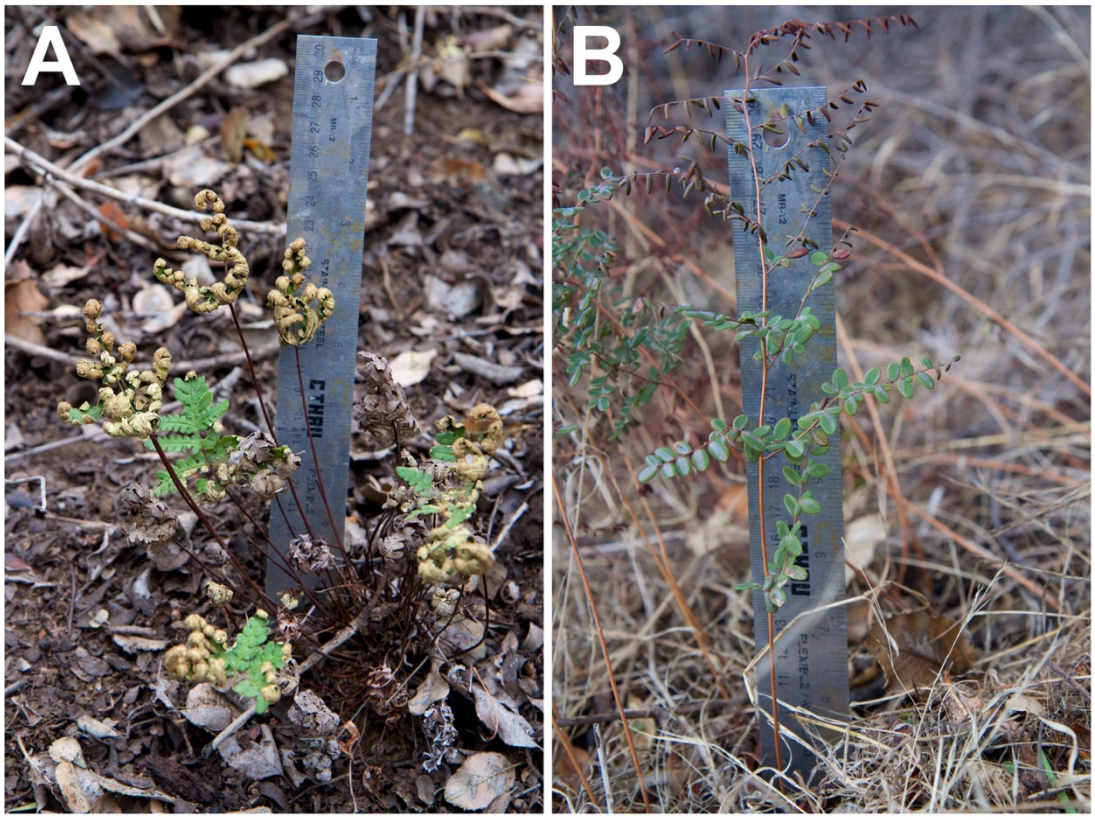

Figure 2: Illustration of three separate experiments used in this study: a natural rain event with bagged and unbagged fronds, dry season root and leaf irrigation, and growth chamber experiments on excised fronds either pressurized or non-pressurized at the cut end of their stipe. (A) The first rain event of the wet season in the Santa Monica Mountains occurred 8-9 Jan 2018. During this rain event, the leaves of some plants were covered (dry leaf treatment), while some leaves were left exposed (wet leaf control). All roots were completely soaked by the rain. (B) At the end of the dry season (Sept-Oct 2017), desiccated plants were irrigated *in situ* at our field sites. The roots of individuals in the root irrigation treatment were watered daily (9.5 L; days 0-15 for a total of 152 L each over 16 days). The leaves of individuals in the leaf irrigation treatment were kept wet continually by spraying with de-ionized water. (C) To determine the importance of applied water pressure to the resurrection of desiccated fronds, excised fronds were resurrected in a growth chamber using either 30 kPa of applied water pressure to the cut end of the frond or capillary action alone (0 kPa control).

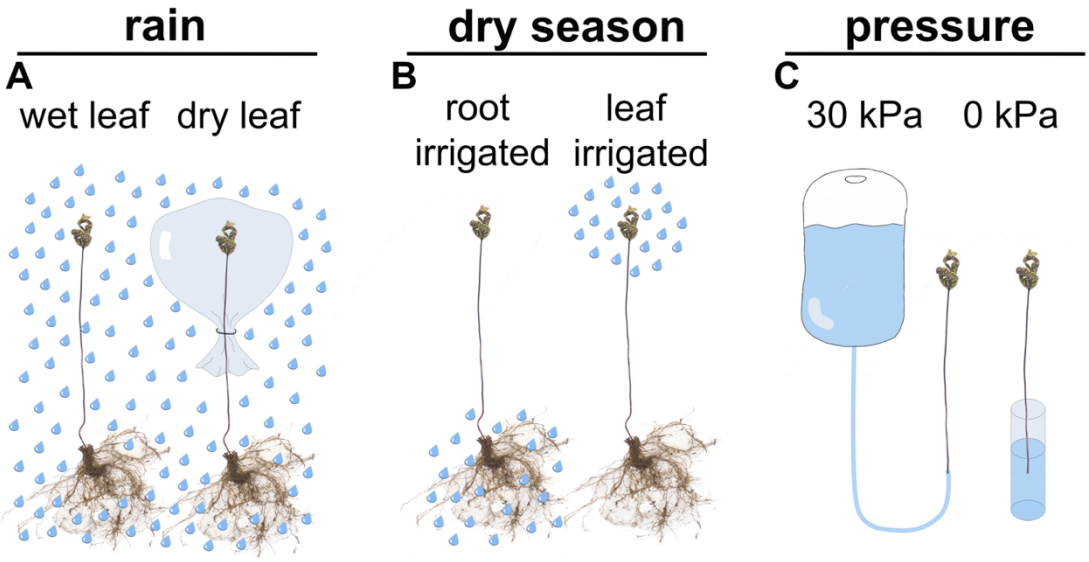
rain
A
wet leaf
dry leaf
dry season
B
root irrigated
leaf irrigated
pressure
C
30 kPa
0 kPa

Figure 3: Recovery of *Pentagramma triangularis* plants in the field following a natural rain event of 69 mm (A-C), root irrigation treatment during the dry season (D-F), and leaf irrigation treatment during the dry season (G-I). During the rain experiment (A-C), leaves were either allowed to be soaked by the rain (wet leaf control, black) or covered to keep them dry during the rain event (dry leaf treatment, gray). During recovery, fronds uncurl and regain photosynthetic capacity of photosystem II. We quantified recovery by measuring daily dark-adapted chlorophyll fluorescence, F_v/F_m (A, D, G), frond width (B, E, H), and root pressure on day 2 post rehydration for the rain experiment (C) or days 2 and 16 for the organ-specific irrigation experiments in the dry season (F, I). Data shown are mean ± se, n = 4-6. The proportions at the bottom indicate how many plants showed root pressure greater than 3 kPa (C, F, I see methods). Post rain p-values indicate the significance ($p < 0.05$) of the interaction between time and treatment effects using a repeated measures ANOVA with a G-G correction factor (F_v/F_m, frond width, significant) or a Student's t test (root pressure, not significant). Water potential values (Ψ) indicate the water potential (MPa) of the leaf tissue or soil at the end of the experiment (n = 6).

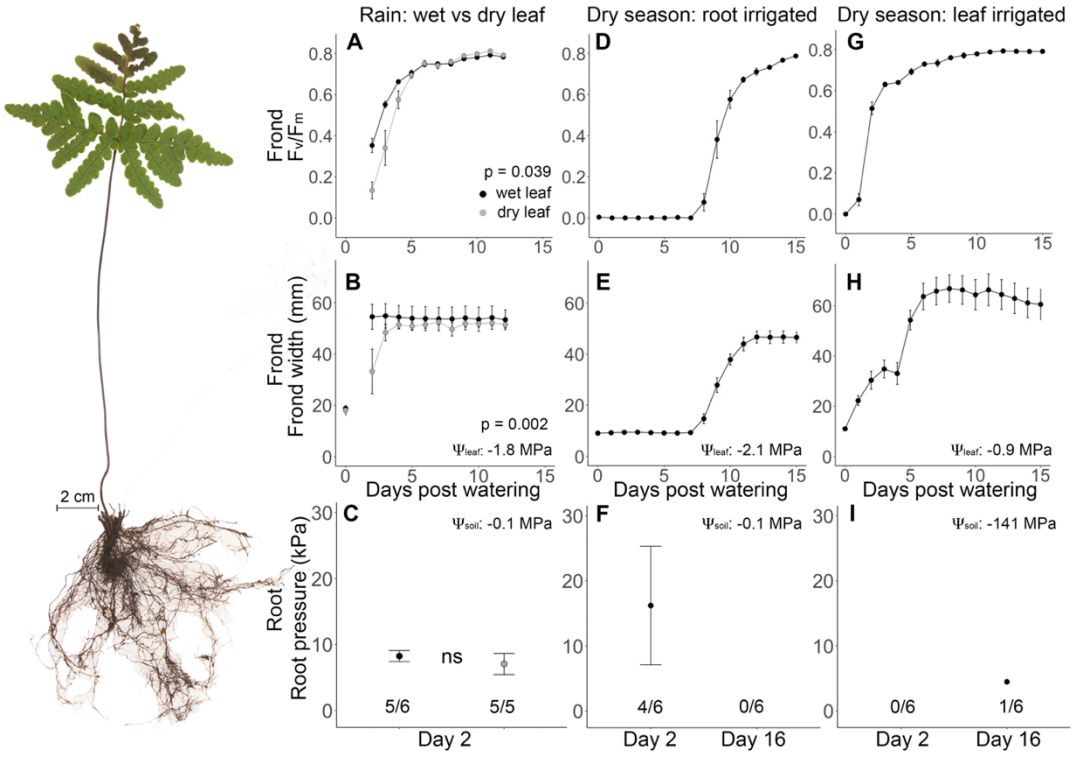
Rain: wet vs dry leaf
Dry season: root irrigated
Dry season: leaf irrigated
A
D
G
B
E
H
C
F
I
Frond F_v/F_m
p = 0.039
wet leaf
dry leaf
Frond width (mm)
p = 0.002
Ψ_{leaf}: -1.8 MPa
Ψ_{leaf}: -2.1 MPa
Ψ_{leaf}: -0.9 MPa
Days post watering
Root pressure (kPa)
Ψ_{soil}: -0.1 MPa
Ψ_{soil}: -0.1 MPa
Ψ_{soil}: -141 MPa
ns
5/6
5/5
4/6
0/6
0/6
1/6
Day 2
Day 2
Day 16
Day 2
Day 16
2 cm

Figure 4: Recovery of *Pellaea andromedifolia* plants in the field following a natural rain event (69 mm, A-D), root irrigation treatment during the dry season (E-H), and leaf irrigation treatment during the dry season (I-L). During the rain experiment (A-D), leaves were either allowed to be soaked by the rain (wet leaf control, black) or covered to keep them dry during the rain event (dry leaf treatment, gray). We quantified recovery by measuring daily dark-adapted chlorophyll fluorescence, F_v/F_m (A-C, E-G, I-K), and root pressure on day 2 post rehydration for the rain experiment (D) or days 2 and 16 for the organ-specific irrigation experiments in the dry season (H, L). Data shown are mean ± se, n = 5-6. The proportions at the bottom indicate how many plants showed root pressure greater than 3 kPa (D, H, L, see methods). Post rain p-values indicate the significance ($p < 0.05$) of the interaction between time and treatment effects using a repeated measures ANOVA with a G-G correction factor (F_v/F_m, not significant) or a Student's t test (root pressure, not significant). Water potential values (Ψ) indicate the water potential (MPa) of the leaf, stele, or soil at the end of the experiment (n = 5-6).

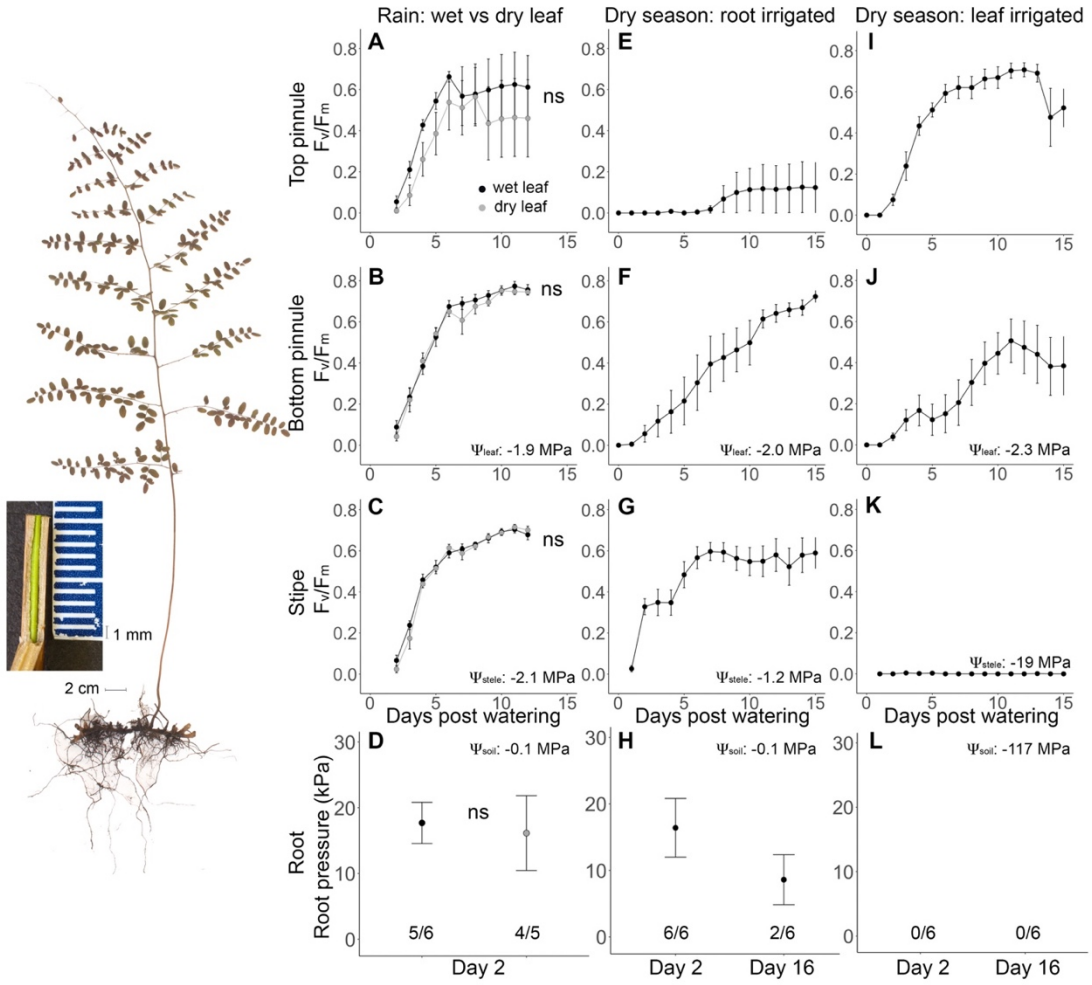
Rain: wet vs dry leaf
Dry season: root irrigated
Dry season: leaf irrigated
A
E
I
B
F
J
C
G
K
D
H
L
Top pinnule Fv/Fm
Bottom pinnule Fv/Fm
Stipe Fv/Fm
Root pressure (kPa)
ns
wet leaf
dry leaf
Ψleaf: -1.9 MPa
Ψleaf: -2.0 MPa
Ψleaf: -2.3 MPa
Ψstele: -2.1 MPa
Ψstele: -1.2 MPa
Ψstele: -19 MPa
Ψsoil: -0.1 MPa
Ψsoil: -0.1 MPa
Ψsoil: -117 MPa
Days post watering
5/6
4/5
6/6
2/6
0/6
0/6
Day 2
Day 16
1 mm
2 cm

Figure 5: Recovery of *Pellaea andromedifolia* plants in the field following a natural rain event (69 mm, A-B), root irrigation treatment during the dry season (C-D), and leaf irrigation treatment during the dry season (E-F). During the rain experiment, leaves were either allowed to be soaked by the rain (wet leaf control, black) or covered to keep them dry during the rain event (dry leaf treatment, gray). We quantified recovery by measuring daily pinnule width with digital Vernier calipers. Data shown are mean ± se, n = 5-6. Post-rain p-values indicate the significance ($p < 0.05$) of the interaction between time and treatments effects using a repeated measures ANOVA with a G-G correction factor (not significant).

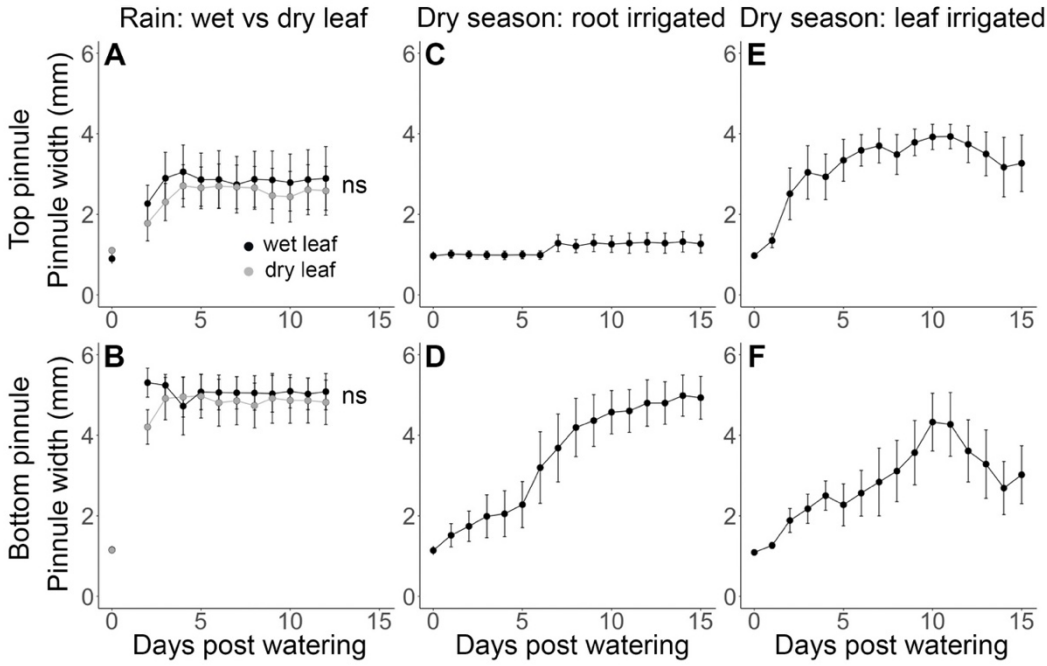

Figure 6: Recovery of F_v/F_m and frond width (mm) in excised fronds of *Pentagramma triangularis* (A, D). Also, recovery of F_v/F_m and pinnule width at top and bottom of *Pellaea andromedifolia* fronds (B-C, E-F). The excised fronds were either subjected to pressure applied to the cut end of the frond (30 kPa, solid line) or capillary action alone (0 kPa, dashed line). At no time was liquid water applied to fronds or pinnules to promote foliar water uptake. Data are mean ± se, n = 6. For F_v/F_m data, there was no significant difference between pressure and non-pressure treatments for the bottom pinnules of *P. andromedifolia*, but there was an overall difference between treatments with time for the top pinnules of *P. andromedifolia* ($p = 0.004$) and for the fronds of *P. triangularis* ($p = 0.014$). Consistent with this observation, there were no significant differences in pinnule width between treatments in the bottom pinnules of *P. andromedifolia*, but there was a significant difference for top pinnules of *P. andromedifolia* ($p = 0.022$) and a marginally significant differences for the fronds of *P. triangularis* ($p = 0.051$). P-values indicate the significance of the interaction between time and treatment effects using a repeated measures ANOVA with a G-G correction factor.

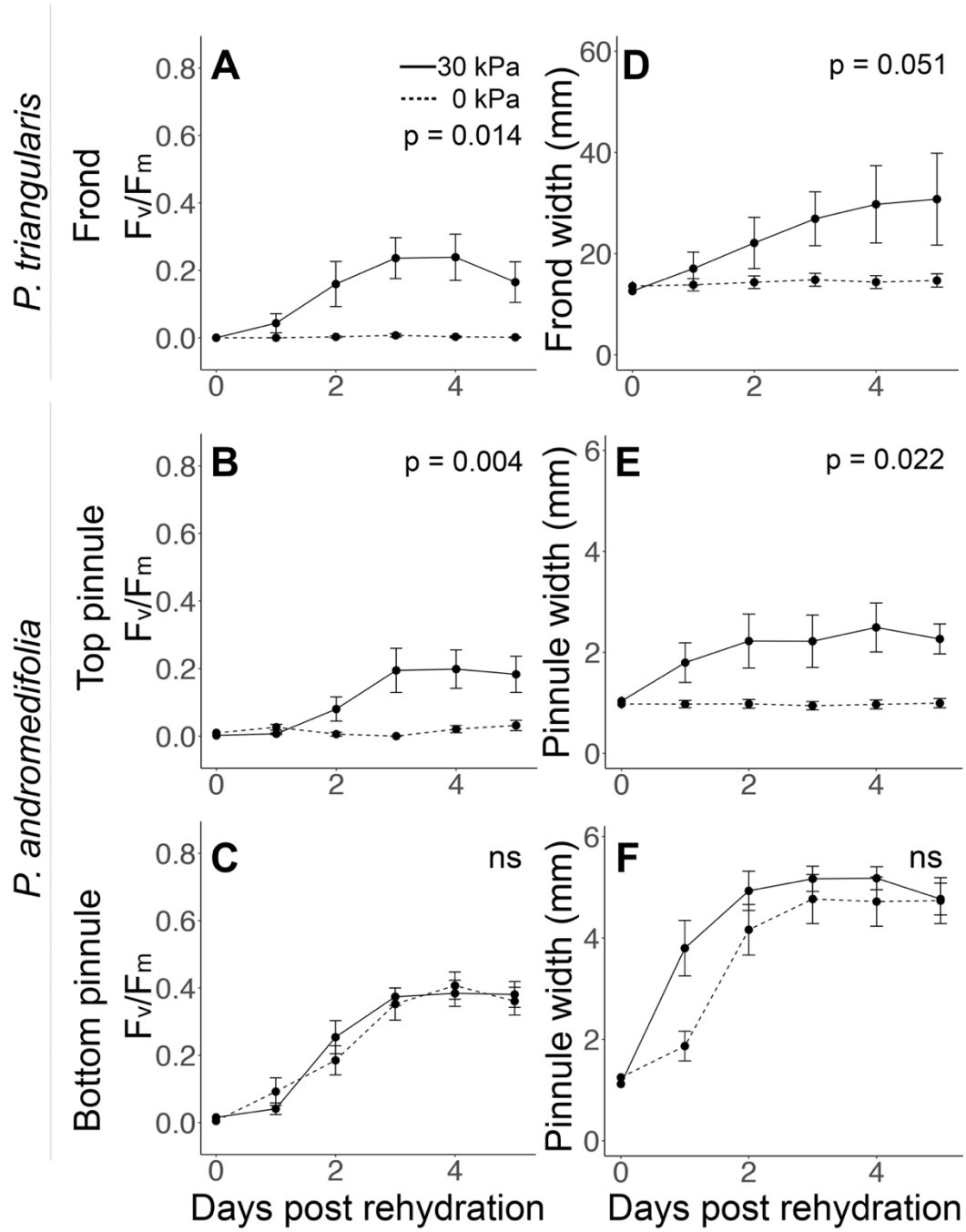
P. triangularis
P. andromedifolia
A
B
C
D
E
F
Frond
Top pinnule
Bottom pinnule
Fv/Fm
Frond width (mm)
Pinnule width (mm)
30 kPa
0 kPa
p = 0.014
p = 0.051
p = 0.004
p = 0.022
ns
ns
Days post rehydration
Days post rehydration

Figure 7: Total non-structural carbohydrate content by organ in recovering individuals of *P. andromedifolia* immediately before (day 0) and following (days 2, 5, 8) a natural rain event of 69 mm on 8-9 January 2018. Asterisks and letters indicate significant difference among days within an organ ($p < 0.05$) as determined by a one-way ANOVA followed by a Tukey's HSD post-hoc test. Boxplots represent first and third quartile, median, and 95% confidence intervals with outliers shown (n = 6). Plants were not repeatedly sampled to avoid artifacts from damaged individuals. Thus, different plants were sampled (n = 6) from the population each day.

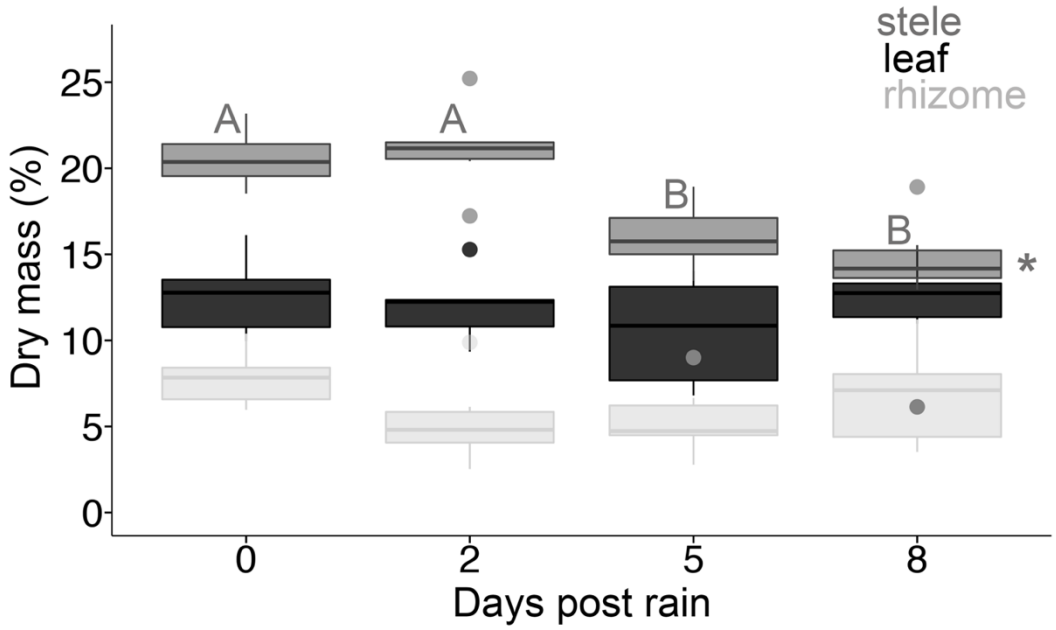

Figure 8: Non-structural carbohydrate content by sugar type in recovering individuals of *P. andromedifolia* immediately before (day 0) and following (days 2, 5, 8) a natural rain event of 69 mm on 8-9 January 2018. Data are shown for the leaf tissue (A), stele (B), and rhizomes (C) for starch content (black), sucrose content (dark gray), and combined glucose and fructose content (light gray). Asterisks and letters indicate significant difference among days within a given organ and sugar type ($p < 0.05$) as determined by a one-way ANOVA followed by a Tukey's HSD post-hoc test. Boxplots represent first and third quartile, median, and 95% confidence intervals with outliers shown ($n = 6$). Plants were not repeatedly sampled to avoid artifacts from damaged individuals. Thus, different plants were sampled ($n = 6$) from the population each day.

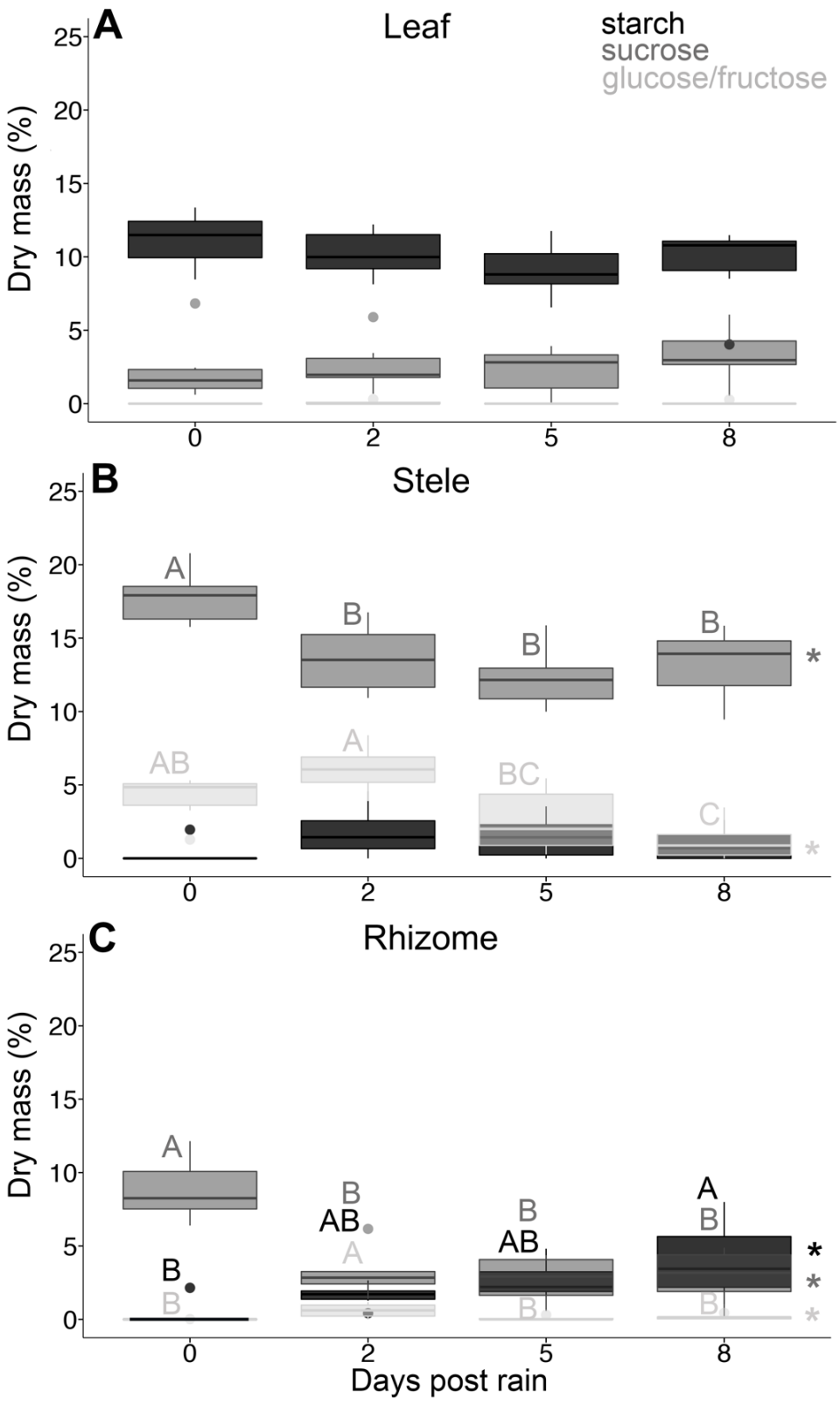
A
Leaf
starch
sucrose
glucose/fructose
Dry mass (%)
25
20
15
10
5
0
0
2
5
8
B
Stele
Dry mass (%)
A
B
B
B
*
AB
A
BC
C
*
C
Rhizome
Dry mass (%)
A
B
AB
A
B
AB
A
B
B
B
*
*
*
Days post rain

Chapter 3

High-resolution computed tomography reveals dynamics of desiccation and rehydration in fern petioles of a desiccation-tolerant fern

Abstract

Desiccation-tolerant (DT) plants can dry past -100 MPa and subsequently recover function upon rehydration. Vascular DT plants face the unique challenges of desiccating and rehydrating complex tissues without causing structural damage. However, these dynamics have not been studied in intact DT plants. We used high resolution micro-computed tomography (microCT), light microscopy, and fluorescence microscopy to characterize the dynamics of tissue desiccation and rehydration in petioles (stipes) of intact DT ferns. During desiccation, xylem conduits in stipes embolized before cellular dehydration of living tissues within the vascular cylinder. During resurrection, the chlorenchyma and phloem within the stipe vascular cylinder rehydrated prior to xylem refilling. We identified unique stipe traits that may facilitate desiccation and resurrection of the vascular system, including xylem conduits containing pectin (which may confer flexibility and wettability); chloroplasts within the vascular cylinder; and an endodermal layer impregnated with hydrophobic substances that impede apoplastic leakage while facilitating the upward flow of water within the vascular cylinder. Resurrection ferns are a novel system for studying extreme dehydration recovery and embolism repair in the petioles of intact plants. The unique anatomical traits identified here may contribute to the spatial and temporal dynamics

of water movement observed during desiccation and resurrection.

Introduction

Desiccation-tolerant (DT) plants can survive near-complete water loss and subsequently recover following rehydration (Alpert, 2005). Desiccation tolerance allowed early plants to colonize dry land before the evolution of a cuticle, stomata, and a vascular system (Oliver *et al*., 2000). While today most plants remain DT at the seed or spore stage, relatively few vascular plants have re-evolved DT in their vasculature-dependent leaves, stems, and roots (Oliver *et al*., 2000). Such plants are aptly named "resurrection plants" for this ability to recover from apparent death. Resurrection plants persist in dry habitats, including rocky outcrops with shallow soil (Porembski & Bartholt, 2000; Holmlund *et al*., 2016). Desiccation tolerance may allow plants to survive in regions affected by seasonal drought, such as the mediterranean-type chaparral ecosystem (Holmlund *et al*., 2016) and other arid or semi-arid ecosystems (Gaff, 1977; Gaff & Latz, 1978; Gaff, 1987). Desiccation tolerance of the leaves, stems, and roots (vegetative DT) has evolved several times, allowing diversity and distinction between groups of DT plants (Gaff & Oliver, 2013). For instance, *Pleopeltis polypodioides* is a DT fern that thrives as an epiphyte in subtropical moist regions, albeit in a dry epiphytic habitat.

In addition to orchestrating revival processes at the molecular and cellular levels, vascular DT plants must also transport water to dry distal tissues with varied composition and function. Thus, vascular DT plants face three challenges unique to

vascular plants. First, they need to experience orderly desiccation of distinct tissue types (e.g., xylem, phloem, chlorenchyma, parenchyma) in order to prevent damage during desiccation. Tough and flexible tissue may facilitate a successful transition to the desiccated state. Second, vascular DT plants also need to resurrect distinct tissue types in a specific and orderly manner. Finally, they need to restore hydraulic flow through xylem conduits in order to transport water to distal desiccated tissues lacking abundant access to water.

Studies of the mechanisms of DT whole-plant recovery have been limited either by the need to cut the plant open to observe anatomical changes or by the need to infer internal processes from external physiological measurements (Sherwin *et al*., 1998; Schneider *et al*., 2000). Such invasive and destructive techniques have the potential to introduce artifacts. While these destructive studies have led to important insights into DT, a complement to such studies is to use advanced imaging techniques such as high-resolution micro-computed tomography (microCT) that uses tissue penetrating x-rays to visualize the internal details of a plant without cutting it open and disturbing function. In the last decade, microCT technology has developed and has been used to image the reversal of gas embolism inside xylem conduits of woody plants (Brodersen *et al*., 2010). Here we report that microCT is also a useful tool to visualize the dynamics of desiccation and resurrection in the stipes of DT ferns.

Resurrection in vascular DT ferns represents an extreme case of embolism repair, since the xylem conduits are completely gas-filled in a deeply-desiccated state

(<-100 MPa). In this study, we used microCT to characterize the desiccation and resurrection processes in the stipes of intact resurrection ferns. Given the seasonal water potentials reported in Holmlund *et al*. (2016), we hypothesized that water under tension in xylem conduits would cavitate early in desiccation (approx. -1 to -3 MPa), while solutes in living phloem and parenchyma cells would retain some water when desiccated. We also hypothesized that xylem conduits would rehydrate before phloem cells, because gas-filled xylem conduits may provide less resistance to water flow than desiccated living cells containing membranes and organelles. Therefore, we predicted that the xylem tissue would be the first to desiccate and the first to rehydrate.

Additionally, vascular DT ferns likely have differences in chemical composition among the distinct tissue types found in stipes to regulate desiccation and resurrection. Because of their pivotal location for water transport between soil and leaves, stipe tissues were examined for any unique traits that might explain the desiccation and rehydration patterns found with microCT. We used staining combined with light and fluorescence microscopy to identify the chemical composition of tissues inside the stipe. Of particular interest were cellular compounds that confer toughness (lignin) or flexibility (pectin), as well as cellular structures that impede the flow of water, such as the Casparian-like strip in the endodermis.

Materials and Methods

Plant material

We grew individuals of *Pentagramma triangularis* (Kaulf.) in a greenhouse at the University of California, Santa Cruz, from locally obtained spores. Plants were grown in 7.5 cm pots under partial shade with regular watering. Plants dried naturally during the desiccation experiment, and each of the 15 plants was only imaged one time with microCT. A different group of plants was used for the resurrection experiment. These plants dried naturally before the experiment with no prior exposure to x-ray radiation. During the resurrection experiment, we watered the plants at the roots and sealed them inside a plastic bag to increase the humidity. To reduce variation in recovery dynamics, we consistently resurrected plants under low light (PPFD = c.15 μmol m^{-2} s^{-1}). During resurrection, we imaged each of ten plants one to four times. Images were timed to capture the full range of hydration, starting with desiccated plants (pre-watering) through rehydrated plants (up to 25 hrs post watering). The ferns resurrected similarly regardless of how many times they were imaged, and no signs of radiation damage were observed (Petruzzellis *et al*., 2018). In several plants, we conducted repeat scans to confirm expansion of the outer stele early in the resurrection process, since there was variation in the size of the dry stele (Fig. S1).

High resolution micro-computed tomography (microCT)

During desiccation and resurrection, we imaged the stipes of intact plants using

high resolution computed tomography (microCT and also abbreviated as HRCT; Bruker Corporation, Skyscan 2211, Kontich, Belgium). To avoid root damage, the entire contents of each pot were wrapped in parafilm and attached to a rotating pedestal inside the scanner. We stabilized fronds by securing them with plastic wrap to a bamboo stick, allowing 1-4 stipes to be imaged on each plant. Stipes were scanned 7 cm above the root base at 1-3 μm resolution, with most scans lasting 10-20 min. We took longitudinal images every 0.15-0.25 degrees over a range of 180 degrees, and the x-ray energy used was 40 kV and 600 μA. From these images, we built 3D reconstructions of each stipe using InstaRecon software (InstaRecon, Champaign, IL, USA). Distinct tissue types became apparent based on differences in x-ray absorption, including the cortex, phloem/chlorenchyma layer, and gas-filled xylem (Fig. 1). A 2-dimensional cross section was extracted from the middle of each 3D reconstruction to measure relative area of each tissue type (CTAn software, Bruker Corporation, Billerica, MA, USA).

After the stipes appeared fully resurrected as seen using microCT, we wished to confirm that the water in the xylem conduits was moving (i.e., the conduits were functional, not just water-filled). We excised two resurrected stipes under water and placed them into 150 mM iohexol solution for 1-2 hrs while illuminating them with light (PPFD = c. 200 μmol m^{-2} s^{-1}; Pratt & Jacobsen, 2018). Iohexol is an x-ray dense molecule with a topological polar surface area of 2 nm^2, small enough to pass in solution through xylem pit membranes but large enough to stay in the apoplast (Pratt

& Jacobsen, 2018). Thus, transpirational uptake of iohexol solution confirmed that most (and possibly all) of the refilled xylem conduits were capable of transporting water (Fig. 1H).

Leaf water potential

Throughout desiccation and resurrection, we measured leaf water potential (Ψ_{leaf}) of individual plants at the time of microCT imaging. Ψ_{leaf} was measured twice in most plants during the resurrection experiment: once in the desiccated state and once after the last image was taken of that plant resurrecting. (No stipes were imaged after the leaf was removed.) We measured Ψ_{leaf} using WP4C dew point hygrometers that are capable of measuring samples from zero to -300 MPa (Decagon Devices, Pullman, WA, USA). We excised leaves from stipes shortly after the plant was imaged with microCT or from an adjacent frond immediately before imaging. We sealed the leaf tissue in two plastic bags for any interim time. The leaf tissue was quickly cut into narrow strips (<1 mm) inside a humid bag and then placed inside the chamber of the dew point hygrometer for the reading. The hygrometer internally sealed the chamber adjacent to a small mirror and adjusted the temperature of the mirror until the fogging point (dew point) was determined. Equilibration time was usually 15 to 30 min. Cutting the leaf tissue into narrow strips expedited equilibration time.

Furthermore, since the desiccation time for each plant was variable, Ψ_{leaf} provided a better predictor of changes in tissue status than time since watering (Fig.

2C-J). Unless distinct differences were apparent among fronds on a single plant (e.g., drastic difference in height or resurrection status), Ψ_{leaf} of a single leaf was measured to represent all stipes on the plant at that time.

Light and fluorescence microscopy

We examined stipe cross-sections using light and fluorescence microscopy to identify traits that may facilitate the desiccation and resurrection processes (Fig. 3). Fresh cross-sections were prepared by hand using razor blades (GEM single edge stainless steel PTFE-coated blades, Electron Microscopy Sciences, Hatfield, PA, USA) to cut thin sections that were then mounted in water for microscopic examination. Other fern stipes were placed in 10% neutral buffered formalin solution (Fisher Scientific, Protocol, Kalamazoo, MI, USA), for a minimum of 48 hrs prior to being sectioned. Then we viewed samples either unstained or following staining with phloroglucinol-HCl or acid fuchsin with stains prepared following Ruzin (1999). Lignin was identified by staining with phloroglucinol-HCl (Jensen, 1962; Fig. 3E-F), and glycoproteins were stained with acid fuchsin (Fulcher & Wong, 1982; Crews *et al*., 1998; Fig. 4G-H). Cross-sections were viewed either using light microscopy or fluorescence microscopy (Zeiss Stereo Discover V.12 with Axiocam HRc digital camera, Carl Zeiss Microscopy, LLC, Thornwood, NY, USA). For each sample preparation (fresh v. fixed) or stain (no stain, phloroglucinol-HCl, or acid fuchsin), we examined at least six and often many more sections from different stipes.

Statistical analyses

We conducted all statistical analyses using R (version 3.5.0; R Core Team, 2018). Ψ_{leaf} was log-transformed to fit assumptions of normality. When testing for correlation, we fit data with a standardized major axis regression (smatr package; Warton *et al*., 2012). Although we calculated the regression using the average values from all stipes on a plant (1-4 stipes per plant), we plotted the individual stipes to show variation (Fig. 2C-J). Regressions were considered significant at $p < 0.05$.

Results

Vascular anatomy

MicroCT revealed four important anatomical regions in the stipes of *P. triangularis*: epidermis; cortex; stele, including the vascular cylinder and gas-filled xylem conduits in desiccated samples; and a gap between the cortex and stele in desiccated samples (Fig. 1 and 2B). In transverse section, cortex tissue comprised the majority of the stipe, including the outer sclerenchyma layer and interior parenchyma. This cortex tissue desiccated during development and never rehydrated during resurrection. The vascular cylinder (stele) included chlorenchyma, phloem, and xylem. The phloem and chlorenchyma tissue were indistinguishable using microCT, but these tissues could be identified using light and fluorescence microscopy (Fig. 3). Fluorescence microscopy revealed a Casparian-like strip within the endodermal layer surrounding the vascular cylinder, but this layer could not be distinguished from the

other tissues using microCT (see Fig. 3).

The stages of development affected which tissues were gas-filled. The stipes of mature fronds had dry cortex tissue, whereas young stipes had hydrated cortex tissue (image not shown). Hydrated cortex cells would have been necessary for early stipe growth because turgor pressure is a prerequisite for cell enlargement. Interestingly, little to no native gas embolism in xylem conduits was observed in any mature fronds before the start of desiccation (Fig. 1A).

Desiccation

We desiccated individuals of *P. triangularis* in pots to observe the tissue responses in their stipes. Based on all the images collected during the desiccation process, we identified three clearly differentiated stages of desiccation (summarized in Fig. 1). First, consistent with our initial hypothesis on desiccation sequence, embolized xylem conduits became clearly visible early in the desiccation process (Fig. 1B). Second, subsequent to initial embolism of xylem conduits, phloem and chlorenchyma tissues shrunk, progressively pulling the outermost endodermal layer of the stele away from the cortex, thus forming a widening gap between the collapsing vascular cylinder and the cortex (Fig. 1C). We observed large quantities of embolized conduits in all images with shrinking phloem and chlorenchyma tissue (Fig. 1C), indicating that the majority of cavitation in the xylem likely occurs before the living tissue condenses. Third, additional desiccation caused further compression of the phloem and chlorenchyma (Fig. 1D).

Resurrection

We watered the soil of intact, desiccated individual plants in pots and kept them inside sealed bags to maintain a humid environment. Desiccated fronds showed gas-filled cortex and xylem cells and shrunken phloem and chlorenchyma (Fig. 1E). However, in contrast to expectation, the phloem and chlorenchyma rehydrated first, not the xylem, filling the gap between the vascular cylinder and cortex (Fig. 1F). Early expansion of the phloem and chlorenchyma was most apparent in several instances where fronds were re-imaged early in resurrection (Fig. S1). Second, xylem conduits refilled, evident in images that show a mix of both water-filled and gas-filled conduits (Fig. 1G). Lastly, fully resurrected stipes closely resembled never-desiccated stipes in appearance (Fig. 1A, H).

To determine whether resurrected xylem conduits were functional (moving water), we excised resurrected fronds under water and fed iohexol solution to the cut end of the stipe for 1-2 hours while plants were transpiring (Pratt & Jacobsen, 2018). The imaged stipes confirmed that water (iohexol solution) was moving through the refilled xylem conduits (Fig. 1H). The cortex tissue showed no signs of rehydration (Fig. 1F-H).

Changes in tissue area with leaf water potential

Ψ_{leaf} ranged from -125 MPa (desiccated) to approximately -1 MPa (hydrated). Ψ_{leaf} of resurrecting fronds increased with time since watering ($p < 0.0001$, Fig. 2A).

Ψ_{leaf} of desiccating fronds was highly variable, possibly because the leaf tissue of this species is hydraulically disconnected from the stipe following complete xylem embolism around -3 MPa (H. Holmlund, unpublished data). The Ψ_{leaf} of hydrated plants was consistent with the normal range of Ψ_{leaf} in the field (approx. -1 to -2.5 MPa; Holmlund *et al*., 2016). The transverse area of each region within the stipe (total area, gap between cortex and vascular cylinder, stele, gas-filled xylem; Fig. 2B) was measured at varied stages in the desiccation and resurrection processes. The total transverse area of the stipe did not change with decreasing or increasing Ψ_{leaf}, consistent with our observation that the cortex desiccates during development and does not refill during resurrection (Fig. 2C-D). In contrast, other transverse regions of the stipe (gap, stele, and gas-filled xylem) changed area with decreasing or increasing water potential (Fig. 2E-J).

Tissue chemical composition

We used light and fluorescence microscopy to elucidate the role of each tissue in producing the patterns observed with microCT. We observed stipe cross-sections using light microscopy, reactivity to different histological stains (phloroglucinol-HCl for lignin, acid fuchsin for glycoproteins), autofluorescence, and a combination of stains and fluorescence (Fig. 3). Autofluorescence revealed that the cell walls within the cortex tissue included several constituents (Fig. 3A-B). Lignin was present in the cell walls of cortex parenchyma surrounding the stele, as well as in the cell walls of the sclerenchyma tissue near the epidermis (yellow walls, Fig. 3A-B; red stain, Fig. 3E).

Fluorescence also indicated the presence of cellulose, suberin, and pectins within cell walls in the cortex (red and yellow autofluorescence, Fig. 3A-B). Suberized Casparian-like strips occurred between the cells in the endodermis, and the endodermis layer remained joined to the collapsing stele during desiccation (Fig. 3C-D; Casparian-like strips are bright yellow in 3D). A parenchyma layer containing densely packed chloroplasts (chlorenchyma) lay immediately interior to the endodermis (chloroplasts exhibit red autofluorescence in Fig. 3C-D). The chlorenchyma chloroplasts autofluoresced (red) more brightly in the resurrected state (Fig. 3D) than in the desiccated state (Fig. 3C) and less brightly in fixed tissue (Fig. 3F). The xylem conduits contained a small degree of lignin, evidenced by a weak turquoise-blue autofluorescence signal (Fig. 3C-D) and weak staining with phloroglucinol-HCl (Fig. 3E). The xylem conduits also contained pectin, which autofluoresced yellow, blending with the blue lignin signal in Fig. 3C-D. Pectin was also evident based on the yellow fluorescence signal in Fig. 3F. The discrete locations within the vascular cylinder for chlorenchyma and phloem tissues were clear in some samples, particularly when they were fixed prior to sectioning (Fig. 3E-F). Lastly, glycoproteins lined the walls of the xylem conduits, which stained pink with acid fuchsin (Fig. 3G), and this was also evident when stained samples were examined using fluorescence (Fig. 3H).

Discussion

The resurrection fern *P. triangularis* is a novel system for studying embolism formation and repair in the xylem of intact plants. We found that desiccation in *P.*

triangularis dramatically differs from the drying process in desiccation-intolerant plants. In most species, cell membranes are destroyed during the desiccation process (Hoekstra *et al*., 2001). In contrast, *P. triangularis* showed an orchestrated, reversible sequence of events during desiccation and resurrection in the stipe. Since the cortex was gas-filled in all mature stipes, all desiccation and resurrection changes in stipe tissues occurred inside the vascular cylinder. The use of microCT was valuable for elucidating the sequential dynamics of the desiccation and resurrection processes in an intact DT plant.

Conceptual model of desiccation and resurrection

We propose a biophysical model for the desiccation and resurrection processes in *P. triangularis* (Fig. 4). At frond maturity, outer cortex cells in the stipe undergo apoptosis and cellular dehydration, but these cortex tissues remain rigid, providing continued mechanical support for the vascular cylinder. Dry soil in combination with a dry atmosphere causes increased tensions on xylem water in the stele, leading to cavitation and near-complete embolism of xylem conduits. Complete xylem embolism may initiate a controlled, consistent drying speed of the leaf tissue as well as symplastic stipe tissues (phloem and chlorenchyma). The osmotic potential of the living phloem and chlorenchyma cells is likely much lower than that of xylem sap, allowing these tissues to retain water longer than the xylem conduits, although this hypothesis has not been tested in DT ferns. The phloem and chlorenchyma shrink as the tissues lose water.

Following soil rehydration in a humid environment, the stipes rapidly rehydrate,

within 24 hours. First, when the roots are soaked with water, water moves through the roots into the living tissues in the stipe vascular cylinder, rehydrating the chlorenchyma and phloem. The low osmotic potential of the desiccated symplastic cells in the stipe vascular cylinder may provide the driving force for this rapid movement of water. Second, the xylem conduits refill, restoring water flow to the leaves. Three factors may contribute to embolism repair in the xylem conduits. First, capillary rise may facilitate passive refilling of xylem conduits. Second, root pressure generated by the resurrected roots (or rhizome) may push water up the xylem conduits towards the leaves. This hypothesis is supported by previous studies showing that root pressure aided refilling in DT plants (Schneider *et al*., 2000; Holmlund *et al*., 2020 (chapter 2); but see Sherwin *et al*., 1998). Third, densely packed chloroplasts in the chlorenchyma may be associated with high cellular sucrose concentrations, perhaps attracting water by osmosis into the stele via the roots. Desiccated steles of another DT fern species showed high sucrose concentrations (Holmlund *et al*., 2020, chapter 2). This sucrose is likely produced during the dehydration phase and may help with stabilizing cellular structures as a compatible solute during desiccation. This is suggested in our study because we resurrected our plants at very low PPFD and production of abundant sucrose would be unlikely. It could come from hydrolyzing starch during resurrection, but we did not find starch in these tissues using I_2KI staining (data not shown). Rehydrated parenchyma cells adjacent to xylem conduits may assist with refilling, as shown previously in grapevine (Brodersen *et al*., 2010). Furthermore, previous studies have suggested that sucrose may trigger active refilling in xylem conduits (Secchi &

Zwieniecki, 2011); however, this hypothesis remains untested in DT species. Taken together, rehydration likely requires a combination of capillarity, root pressure, and metabolic activity to refill xylem conduits.

This hydraulic model for desiccation and recovery in DT ferns complements studies of embolism repair in non-DT plants. Stems (or stipes) occupy a critical position as the sole pathway for water from the roots to the leaves. Since stem xylem embolism is linked to mortality in non-DT plants, understanding mechanisms of embolism repair is timely and relevant (Pratt *et al*., 2008; Klein *et al*., 2018). Desiccation-tolerant ferns represent an extreme case of embolism formation, since all water is removed from the xylem conduits in the desiccated state. Few vascular plants are DT, and most DT vascular plants are small in stature (Alpert, 2006). Desiccation tolerance in vascular plants may be taxonomically limited partly because recovery from complete xylem embolism is too great a barrier to recovery from the extremely desiccated state. A better understanding of embolism repair in DT ferns may elucidate requirements for the DT trait in other vascular plants. This knowledge is relevant both to the potential development of DT crops and also to our understanding of DT evolution.

Key stipe anatomical traits

The use of light and fluorescence microscopy to illuminate the chemical composition and arrangement of stipe tissues complemented our findings from microCT. For instance, autofluorescence and staining with phloroglucinol-HCl revealed that the tracheid walls in these ferns are likely more flexible than the tracheids

of woody plants. Pectins, glycoproteins, and reduced lignin content may provide the conduits with increased flexibility compared to the strongly lignified conduits of woody plants, preventing the conduits from breaking as the vascular cylinder shrinks during desiccation. This hypothesis is consistent with previous reports of DT leaf cell walls containing arabinan-associated pectins and arabinogalactan proteins, which are hypothesized to contribute to cell wall flexibility during desiccation (Moore *et al*., 2006; Moore *et al*., 2008; Moore *et al*., 2013). Furthermore, this observation is consistent with previous data showing that fern tracheids have an unusually low double wall thickness to diameter ratio, likely conferring increased flexibility and low implosion resistance (Pittermann *et al*., 2011). Additionally, a previous study has proposed that the combination of hydrophilic pectin and hydrophobic lignin increases surface wettability of xylem in maize root vessels (McCully *et al*., 2014). Increased wettability could contribute to capillary rise in xylem conduits, but more detailed anatomical studies are required to determine if xylem conduits in *P. triangularis* show increased wettability compared to conduits in other species.

The vascular cylinder contained densely packed chloroplasts that are likely functionally important. Xylary chloroplasts have previously been linked with embolism repair and improved cavitation resistance (Schmitz *et al*., 2012; De Baerdemaeker *et al*., 2017), but to our knowledge, this is the first report of chloroplasts in the vascular tissue of a DT plant species. Chlorenchyma may provide a source of osmotically active molecules (sucrose), contributing to the movement of water into the chlorenchyma and phloem early in resurrection. Rehydrated parenchyma may have a role in active xylem

refilling, as suggested previously (Hacke & Sperry, 2003; Brodersen *et al*., 2010; Secchi & Zwieniecki, 2011; Secchi & Zwieniecki, 2012; Secchi *et al*., 2017). Furthermore, chloroplasts may provide energy in the form of ATP to facilitate active xylem refilling. Previous studies have suggested that energy has a role in active xylem refilling (Holbrook & Zwieniecki, 1999; Salleo *et al.*, 2004). ATP may facilitate xylem refilling by fueling the active transport of sugars into the xylem conduits to generate an osmotic gradient, but hypothesis remains untested in DT ferns.

Light microscopy also revealed an endodermal layer with Casparian-like strips surrounding the vascular cylinder, analogous to the endodermis found in roots. This endodermal layer is frequently found in fern stipes (Lersten, 1997; Sperry, 2003; Pittermann *et al.,* 2015). In *P. triangularis*, the endodermal layer remains attached to the shrunken vascular cylinder during desiccation (Fig. 3C-D). In a resurrection fern, this endodermal layer may act similarly to that in a root, preventing water from leaking out of the vascular cylinder into the cortex, especially if plasmodesmata between cortex and endodermis were disrupted during development or desiccation and not repaired during rehydration. This may contribute to the lack of cortex rehydration during the resurrection process. If this is the case, the endodermis may facilitate the upward movement of water towards the leaf tissue, rather than outward movement into the cortex.

The desiccated cortex appears to provide mechanical support in both desiccated and rehydrated stipes, because desiccated fronds remain upright (H. Holmlund,

personal observation). In hydrated plants, the cortex appears to desiccate either during development or following even slight desiccation, since all stipes of hydrated plants showed desiccated cortex except for two stipes with immature leaf tissue. This supportive function of desiccated cortex is likely facilitated by the lignin and high cellulose content of the cortex cells in their perennially desiccated state. A previous study has reported that other Cheilanthoid fern species also have lignified cortex tissue (Mahley *et al*., 2018). Rakic *et al*. (2017) also found a gap between the vascular cylinders and the cortex in the desiccated state in DT angiosperms *Ramonda serbica* and *R. nathaliae*. However, these studies did not report findings of desiccated cortex tissue in resurrected intact plants. The phylogenetic extent of dry, lignified cortex tissue may provide insight into the evolutionary history of the DT strategy.

Whole-plant DT in other species

Since vegetative DT has evolved several times in vascular plants (Gaff & Oliver, 2013), other DT species may show contrasting mechanisms of whole-plant resurrection. For instance, *Pleopeltis polypodioides* has been shown to resurrect via specialized scales on the leaf surface (John & Hasenstein, 2017). Consequently, stipe anatomical traits may be less critical for resurrection in this species, as foliar water uptake likely plays a more significant role in the resurrection process. Additionally, several DT angiosperm species have been studied extensively, including *Myrothamnus flabellifolius, Craterostigma wilmsii,* and *Xerophyta* spp.; however, most of these studies have focused on biochemical and molecular processes (Vicre *et al*., 2004;

Farrant, 2007; Moore *et al*., 2007; Farrant *et al*., 2015; but see Sherwin & Farrant, 1996; Sherwin *et al*., 1998). Desiccation and resurrection dynamics in DT angiosperm species likely differ from DT fern species due to differences in vascular anatomy, such as DT angiosperms' lack of an endodermal layer. More anatomical studies of DT fern and angiosperm species may reveal which traits are generally essential for DT.

Pentagramma triangularis may represent the resurrection dynamics in other DT fern species with a similar vascular anatomy and ecological niche. Whole-plant DT has separately evolved several times; thus, varied suites of traits likely contribute to whole-plant DT across the phylogeny. Since DT plants successfully occupy dry niches, it will be interesting to learn what anatomical and physiological traits (or combinations of traits) are most essential for DT. Beyond increasing understanding of the DT strategy, the mechanisms of whole-plant resurrection may provide useful information about xylem refilling.

Author Contributions

This chapter was originally published as the following journal article in *New Phytologist*:

Holmlund HI, Pratt RB, Jacobsen AL, Davis SD, Pittermann J. 2019. High-resolution computed tomography reveals dynamics of desiccation and rehydration in fern petioles of a desiccation-tolerant fern. *New Phytologist* 224(1): 97-105.

All authors contributed to developing the question and experimental design. H.I.H.,

R.B.P, and A.L.J. conducted microCT experiments. A.L.J. conducted staining and light microscopy analyses. All authors contributed to interpretation of results. H.I.H., J.P., and S.D.D. wrote the manuscript with contributions from all authors.

Figure 1: Representative microCT transverse images of *Pentagramma triangularis* stipes during desiccation and resurrection (A-H). Scale bars represent 1 mm. Prior to desiccation, mature, hydrated stipes showed desiccated cortex tissue surrounding a fully hydrated vascular cylinder (A). Early in desiccation, the xylem conduits became gas-filled (B). Subsequently, the living tissues in the vascular cylinder (phloem and chlorenchyma) compressed (C). Fully desiccated stipes showed gas-filled xylem and a shrunken vascular cylinder, leaving a gap between the vascular cylinder and cortex (D-E). Early in resurrection, the phloem and chlorenchyma expanded (F). Later, xylem conduits refilled (G). Fully resurrected stipes resembled mature, never-desiccated stipes (H). Resurrected xylem conduits functioned in water transport, since iohexol solution can be seen in refilled xylem conduits (white region, indicated by arrow in panel H). A cartoon illustrating the stages of desiccation and rehydration is provided below. Stage 3 represents fully hydrated stipes, as in (A) and (H). Stage 2 includes stipes experiencing xylem cavitation or refilling, as in (B) and (G). Stage 1 includes the shrinking or expanding of living tissue inside the vascular bundle (phloem and parenchyma), as in (C-F).

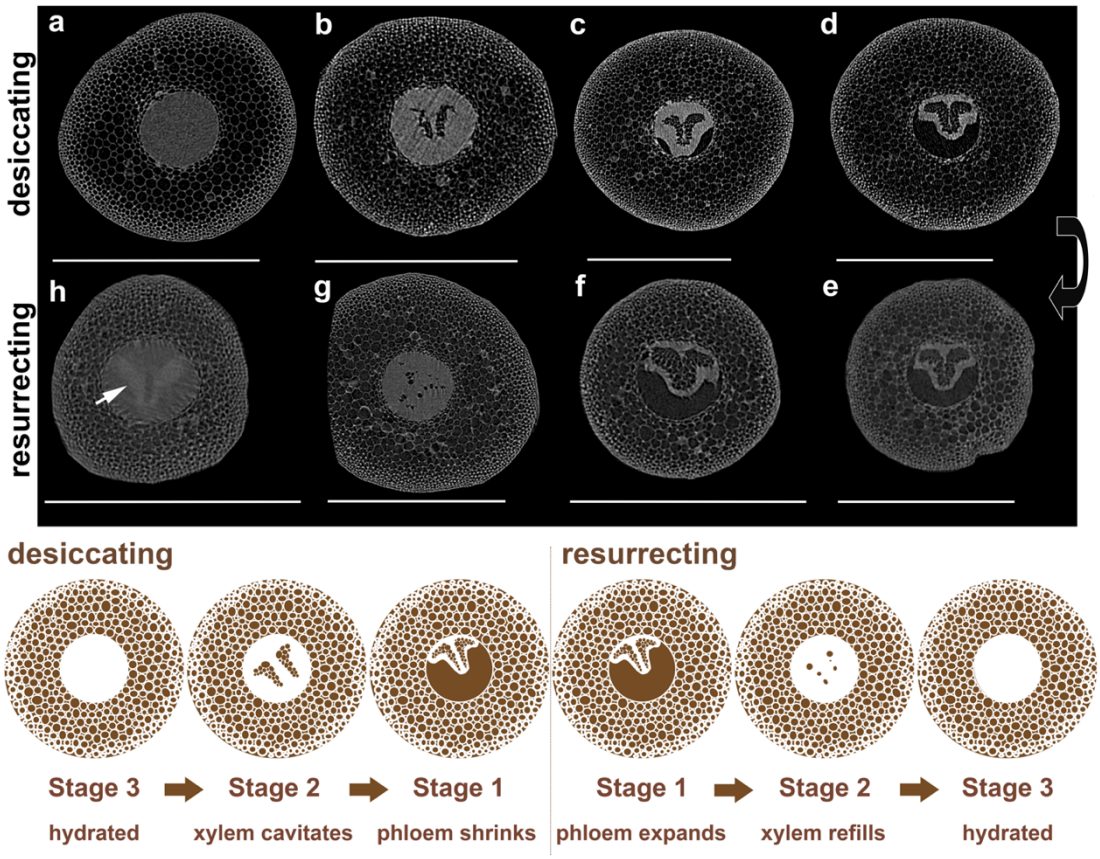
a
b
c
d
desiccating
h
g
f
e
resurrecting
desiccating
resurrecting
Stage 3
Stage 2
Stage 1
Stage 1
Stage 2
Stage 3
hydrated
xylem cavitates
phloem shrinks
phloem expands
xylem refills
hydrated

Figure 2: Changes in leaf water potential (Ψ_{leaf}) with time since watering during the resurrection process (A). Point color and shape correspond to the stage of resurrection, based on observations in Fig. 1. Stage 1 (red circles) includes plants with desiccated stipes and stipes starting to resurrect (expanding phloem and chlorenchyma). Stage 2 (green squares) includes plants with stipes showing partly refilled xylem. Stage 3 (blue triangles) includes plants with fully resurrected stipes. Tissue types distinguishable using microCT are identified in (B). Changes in transverse stipe tissue area with Ψ_{leaf} were observed during desiccation (C, E, G, I) and resurrection (D, F, H, J). No changes were observed in total transverse area with log Ψ_{leaf} (C-D), but area of the gap, stele (vascular cylinder), and gas-filled xylem correlated with log Ψ_{leaf} (E-J; standardized major axis regression, significant when $p < 0.05$). Asterisks indicate significance level (*$p < 0.05$, **$p < 0.01$, ***$p < 0.001$). The standardized major axis regressions were calculated using the mean values of all stipes in a plant (1-4 stipes per plant, n = 15 means for desiccation experiment, n = 16 means for resurrection experiment). However, data points for individual stipe values are plotted to illustrate natural variation among stipes (C-J).

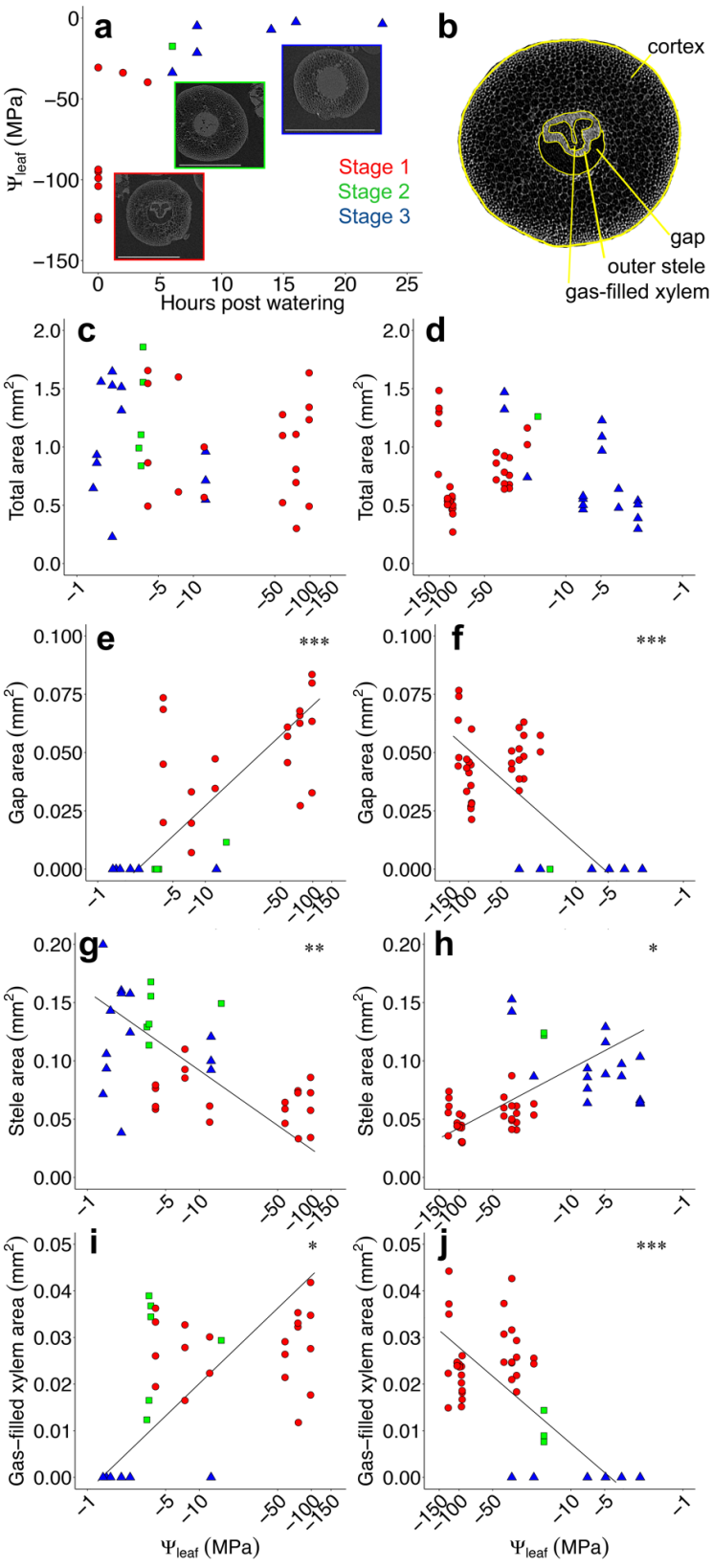
a
b
c
d
e
f
g
h
i
j
Stage 1
Stage 2
Stage 3
Hours post watering
Ψleaf (MPa)
cortex
gap
outer stele
gas-filled xylem
Total area (mm2)
Gap area (mm2)
Stele area (mm2)
Gas−filled xylem area (mm2)
***
**
*

Figure 3. Transverse sections of fresh (A-D) and fixed (E-H) *P. triangularis* stipes. Scale bar represents 100 µm (A, E, F) or 50 µm (B, C, D, G, H). Autofluorescence revealed that the cortex tissue is slightly lignified (blue) and likely contains cellulose (yellow) (A-B). The appearance of the vascular cylinder changed slightly from the desiccated state (C) to the resurrected state (D), but both images showed densely packed chloroplasts in the parenchyma surrounding the xylem and an endodermal layer (arrows) surrounding and attached to the vascular cylinder. The xylem conduits likely contain both lignin (blue) and cellulose or pectin (yellow). Staining with phloroglucinol-HCl revealed some lignin in the xylem conduits and cortex cells, but less lignin than is typical in woody angiosperms, shown with brightfield (E) and fluorescence (F). Staining with acid fuchsin revealed glycoproteins lining the interior of the xylem conduits, shown with brightfield (G) and fluorescence (H).

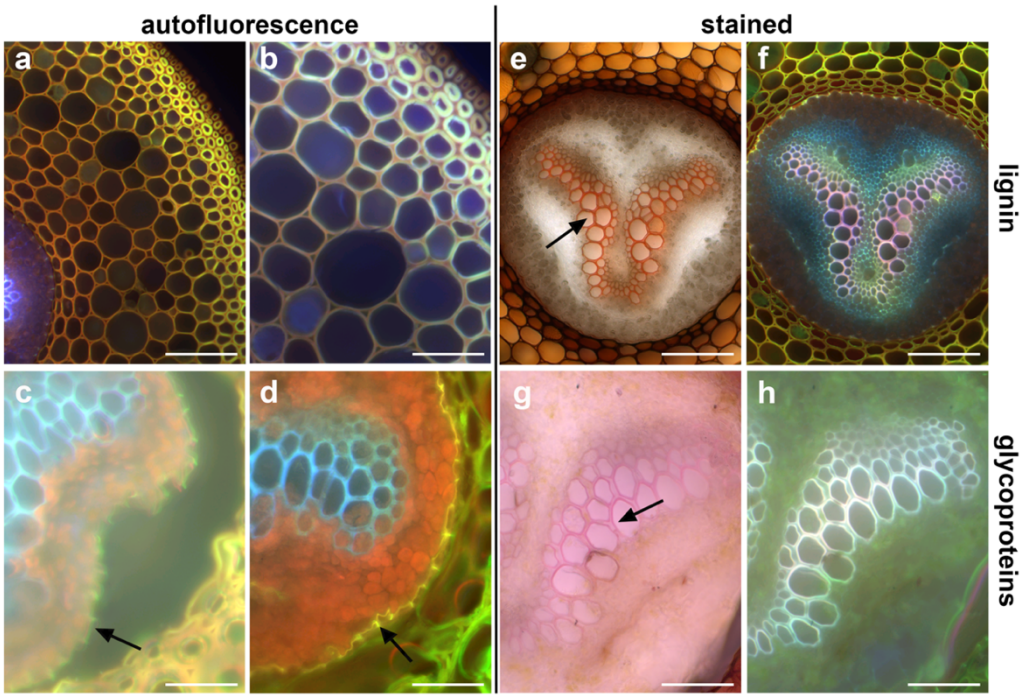

Figure 4. Conceptual diagram summarizing the findings in this study. Fully hydrated *Pentagramma triangularis* plants show desiccated cortex tissue surrounding hydrated chlorenchyma, phloem, and xylem tissue (A). During the early stages of desiccation, the stipe xylem conduits become gas-filled, reducing water flow to the leaves and also to the stipe phloem and chlorenchyma tissue (B). Later in desiccation, the stipe phloem and chlorenchyma tissue shrinks as it loses water (C). During the early stages of rehydration, the stipe phloem and chlorenchyma tissue expands as it begins to rehydrate (D). Later in rehydration, the stipe phloem and chlorenchyma tissue becomes fully expanded and the xylem conduits refill (E). Further studies are needed to fully resolve the dynamics between these three tissues during refilling. Since the phloem and chlorenchyma rehydrate first, it is possible that these tissues aid in xylem refilling (arrows in panel E). However, it is also possible that xylem refilling by capillary action or root pressure aids in the complete rehydration of the phloem and chlorenchyma tissue (arrows in panel E). A fixed cross-section of a representative stipe is shown with all tissue types labeled (F).

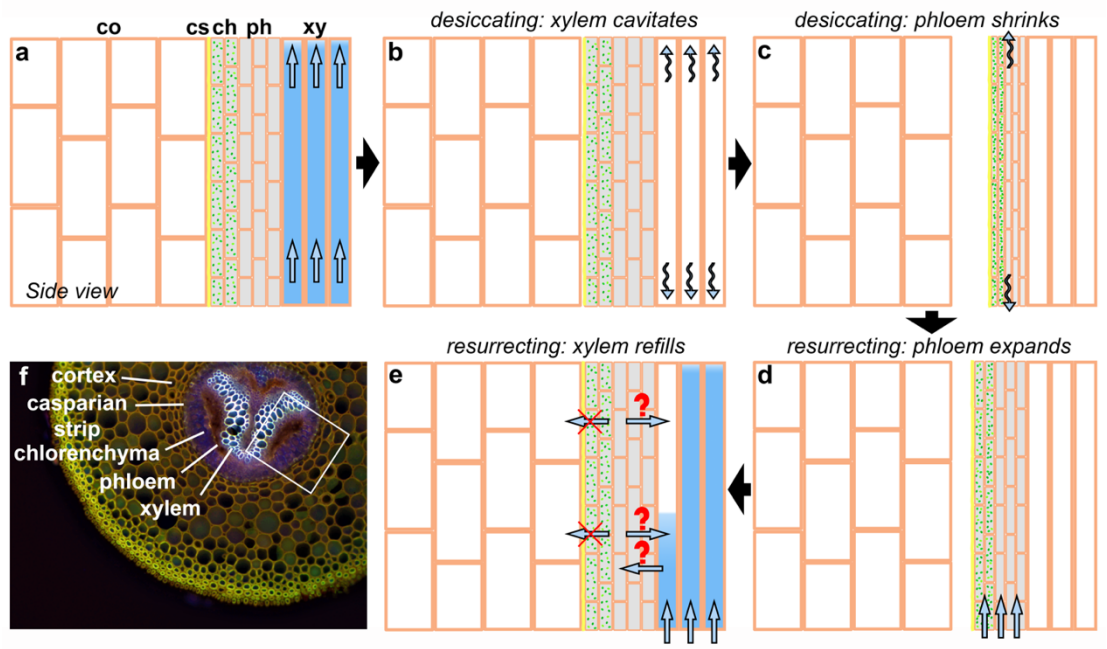
co
cs
ch
ph
xy
a
Side view
desiccating: xylem cavitates
b
desiccating: phloem shrinks
c
d
resurrecting: phloem expands
resurrecting: xylem refills
e
f
cortex
casparian strip
chlorenchyma
phloem
xylem

Conclusion

This dissertation characterizes adaptations to limited fresh water availability in two groups of ferns: the salt-tolerant mangrove ferns and the desiccation-tolerant resurrection ferns. In each system, I combined several methodological approaches to gain a holistic view of the survival strategies employed by these ferns. For the mangrove ferns, I integrated my study of physiological and anatomical traits with CEDX to contextualize the data on water relations with variation in cellular ion concentrations in ferns from high and low salinity sites. My field study captured the natural range of estuarine salinities in which mangrove ferns thrive along with their physiological extremes, and my greenhouse experiments provided insight into the role of plasticity in mangrove ferns. To examine mechanisms of whole-plant recovery in the resurrection ferns, I combined field and laboratory irrigation experiments with analyses of non-structural carbohydrates to provide insight into the role of root pressure in whole-plant recovery. Further analyses using high resolution microCT and fluorescence microscopy revealed anatomical traits that may contribute to observed patterns of desiccation and recovery. Taken together, these varied approaches provided an integrated picture of the strategies used by mangrove and resurrection ferns to thrive in their respective niches.

In **Chapter 1**, I measured physiological, anatomical, and chemical adjustments in the mangrove ferns along a salinity gradient and an atmospheric moisture gradient in tropical Australia. These results provided insight into mangrove fern adaptations

when limited fresh water is available to the roots (due to high salinity) or to the leaves (due to low atmospheric moisture). Limited freshwater availability to the roots altered water relations and gas exchange, leading to more negative osmotic potential, lower rates of carbon assimilation, and lower stomatal conductance to water vapor. Furthermore, cryo-SEM with EDX revealed that ferns growing in saline water accumulated increased Na^+ and Cl^- in their leaf cells. These findings are consistent with previous studies in mangrove tree species showing adaptations along a salinity gradient (Nguyen *et al*., 2015). However, limited freshwater availability to either the roots or leaves caused anatomical changes to limit extreme water potential gradients, such as thicker leaves (high LMA) and smaller, more dense stomata. My greenhouse experiments revealed that water relations and gas exchange did not adjust to increased estuarine salinity in a short time frame (one month), indicating that mangrove ferns might not adjust cellular osmotic potential and leaf carbon assimilation over short time scales.

In **Chapter 2**, my goal was to discover how water moves through desiccated ferns during the resurrection process. My applied pressure experiments showed that positive water pressure applied to the base of the petiole was required to resurrect distal leaf tissue, implying that root pressure has a critical role in whole-plant recovery. Interestingly, the desiccated petioles and rhizomes showed high concentrations of soluble, osmotically-active sugars such as sucrose, glucose, and fructose. Low molecular weight sugars such as sucrose have been previously revealed to protect resurrection plant tissues in the desiccated state by maintaining cellular organization as

water is lost from the cell (Moore *et al*., 2007; Peters *et al*., 2007). While further research is needed to elucidate the role of osmotically-active sugars in generating root pressure, it is possible that these sugars may function both as desiccation protectants and as generators of root pressure in these resurrection ferns.

In **Chapter 3**, I examined the reversible desiccation process in the petioles of resurrection ferns using microCT and fluorescence microscopy. Fern petioles play a key role in water transport, and the timely desiccation and recovery of the petiole vascular tissues is a critical component of the desiccation tolerance strategy. Our microCT time series revealed patterns of water movement unique to these resurrection ferns, including perennially desiccated cortex tissues, compressible phloem tissues, and flexible xylem conduits. Fluorescence microscopy revealed anatomical traits that may explain these patterns of water movement, including lignified cortex parenchyma, a suberized Casparian-like strip surrounding the petiole vascular bundle, chloroplasts in the vascular bundle, and xylem conduits composed of lignin and pectin. Lignified cortex cells have been described previously in Cheilanthoid ferns (Mahley *et al*., 2018), and likely explain how these cells can remain rigid while not turgid, thus functioning in mechanical support for the frond while remaining dry. Densely packed chloroplasts near the xylem (containing high levels of osmotically-active sugars) may aid in osmotically drawing water up the petiole vascular bundle, facilitating rapid recovery. Pectin-containing xylem conduits may be more flexible and also more hydrophilic, preventing conduit fracture during desiccation and aiding capillary rise (Moore *et al*., 2006; Moore *et al*., 2008; Moore *et al*., 2013; McCully *et al*, 2014). Future studies may

further elucidate the roles of histochemical and anatomical traits in the recovery of desiccation-tolerant ferns.

These three chapters each address the overarching goal of my graduate studies: to learn how ferns have adapted to thrive in water-limited niches. While the saltwater mangrove swamp and the arid chaparral ecosystems pose distinct environmental stressors, osmotic adjustments are a common thread between mangrove ferns and resurrection ferns. These data show that mangrove ferns adjust to high salinity by decreasing the osmotic potential of their cells, allowing the plants to draw water out of increasingly saline soil. In contrast, resurrection ferns opt to lose all water during extended seasonal drought. However, high concentrations of osmotically active molecules (including soluble sugars) likely facilitate the rapid recovery of vascular tissues and possibly enable generation of root pressure to reverse embolism in the xylem conduits. Consequently, further research into the role of osmotically active molecules in whole-plant adaptation of mangrove ferns and resurrection ferns may prove particularly fruitful.

It is also worthwhile to note the similarities and differences between fern and angiosperm adaptations to water-limited habitats. Since ferns have adapted to extreme water deficit separately from angiosperms, further research on ferns may reveal novel strategies for coping with water limitation (Schneider *et al*., 2004; Rathinasabapathi, 2006; Pittermann *et al*., 2015). For instance, mangrove ferns and mangrove trees both show evidence of osmotic adjustment to thrive in saline water, but ferns lack many of the other adaptations seen in some angiosperm halophytes, including viviparous

propagules and salt secretion from the leaves. Further research may reveal other fern adaptations to cope with the saltwater habitat, or we may discover trade-offs unique to saltwater ferns lacking these additional halophytic traits. Similarly, resurrection ferns show different anatomical traits and physiological recovery mechanisms compared to resurrection angiosperms. In this case, many of the traits discovered in my dissertation, including perennially desiccated cortex tissue and vascular chloroplasts, seem to be unique to resurrection ferns and lacking in commonly studied resurrection angiosperms. Thus, resurrection ferns may provide a particularly interesting case study for further characterizing the desiccation tolerance strategy in plants.

Both the mangrove ferns and the Cheilanthoid resurrection ferns belong to the Pteridaceae, an anatomically and physiologically diverse family including ferns filling a variety of water-limited ecosystems, such as aquatic, epiphytic, and terrestrial arid habitats (Schuettpelz *et al*., 2007; Schuettpelz *et al*., 2009; Mahley *et al*., 2018). Given this exceptional diversity, further research on the Pteridaceae may prove particularly informative in the study of fern adaptations to water-limited habitats, especially considering that most other fern species are restricted to habitats with abundant fresh water. Although the earliest ferns pre-date the appearance of angiosperms, most modern ferns (including the Pteridaceae) radiated "in the shadow of angiosperms," filling the niches created by angiosperm architects (Schneider *et al*., 2004; Schuettpelz *et al*., 2009). The Pteridaceae seem particularly adept at exploiting niches where many other ferns and angiosperms cannot survive. Consequently, it will be interesting to consider the potential of ferns (and especially the Pteridaceae) to adapt to a changing

climate. While many ferns require abundant water to thrive, fern living in the extremes (such as arid or saline habitats) may be particularly resilient in the face of climate change.

Appendix 1

Supplementary Figures for Chapter 1

Figure S1: Maps of field sites in this study. Small box in Panel A indicates the area shown in Panel B. I measured ferns growing on Lizard Island (Panel A; "Island") and on the mainland along the Daintree River (Panel A; "Mainland"). Ferns on Lizard Island received less rainfall than ferns on the mainland. Along the Daintree River, I measured ferns at the extremes of their distribution, from high estuarine salinity near the mouth of the river (Panel B; 94% seawater) to low estuarine salinity upstream (Panel B; 18% seawater). Scale bars indicate 20 km (Panel A) and 2 km (Panel B).

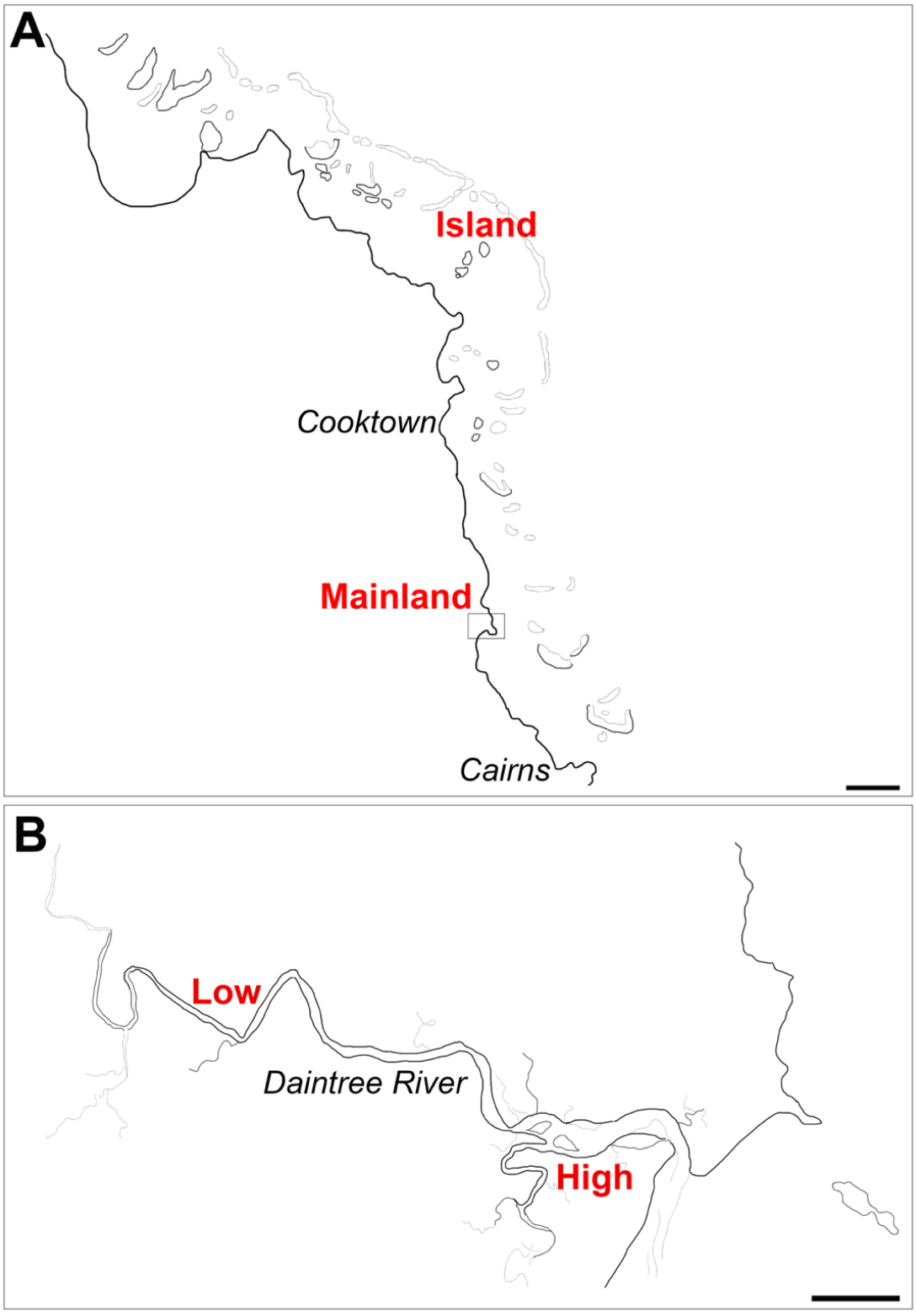
A
Island
Cooktown
Mainland
Cairns
B
Low
Daintree River
High

Figure S2: Soil water content (%) at each site. Soil samples were collected at each site and weighed before and after drying. Soil water content was calculated as the mass of water as a percent of the total mass. Differences were determined using a one-way ANOVA with a Tukey's HSD post-hoc test (letters indicate significant difference, $p < 0.05$).

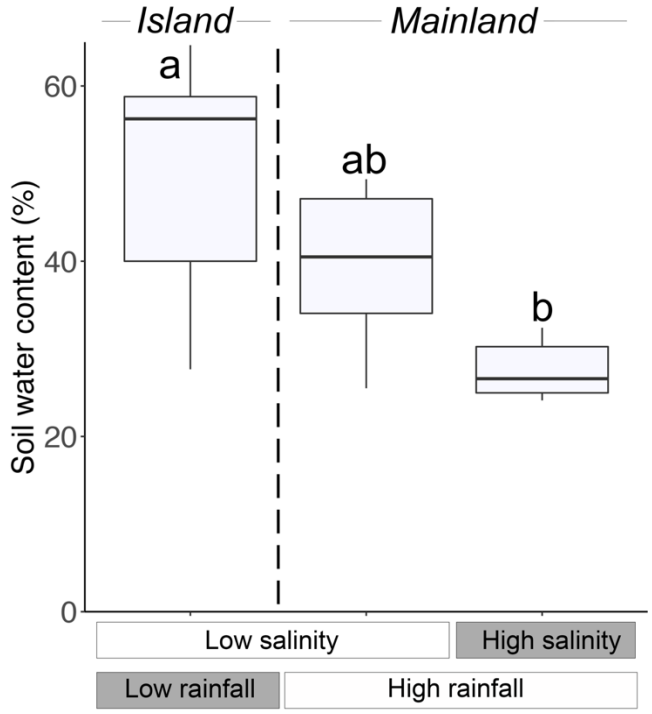

Figure S3: Calibration curves used to determine cellular element concentrations for cryo-SEM with energy dispersive x-ray (CEDX) analyses. The calibration curves were created by conducting CEDX analyses on drops taken from serial dilutions of each element.

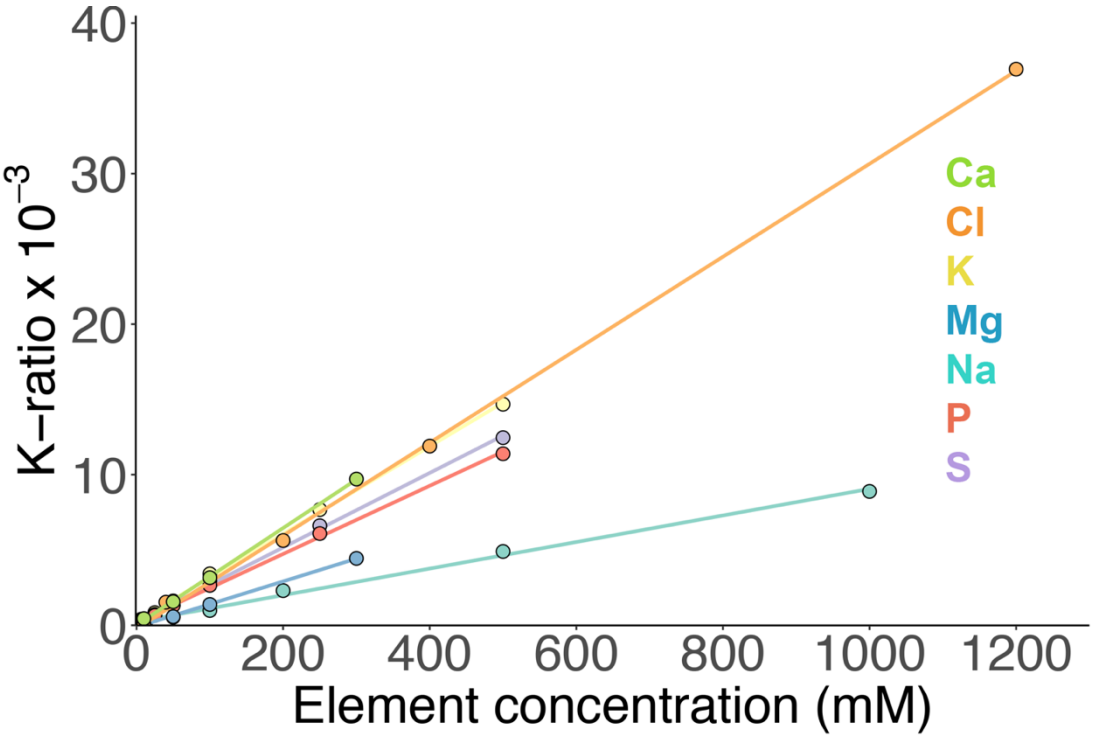

Appendix 2

Supplementary Figures for Chapter 3

Figure S1: Repeat scans of two *Pentagramma triangularis* stipes early in the resurrection process, showing expansion of the phloem and chlorenchyma prior to xylem refilling (stipe 1: A-B, stipe 2: C-D). Stipe 1 was imaged in the desiccated state (A) and 6 hrs post watering (B). Stipe 2 was imaged in the desiccated state (C) and 8 hrs post watering (D). Scale bar represents 1 mm.

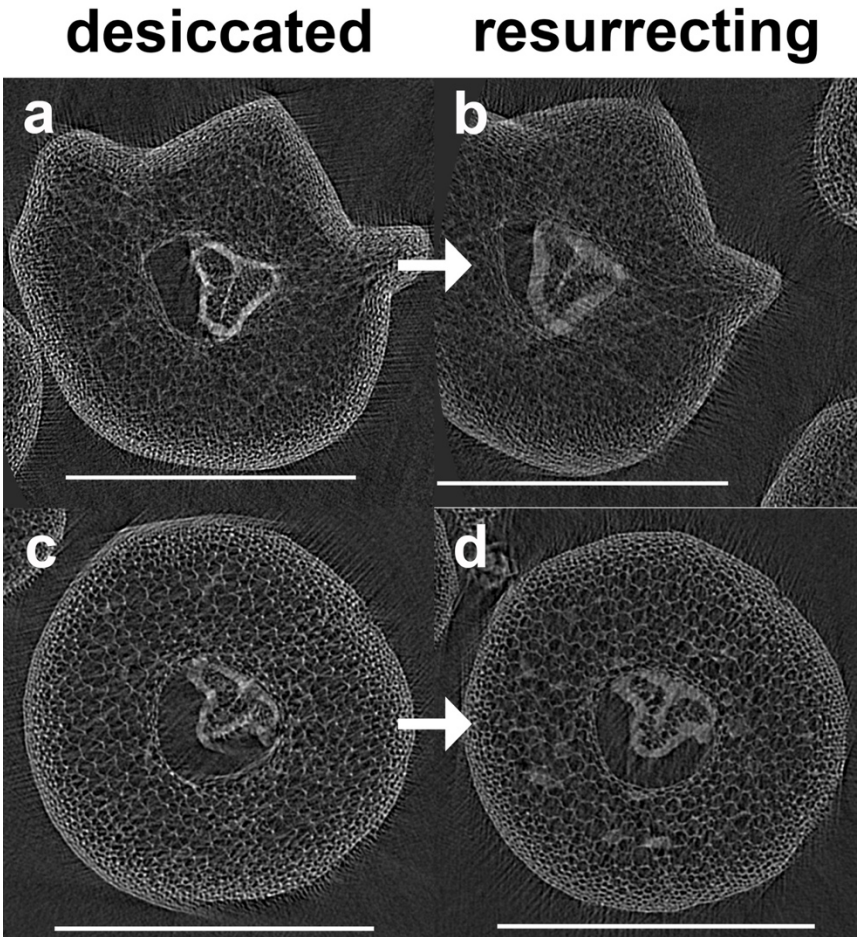

Literature Cited

Adams DC, Tomlinson PB. 1979. *Acrostichum* in Florida. *American Fern Journal* 69: 42-46.

Alcantara S, Mello-Silva R de, Teodoro GS, Drequeceler K, Ackerly DD, Oliveira RS. 2015. Carbon assimilation and habitat segregation in resurrection plants: a comparison between desiccation- and non-desiccation-tolerant species of Neotropical Velloziaceae (Pandanales). *Functional Ecology* 29: 1499–1512.

Alpert P. 2005. The limits and frontiers of desiccation-tolerant life. *Integrative and Comparative Biology* 45: 685-695.

Alpert P. 2006. Constraints of tolerance: why are desiccation-tolerant organisms so small or rare? *Journal of Experimental Biology* 209: 1575-1584.

Baldwin BG, Goldman DH, Keil DJ, Patterson R, Rosatti TJ, Wilken DH. [eds.] 2012. *The Jepson manual: Vascular plants of California.* Berkeley, California, USA: University of California Press.

Ball MC. 1988a. Ecophysiology of mangroves. *Trees* 2: 129-142.

Ball M, Cowan IR, Farquhar GD. 1988b. Maintenance of leaf temperature and the optimisation of carbon gain in relation to water loss in a tropical mangrove forest. *Functional Plant Biology* 15: 263-276.

Ball MC. 1988c. Salinity tolerance in the mangroves, *Aegiceras corniculatum* and *Avicennia marina.* I. Water use in relation to growth, carbon partitioning and salt balance. *Australian Journal of Plant Physiology* 15: 447-464.

Ball MC, Pidsley SM. 1995. Growth responses to salinity in relation to distribution of two mangrove species, *Sonneratia alba* and *S. lanceolata*, in northern Australia. *Functional Ecology* 9: 77-85.

Ball MC. 1996. Comparative ecophysiology of mangrove forest and tropical lowland moist rainforest. In: Mulkey SS, Chazdon RL, Smith, AP, eds. *Tropical Forest Plant Ecophysiology.* Boston, MA: Springer, 461-496.

Bartlett MK, Scoffoni C, Sack L. 2012. The determinants of leaf turgor loss point and prediction of drought tolerance of species and biomes: a global meta-analysis. *Ecology Letters* 15: 393-405.

Boyce CK, Brodribb TJ, Feild TS, Zwieniecki MA. 2009. Angiosperm leaf vein evolution was physiologically and environmentally transformative. *Proceedings of the Royal Society B: Biological Sciences* 276: 1771-1776.

Brander LM, Wagtendonk AJ, Hussain SS, McVittie A, Verburg PH, de Groot RS, van der Ploeg S. 2012. Ecosystem service values for mangroves in Southeast Asia: A meta-analysis and value transfer application. *Ecosystem Services* 1: 62-69.

Brodersen CR, McElrone AJ, Choat B, Matthews MA, Shackel KA. 2010. The dynamics of embolism repair in xylem: in vivo visualizations using high resolution computed tomography. *Plant Physiology* 154: 1088-1095.

Brodersen CR, McElrone AJ, Choat B, Matthews MA, Shackel KA. 2010. The dynamics of embolism repair in xylem: *in vivo* visualizations using high resolution computed tomography. *Plant Physiology* 154: 1088-1095.

Canny MJ. 2000. Water transport at the extreme – restoring the hydraulic system in a resurrection plant. *New Phytologist* 148: 187–189.

Cowling RM, Rundel PW, Lamont BB, Kalin Arroyo M, Arianoutsou M. 1996. Plant diversity in mediterranean-climate regions. *Trends in Ecology & Evolution* 11: 362–366.

Crews LJ, McCully ME, Canny MJ, Huang CX, Ling LE. 1998. Xylem feeding by spittlebug nymphs: some observations by optical and cryo-scanning electron microscopy. *American Journal of Botany* 85: 449-460.

De Baerdemaeker NJ, Salomón RL, De Roo L, Steppe K. 2017. Sugars from woody tissue photosynthesis reduce xylem vulnerability to cavitation. *New Phytologist* 216: 720-727.

Duke N, Ball MC, Ellison J. 1998. Factors influencing biodiversity and distributional gradients in mangroves. *Global Ecology & Biogeography Letters* 7: 27-47.

Ewers FW, Cochard H, Tyree MT. 1997. A survey of root pressures in vines of a tropical lowland forest. *Oecologia* 110: 191–196.

Farrant JM. 2007. Mechanisms of desiccation tolerance in angiosperm resurrection plants. In: Jenks MA, Wood AJ, eds. *Plant desiccation tolerance*. Oxford, UK: Blackwell Publishing, 51-90.

Farrant JM, Brandt W, Lindsey GG. 2007. An overview of mechanisms of desiccation tolerance in selected angiosperm resurrection plants. *Plant Stress* 1: 72-84.

Farrant JM, Cooper K, Hilgart A, Abdalla KO, Bentley J, Thomson JA, Dace HJ, Peton N, Mundree SG, Rafudeen MS. 2015. A molecular physiological review of vegetative desiccation tolerance in the resurrection plant *Xerophyta viscosa* (Baker). *Planta* 242: 407-426.

Fisher JB, Guillermo Angeles A, Ewers FW, Lopez-Portillo J. 1997. Survey of root pressure in tropical vines and woody species. *International Journal of Plant Sciences* 158: 44-50.

Flowers TJ. 2004. Improving crop salt tolerance. *Journal of Experimental Botany* 55: 307-319.

Flowers TJ, Colmer TD. 2008. Salinity tolerance in halophytes. *New Phytologist* 179: 945-963.

Flowers TJ, Galal HK, Bromham L. 2010. Evolution of halophytes: multiple origins of salt tolerance in land plants. *Functional Plant Biology* 37: 604-612.

Flowers TJ, Munns R, Colmer TD. 2015. Sodium chloride toxicity and the cellular basis of salt tolerance in halophytes. *Annals of Botany* 115: 419-431.

Franks PJ, Beerling DJ. 2009. Maximum leaf conductance driven by CO_2 effects on stomatal size and density over geologic time. *PNAS* 106: 10343-10347.

Franks PJ, Drake PL, Beerling DJ. 2009. Plasticity in maximum stomatal conductance constrained by negative correlation between stomatal size and density: an analysis using *Eucalyptus globulus*. *Plant, Cell & Environment* 32: 1737-1748.

Fuenzalida TI, Bryant CJ, Ovington LI, Yoon HJ, Oliveira RS, Sack L, Ball MC. 2019. Shoot surface water uptake enables leaf hydraulic recovery in *Avicennia marina*. *New Phytologist* 224: 1504-1511.

Fulcher RG, Wong SI. 1982. Fluorescence microscopy of cereal grains. *Canadian Journal of Botany* 60: 325-329.

Gaff DF. 1977. Desiccation tolerant vascular plants of southern Africa. *Oecologia* 31: 95–109.

Gaff DF, Latz PK. 1978. The occurrence of resurrection plants in the Australian flora. *Australian Journal of Botany* 26: 485-492.

Gaff DF. 1987. Desiccation tolerant plants in South America. *Oecologia* 74: 133–136.

Gaff DF, Oliver M. 2013. The evolution of desiccation tolerance in angiosperm plants: a rare yet common phenomenon. *Functional Plant Biology* 40: 315-328.

George LO, Bazzaz FA. 1999. The fern understory as an ecological filter: growth and survival of canopy-tree seedlings. *Ecology* 80: 846-856.

Hacke UG, Sperry JS. 2003. Limits to xylem refilling under negative pressure in *Laurus nobilis* and *Acer negundo*. *Plant, Cell & Environment* 26: 303-311.

Harvey HW. 1966. *The Chemistry and Fertility of Seawater.* Cambridge, UK: Cambridge University Press.

Hietz, P. 2010. Fern adaptations to xeric environments. In: Mehltreter K, Walker LR, Sharpe JM, eds. *Fern Ecology*. Cambridge, UK: Cambridge University Press, 140-177.

Hoekstra FA, Golovina EA, Buitink J. 2001. Mechanisms of plant desiccation tolerance. *Trends in Plant Science* 6: 431-438.

Holbrook NM, Zwieniecki MA. 1999. Embolism repair and xylem tension: do we need a miracle? *Plant Physiology* 120: 7-10.

Holmlund HI, Lekson VM, Gillespie BM, Nakamatsu NA, Burns AM, Sauer KE, Pittermann J, Davis SD. 2016. Seasonal changes in tissue-water relations for eight species of ferns during historic drought in California. *American Journal of Botany* 103: 1607-1617.

Holmlund HI, Pratt RB, Jacobsen AL, Davis SD, Pittermann J. 2019. High-resolution computed tomography reveals dynamics of desiccation and rehydration in fern petioles of a desiccation-tolerant fern. *New Phytologist* 224: 97-105.

Holmlund HI, Davis SD, Ewers FW, Aguirre NM, Sapes G, Sala A, Pittermann J. 2020. Positive root pressure is critical for whole-plant desiccation recovery in two species of terrestrial resurrection ferns. *Journal of Experimental Botany* 71: 1139-1150.

Jensen WA. 1962. *Botanical Histochemistry: Principles and Practices.* San Francisco, CA, USA: WH Freeman and Co.

John SP, Hasenstein KH. 2017. The role of peltate scales in desiccation tolerance of *Pleopeltis polypodioides. Planta* 245: 207-220.

Kirkpatrick REB. 2008. Phylogenetic analysis and desiccation tolerance of the homosporous fern genus *Pellaea* link (Pteridaceae) and relatives. PhD thesis, University of California, Berkeley, Berkeley, CA, USA.

Klein T, Zeppel MJ, Anderegg WR, Bloemen J, De Kauwe MG, Hudson P, Ruehr NK, Powell TL, von Arx G, Nardini A. 2018. Xylem embolism refilling and resilience against drought-induced mortality in woody plants: processes and trade-offs. *Ecological Research* 33: 839-855.

Lersten NR. 1997. Occurrence of endodermis with a casparian strip in stem and leaf. *The Botanical Review* 63: 265-272.

Lloret F, Sapes G, Rosas T, Galiano L, Saura-Mas S, Sala A, Martínez-Vilalta J. 2018. Non-structural carbohydrate dynamics associated with drought-induced die-off in woody species of a shrubland community. *Annals of Botany* 121: 1383-1396.

Maguire DA, Forman RT. 1983. Herb cover effects on tree seedling patterns in a mature hemlock-hardwood forest. *Ecology* 64: 1367-1380.

Mahley JN, Pittermann J, Rowe N, Baer A, Watkins JE, Schuettpelz E, Wheeler JK, Mehltreter K, Windham M, Testo W, Beck J. 2018. Geometry, allometry and biomechanics of fern leaf petioles: their significance for the evolution of functional and ecological diversity within the Pteridaceae. *Frontiers in Plant Science* 9: 197.

Marshall AT. 2017. Quantitative x-ray microanalysis of model biological samples in the SEM using remote standards and the XPP analytical model. *Journal of Microscopy* 266: 231-238.

Martínez-Vilalta J, Sala A, Asensio D, Galiano L, Hoch G, Palacio S, Piper FI, Lloret F. 2016. Dynamics of non-structural carbohydrates in terrestrial plants: a global synthesis. *Ecological Monographs* 86: 495-516.

Maxwell K, Johnson GN. 2000. Chlorophyll fluorescence—a practical guide. *Journal of Experimental Botany* 51: 659-668.

McCully ME, Shane MW, Baker AN, Huang CX, Ling LEC, Canny MJ. 2000. The reliability of cryo-SEM for the observation and quantification of xylem embolisms and quantitative analysis of xylem sap *in situ*. *Journal of Microscopy* 198: 24-33.

McCully ME, Canny MJ, Huang CX, Miller C, Brink F. 2010. Cryo-scanning electron microscopy (CSEM) in the advancement of functional plant biology: energy

dispersive X-ray microanalysis (CEDX) applications. *Functional Plant Biology* 37: 1011-1040.

McCully M, Canny M, Baker A, Miller C. 2014. Some properties of the walls of metaxylem vessels of maize roots, including tests of the wettability of their lumenal wall surfaces. *Annals of Botany* 113: 977-989.

McElwain JC, Yiotis C, Lawson T. 2016. Using modern plant trait relationships between observed and theoretical maximum stomatal conductance and vein density to examine patterns of plant macroevolution. *New Phytologist* 209: 94-103.

Medina E, Cuevas E, Popp M, Lugo AE. 1990. Soil salinity, sun exposure, and growth of *Acrostichum aureum*, the mangrove fern. *Botanical Gazette* 151: 41-49.

Moon GJ, Clough BF, Peterson CA, Allaway WG. 1986. Apoplastic and symplastic pathways in *Avicennia marina* (Forsk.) Vierh. roots revealed by fluorescent tracer dyes. *Functional Plant Biology* 13: 637-648.

Moore JP, Nguema-Ona E, Chevalier L, Lindsey GG, Brandt WF, Lerouge P, Farrant JM, Driouich A. 2006. Response of the leaf cell wall to desiccation in the resurrection plant *Myrothamnus flabellifolius*. *Plant Physiology* 141: 651-662.

Moore JP, Hearshaw M, Ravenscroft N, Lindsey GG, Farrant JM, Brandt WF. 2007. Desiccation-induced ultrastructural and biochemical changes in the leaves of the resurrection plant *Myrothamnus flabellifolia. Australian Journal of Botany* 55: 482-491.

Moore JP, Farrant JM, Driouich A. 2008. A role for pectin-associated arabinans in maintaining the flexibility of the plant cell wall during water deficit stress. *Plant Signaling and Behavior* 3: 102-104.

Moore JP, Nguema-Ona EE, Vicré-Gibouin M, Sørensen I, Willats WG, Driouich A, Farrant JM. 2013. Arabinose-rich polymers as an evolutionary strategy to plasticize resurrection plant cell walls against desiccation. *Planta* 237: 739-754.

Nguyen HT, Stanton DE, Schmitz N, Farquhar GD, Ball MC. 2015. Growth responses of the mangrove *Avicennia marina* to salinity: development and function of shoot hydraulic systems require saline conditions. *Annals of Botany* 115: 397-407.

Nguyen HT, Meir P, Sack L, Evans JR, Oliveira RS, Ball MC. 2017. Leaf water storage increases with salinity and aridity in the mangrove *Avicennia marina:*

integration of leaf structure, osmotic adjustment and access to multiple water sources. *Plant, Cell & Environment* 40: 1576-1591.

Nobel PS. 1978. Microhabitat, water relations, and photosynthesis of a desert fern, *Notholaena parryi*. *Oecologia* 31: 293-309.

Oliver MJ, Tuba Z, Mishler BD. 2000. The evolution of vegetative desiccation tolerance in land plants. *Plant Ecology* 151: 85-100.

Parkhurst DF, Loucks OL. 1972. Optimal leaf size in relation to environment. *Journal of Ecology* 60: 505-537.

Peters S, Mundree SG, Thomson JA, Farrant JM, Keller F. 2007. Protection mechanisms in the resurrection plant *Xerophyta viscosa* (Baker): both sucrose and raffinose family oligosaccharides (RFOs) accumulate in leaves in response to water deficit. *Journal of Experimental Botany* 58: 1947–1956.

Petruzzellis F, Pagliarani C, Savi T, Losso A, Cavalletto S, Tromba G, Dullin C, Bär A, Ganthaler A, Miotto A, Mayr S. 2018. The pitfalls of *in vivo* imaging techniques: evidence for cellular damage caused by synchrotron X-ray computed micro-tomography. *New Phytologist* 220: 104-110.

Pittermann J, Limm E, Rico C, Christman MA. 2011. Structure–function constraints of tracheid-based xylem: a comparison of conifers and ferns. *New Phytologist* 192: 449-461.

Pittermann J, Brodersen CB, Watkins J. 2013. The physiological resilience of fern sporophytes and gametophytes: advances in water relations offer new insights into an old lineage. *Frontiers in Plant Science* 4: 285.

Pittermann J, Watkins JE, Cary KL, Schuettpelz E, Brodersen C, Smith AR, Baer A. 2015. The structure and function of xylem in seed-free vascular plants: an evolutionary perspective. In: Hacke U, ed. *Functional and ecological xylem anatomy*. Heidelberg, Germany: Springer Cham, 1-37.

Porembski S, Barthlott W. 2000. Granitic and gneissic outcrops (inselbergs) as centers of diversity for desiccation-tolerant vascular plants. *Plant Ecology* 151: 19-28.

PPG I, 2016. A community-derived classification for extant lycophytes and ferns. *Journal of Systematics and Evolution* 54: 563-603.

Pratt RB, Jacobsen AL, Mohla R, Ewers FW, Davis SD. 2008. Linkage between water stress tolerance and life history type in seedlings of nine chaparral species (Rhamnaceae). *Journal of Ecology* 96: 1252-1265.

Pratt RB, Jacobsen AL. 2018. Identifying which conduits are moving water in woody plants: a new HRCT-based method. *Tree Physiology* 38: 1200-1212.

Proctor MC. 2000. The bryophyte paradox: tolerance of desiccation, evasion of drought. *Plant Ecology* 151: 41–49.

Proctor MC, Tuba Z. 2002. Poikilohydry and homoihydry: antithesis or spectrum of possibilities? *New Phytologist* 156: 327-349.

Proctor MCF, Oliver MJ, Wood AJ, Alpert P, Stark LR, Cleavitt NL, Mishler BD. 2007. Desiccation-tolerance in bryophytes: a review. *The Bryologist* 110: 595–621.

R Core Team. 2018. R: A language and environment for statistical computing. R Foundation for Statistical Computing, Vienna, Austria. URL https://www.R-project.org/.

Rakić T, Jansen S, Rančić D. 2017. Anatomical specificities of two paleoendemic flowering desiccation tolerant species of the genus *Ramonda* (Gesneriaceae). *Flora* 233: 186-193.

Rathinasabapathi B. 2006. Ferns represent an untapped biodiversity for improving crops for environmental stress tolerance. *New Phytologist* 172: 385-390.

Raven JA. 2014. Speedy small stomata? *Journal of Experimental Botany* 65: 1415-1424.

Ruzin SE. 1999. *Plant microtechnique and microscopy*. Oxford, UK: Oxford University Press.

Sack L, Frole K. 2006. Leaf structural diversity is related to hydraulic capacity in tropical rain forest trees. *Ecology* 87: 483–491.

Sack L, Scoffoni C, McKown AD, Frole K, Rawls M, Havran JC, Tran H, Tran T. 2012. Developmentally based scaling of leaf venation architecture explains global ecological patterns. *Nature Communications* 3: 1-10.

Salleo S, Lo Gullo MA, Trifilo P, Nardini A. 2004. New evidence for a role of vessel-associated cells and phloem in the rapid xylem refilling of cavitated stems of *Laurus nobilis* L. *Plant, Cell & Environment* 27: 1065-1076.

Savi T, Casolo V, Luglio J, Bertuzzi S, Lo Gullo MA, Nardini A. 2016. Species-specific reversal of stem xylem embolism after a prolonged drought correlates

to endpoint concentration of soluble sugars. *Plant Physiology and Biochemistry* 106: 198-207.

Schmitz N, Egerton JJG, Lovelock CE, Ball MC. 2012. Light-dependent maintenance of hydraulic function in mangrove branches: do xylary chloroplasts play a role in embolism repair? *New Phytologist* 195: 40-46.

Schneider H, Wistuba N, Wagner HJ, Thürmer F, Zimmermann U. 2000. Water rise kinetics in refilling xylem after desiccation in a resurrection plant. *New Phytologist* 148: 221-238.

Schneider H, Schuettpelz E, Pryer KM, Cranfill R, Magallón S, Lupia R. 2004. Ferns diversified in the shadow of angiosperms. *Nature* 428: 553-557.

Scholander PF, Hammel HT, Hemmingsen EA, Bradstreet ED. 1964. Hydrostatic pressure and osmotic potential in leaves of mangroves and some other plants. *PNAS* 52: 119-125.

Scholander PF, Bradstreet ED, Hammel HT, Hemmingsen EA. 1966. Sap concentrations in halophytes and some other plants. *Plant Physiology* 41: 529-532.

Scholander PF. 1968. How mangroves desalinate seawater. *Physiologia Plantarum* 21: 251-261.

Schuettpelz E, Schneider H, Huiet L, Windham MD, Pryer KM. 2007. A molecular phylogeny of the fern family Pteridaceae: assessing overall relationships and the affinities of previously unsampled genera. *Molecular Phylogenetics and Evolution* 44: 1172-1185.

Schuettpelz E, Pryer KM. 2009. Evidence for a Cenozoic radiation of ferns in an angiosperm-dominated canopy. *PNAS* 106: 11200-11205.

Schuettpelz E, Pryer KM, Windham MD. 2015. A unified approach to taxonomic delimitation in the fern genus *Pentagramma* (Pteridaceae). *Systematic Botany* 40: 629-644.

Scoffoni C, Rawls M, McKown A, Cochard H, Sack L. 2011. Decline of leaf hydraulic conductance with dehydration: relationship to leaf size and venation architecture. *Plant Physiology* 156: 832-843.

Scott P. 2000. Resurrection plants and the secrets of eternal leaf. *Annals of Botany* 85: 159–166.

Secchi F, Zwieniecki MA. 2011. Sensing embolism in xylem vessels: the role of sucrose as a trigger for refilling. *Plant, Cell & Environment* 34: 514-524.

Secchi F, Zwieniecki MA. 2012. Analysis of xylem sap from functional (non-embolized) and non-functional (embolized) vessels of *Populus nigra* – chemistry of refilling. *Plant Physiology* 160: 955-964.

Secchi F, Pagliarani C, Zwieniecki MA. 2017. The functional role of xylem parenchyma cells and aquaporins during recovery from severe water stress. *Plant, Cell & Environment* 40: 858-871.

Sharpe JM. 2010. Responses of the mangrove fern *Acrostichum danaeifolium* Langsd. & Fisch. (Pteridaceae, Pteridophyta) to disturbances resulting from increased soil salinity and hurricane Georges at the Jobos Bay National Estuarine Research Reserve, Puerto Rico. *Wetlands Ecology and Management*, 18: 57-68.

Sherwin HW, Farrant JM. 1996. Differences in rehydration of three desiccation-tolerant angiosperm species. *Annals of Botany* 78: 703-710.

Sherwin HW, Pammenter N, February E, Willigen CV, Farrant JM. 1998. Xylem hydraulic characteristics, water relations and wood anatomy of the resurrection plant *Myrothamnus flabellifolius* Welw. *Annals of Botany* 81: 567–575.

Sommerville KE, Gimeno TE, Ball MC. 2010. Primary nerve (vein) density influences spatial heterogeneity of photosynthetic response to drought in two *Acacia* species. *Functional Plant Biology* 37: 840-848.

Sommerville KE, Sack L, Ball MC. 2012. Hydraulic conductance of *Acacia* phyllodes (foliage) is driven by primary nerve (vein) conductance and density. *Plant, Cell and Environment* 35: 158-168.

Spalding MD, Blasco E, Field CD. [eds.] 1997. *World Mangrove Alias*. Okinawa, Japan: The International Society for Mangrove Ecosystems.

Sperry JS. 1983. Observations on the structure and function of hydathodes in *Blechnum lehmannii. American Fern Journal* 73: 65-72.

Sperry JS. 2003. Evolution of water transport and xylem structure. *International Journal of Plant Sciences* 164: S115-S127.

Stuart SA, Choat B, Martin KC, Holbrook NM, Ball MC. 2007. The role of freezing in setting the latitudinal limits of mangrove forests. *New Phytologist* 173: 576-583.

Toldi O, Tuba Z, Scott P. 2009. Vegetative desiccation tolerance: is it a goldmine for bioengineering crops? *Plant Science* 176: 187-199.

Tomlinson PB. 2016. *The botany of mangroves*. Cambridge, UK: Cambridge University Press.

VanBuren R, Wai CM, Zhang Q, Song X, Edger PP, Bryant D, Michael TP, Mockler TC, Bartels D. 2017. Seed desiccation mechanisms co-opted for vegetative desiccation in the resurrection grass *Oropetium thomaeum. Plant, Cell & Environment* 40: 2292-2306.

Vicré M, Lerouxel O, Farrant J, Lerouge P, Driouich A, 2004. Composition and desiccation-induced alterations of the cell wall in the resurrection plant *Craterostigma wilmsii. Physiologia Plantarum* 120: 229-239.

Warton DI, Duursma RA, Falster DS, Taskinen S. 2012. smatr 3 - an R package for estimation and inference about allometric lines. *Methods in Ecology and Evolution* 3: 257-259.

Watkins JE, Mack MC. Sinclair TR, Mulkey SS. 2007. Ecological and evolutionary consequences of desiccation tolerance in tropical fern gametophytes. *New Phytologist* 176: 708-717.

Werth M, Mehltreter K, Briones O, Kazda M. 2015. Stable carbon and nitrogen isotope compositions change with leaf age in two mangrove ferns. *Flora-Morphology, Distribution, Functional Ecology of Plants* 210: 80-86.

Wickham H. 2016. *ggplot2: Elegant Graphics for Data Analysis.* New York, NY, USA: Springer-Verlag. ISBN 978-3-319-24277-4, https://ggplot2.tidyverse.org

Xiao-Ping LI, Bee-Lian ONG. 1998. Tolerance of gametophytes of *Acrostichum aureum* (L.) to salinity and water stress. *Photosynthetica* 34: 21-30.

Zwieniecki MA, Boyce CK, Holbrook NM. 2004. Hydraulic limitations imposed by crown placement determine final size and shape of *Quercus rubra* L. leaves. *Plant, Cell & Environment* 27: 357-365.